

EPA-600/2-75-037

August 1975

Environmental Protection Technology Series

TEST EVALUATION OF CAT-OX HIGH EFFICIENCY ELECTROSTATIC PRECIPITATOR



**Industrial Environmental Research Laboratory
Office of Research and Development
U.S. Environmental Protection Agency
Research Triangle Park, N.C. 27711**

TEST EVALUATION OF
CAT-OX HIGH EFFICIENCY
ELECTROSTATIC PRECIPITATOR

by

E. M. Jamgochian, N. T. Miller, and R. Reale

The Mitre Corporation
Westgate Research Park
McLean, Virginia 22101

Contract No. 68-02-0650
ROAP No. 21ACZ-003
Program Element No. 1AB013

EPA Project Officer: C. J. Chatlynne

Industrial Environmental Research Laboratory
Office of Energy, Minerals, and Industry
Research Triangle Park, NC 27711

Prepared for

U.S. ENVIRONMENTAL PROTECTION AGENCY
Office of Research and Development
Washington, DC 20460

August 1975

RESEARCH REPORTING SERIES

Research reports of the Office of Research and Development, U.S. Environmental Protection Agency, have been grouped into five series. These five broad categories were established to facilitate further development and application of environmental technology. Elimination of traditional grouping was consciously planned to foster technology transfer and a maximum interface in related fields. The five series are:

1. Environmental Health Effects Research
2. Environmental Protection Technology
3. Ecological Research
4. Environmental Monitoring
5. Socioeconomic Environmental Studies

This report has been assigned to the ENVIRONMENTAL PROTECTION TECHNOLOGY STUDIES series. This series describes research performed to develop and demonstrate instrumentation, equipment and methodology to repair or prevent environmental degradation from point and non-point sources of pollution. This work provides the new or improved technology required for the control and treatment of pollution sources to meet environmental quality standards.

This report has been reviewed by the U.S. Environmental Protection Agency and approved for publication. Approval does not signify that the contents necessarily reflect the views and policies of the Agency, nor does mention of trade names or commercial products constitute endorsement or recommendation for use.

This document is available to the public through the National Technical Information Service, Springfield, Virginia 22151.

ABSTRACT

The general objective of the test program was to measure the performance of the high-efficiency Research-Cottrell electrostatic precipitator (ESP) located at the Wood River Power Station in East Alton, Illinois. The overall efficiency of the precipitator was measured as a function of steam generator and ESP operating conditions. Of particular interest was the efficiency of the precipitator as a function of particle size over the range from 0.01 μm to 5 μm . In addition, fly ash resistivity, gas concentrations, coal analyses, and fly ash analyses were determined. The measured results were compared with those generated by an idealized computer simulation model developed by the Southern Research Institute.

TABLE OF CONTENTS

	<u>Page</u>
ABSTRACT	iii
LIST OF FIGURES	vi
LIST OF TABLES	ix
CONCLUSIONS	1
INTRODUCTION	4
MEASUREMENT PROGRAM	6
Test Conditions	6
Parameters and Measurement Methods	10
TEST RESULTS	16
Mass Loading and Precipitator Efficiency	16
Particle Size Distribution and Fractional Efficiency	21
In Situ Resistivity Measurements	25
Sulfur Trioxide, Sulfur Dioxide, and Water Vapor Measurements	32
Coal and Fly Ash Analysis	33
COMPARISON OF RESULTS OF COMPUTER SIMULATION	43
APPENDICES	
I. Catalytic Oxidation Precipitator Performance at Wood River Power Station	49
II. Flue Gas Composition and Volume Flow Measurements	77
III. ESP Inlet and Outlet Ducts	89
IV. Conversion Factors	95

LIST OF FIGURES

<u>Figure Number</u>		<u>Page</u>
1	ESP Efficiency vs. Current Density	19
2	ESP Efficiency vs. Current Density	19
3	ESP Efficiency vs. Load	19
4	ESP Efficiency with 4th Section Off	20
5	ESP Efficiency During Soot Blowing	20
6	ESP Efficiency for Low Sulfur Coal	20
7	Fractional Efficiencies for the Cat-Ox Precipitator	24
8	Comparison of Optical and Impactor Data	27
9	dM/d Log D Versus Geometric Mean Diameter for 103 MW Load Tests	28
10	dM/d Log D Versus Geometric Mean Diameter for 85 MW Load Tests	29
11	dM/d Log D Versus Geometric Mean Diameter for 70 MW Load Tests	30
12	Inlet Mass Distribution Calculated from Cascade Impactor Data	31
13	Resistivity as a Function of Temperature by the Electric Field-Current Density Method	34
14	Comparison of Computer Simulated and Measured ESP Efficiencies	44
15	Comparison of Computed and Measured Size Fractional Efficiencies for 10 Microamperes Per Square Foot Current Density	45
16	Comparison of Computed and Measured Size Fractional Efficiencies for 20 Microamperes Per Square Foot Current Density	46
17	Comparison of Computed and Measured Size Fractional Efficiencies for 30 Microamperes Per Square Foot Current Density	47
18	Inlet Mass Distribution Calculated from Cascade Impactor Data	53
19	Inlet Particle-Size Distribution	54
20	Fractional Efficiencies for the Wood River Precipitator	56
21	Resistivity as a Function of Temperature by the Electric Field-Current Density Method for the Wood River Catalytic Oxidation Project Tests	60
22	Voltage vs. Current Characteristics for Power Supply No. 2 for the Low Sulfur Test Conditions	61

LIST OF FIGURES (Continued)

		<u>Page</u>
<u>Figure Number</u>		
23	Voltage vs. Current Characteristics for Power Supply No. 4 for the Low Sulfur Test Conditions	62
24	Voltage vs. Current Characteristics for Power Supply No. 5 for the Low Sulfur Test Conditions	63
25	Voltage vs. Current Characteristics for Power Supply No. 8 for the Low Sulfur Test Conditions	64
26	Voltage vs. Current Characteristics for Power Supply No. 2 for the High Sulfur Test Conditions	65
27	Voltage vs. Current Characteristics for Power Supply No. 4 for the High Sulfur Test Conditions	66
28	Voltage vs. Current Characteristics for Power Supply No. 5 for the High Sulfur Test Conditions	67
29	Voltage vs. Current Characteristics for Power Supply No. 8 for the High Sulfur Test Conditions	68
30	Actual Efficiency from Inlet and Outlet Dust Loading Measurements with All Data Points Included	70
31	Actual Efficiency from Inlet and Outlet Dust Loading Measurements with Soot Blowing, Non-Isokinetic and Fourth Electrical Section Points Removed	71
32	Computed and Measured Size Fractional Efficiencies for 10 Microamperes per Square Foot for the Cat-Ox [®] Tests. The region identified as lower limit region is that corresponding to acid condensation in the measurement system	72
33	Computed and Measured Size Fractional Efficiencies for 20 Microamperes per Square Foot for the Cat-Ox [®] Tests. The region identified as lower limit region is that corresponding to acid condensation in the measurement system	73

LIST OF FIGURES (Continued)

		<u>Page</u>
<u>Figure Number</u>		
34	Computed and Measured Size Fractional Efficiencies for 30 Microamperes per Square Foot for the Cat-Ox® Tests. The region identified as lower limit region is that corresponding to acid condensation in the measurement system	74
35	Test #14 Strip Chart Showing Transition From Low Sulfur to High Sulfur Coal	81
36	Gas Volume Flow Versus Load for Traverses	86
37	Gas Volume Flow Versus Load for Rakes	87
38	Point 1 - Input Electrostatic Precipitator (Left Side Facing Power Plant)	91
39	Point 1 - Input Electrostatic Precipitator (Right Side Facing Power Plant)	92
40	Point 3 - Output Electrostatic Precipitator	93

LIST OF TABLES

		<u>Page</u>
<u>Table Number</u>		
1	Electrostatic Precipitator Test Program	7
2	Breakdown and Repair of Unit 4 Steam Generator	8
3	Parameters Measured During Test Program	11
4	Measurement Methods	12
5	ESP Mass Loading and Efficiency at Various Operating Conditions	17
6	Fractional Efficiency from SRI Diffusional and Optical Data	23
7	Fractional Efficiencies from MRI Impactor Data	26
8	Measured SO ₃ Concentrations and Mass Flow	35
9	Average SO ₃ Concentrations and Mass Flow	36
10	Comparison of SO ₃ and SO ₂ Concentrations	37
11	Water Vapor Measurements	38
12	Proximate and Ultimate Analysis of Coal - As Received Basis	39
13	Proximate and Ultimate Analysis of Coal - Dry Basis	40
14	Chemical Content of Fly-Ash Sampled at ESP Inlet	42
15	Fractional Efficiency Data	55
16	Comparison Between the Resistivity Determined by Each Method at a Current Density of 0.2 A/cm ² , Test Date 10/1/73	59
17	Flue Gas Composition at Economizer and Input/Out- put of ESP	79
18	Flue Gas Composition for Repeat Tests	80
19	Pressure and Temperature Measurements at Economizer and Stack Using Rakes	83
20	Gas Volume Flow at Economizer and Stack Using Rakes	84
21	Comparison of Traverse and Rake Volume Flow Measurements	85
22	Conversion Factors	96

ACKNOWLEDGEMENTS

The work described in this paper was performed jointly by the MITRE Corporation, the Southern Research Institute (SRI), and the Midwest Research Institute (MRI), under the sponsorship of Mr. G. S. Haselberger and Mr. R. C. Lorentz of the Industrial Environmental Research Laboratory (RTP), Office of Research and Development, U.S. Environmental Protection Agency. The Illinois Power Company made its facilities available, and the Wood River Power Station supervisory and operating personnel fully cooperated in the establishment of the proper test operating conditions. Mr. D. Korneman provided the supervisory interface.

Mr. G. B. Nichols headed up the SRI field team and Messrs. W. H. Maxwell and R. C. Tussey, Jr., the MRI field team. Dr. R. Statnick of the Industrial Environmental Research Laboratory (RTP) provided consultation on testing techniques, participated in the first week of field testing, and was subsequently responsible for reduction of the impactor data. Mr. J. McCain of SRI, in addition to performing the condensation nuclei and optical particle sizing, provided consultation on the impactor measurements.

In addition to the basic MITRE team consisting of Mr. E. M. Jamgochian, program task leader, Mr. N. T. Miller, and Mr. R. Reale, periodic field support was provided by Mr. J. Findley, Mr. J. Miller, and Mr. R. W. Spewak. Mr. J. Elliott assisted in the reduction of the gas concentration and gas volume flow data. Mr. G. Erskine initially proposed this program and also participated in some of the field tests.

CONCLUSIONS

In the normal mode of operation for the Unit 4 steam generator, (i.e., 103 MW load, high-sulfur coal, and ESP functioning automatically), the total ESP efficiency was measured to be in the 99.43 to 99.70 percent range, indicating that the ESP was operating either at or close to the design efficiency (99.6 percent). A change to low-sulfur coal (1.11 percent S, as received) under these same operating conditions showed no significant loss in efficiency.

A decrease in load from 103 MW to 70 MW, with a corresponding decrease in gas volume flow from an average of 308,000 SCFM to 203,750 SCFM, resulted in a decrease of ESP efficiency as opposed to the expected increase in efficiency. An explanation of this result cannot be made based on the available data; more data are required, particularly at the lower load levels, to provide a definitive statistical result.

The ESP efficiency is nearly constant for ESP current densities from $55 \mu\text{A}/\text{ft}^2$ (automatic) to $30 \mu\text{A}/\text{ft}^2$, increasing slightly at $30 \mu\text{A}/\text{ft}^2$. Between 30 and $20 \mu\text{A}/\text{ft}^2$, the efficiency begins to drop, reaching a value ranging from 96.18 percent to 97.31 percent at a current density of $10 \mu\text{A}/\text{ft}^2$. Conversely, the fly ash penetration increased to values of 2.69 percent to 3.82 percent at $10 \mu\text{A}/\text{ft}^2$ from values of 0.17 percent to 0.22 percent at $30 \mu\text{A}/\text{ft}^2$. Therefore, on the average, penetration increased by a factor of approximately 16 for a factor of 3 decrease in current density.

With the fourth section of the ESP off, a loss in efficiency of one percent with a corresponding tripling of the fly ash penetration was observed. This result shows the effect of having a smaller precipitator, shorter in length by approximately 10 feet (25 percent of total length).

Soot blowing using only the wall blowers had no discernible effect on ESP efficiency or outlet grain loading; however, soot blowing using the retractable blowers dropped the efficiency by 0.3 to 0.6 percent and caused approximately a doubling of the fly ash penetration.

The data involving measurement of particle size efficiency resulted in some difficulties. One problem was contamination of impactor data at the precipitator outlet by condensation of H_2SO_4 . In addition, similar contamination was observed in the condensation nuclei apparatus; however, good results were obtained with the Climet optical counter in the 1.5 μm to 0.46 μm size range. A drop in efficiency from 99.85 to 96.80 percent from the large particle size to the small particle size was determined for the ESP in the automatic mode of operation.

Even though the CN results were contaminated by H_2SO_4 condensation, a lower limit of efficiency was determined in the diffusional size range from 0.01 μm to 0.15 μm . The ESP efficiency was greater than 97 percent over this range.

The resistivity measurements of the low-sulfur coal were approximately the same as for the high-sulfur coal, corroborating the high ESP efficiency obtained during the low-sulfur coal test. The resistivity may have been dominated by surface conductivity in the presence of high concentrations of water vapor and SO_3 .

The ESP efficiencies determined from the measured data were compared to efficiencies determined by the SRI ESP computer systems model. In a comparison of total efficiency versus gas volume flow, the measured data verified the validity of the simulation model at the lower current densities, but deviated from the model at the

higher current densities. Comparisons were also made of measured fractional efficiencies and computed efficiencies. There was general agreement between the measured and computed data.

INTRODUCTION

The general objective of the test program was to measure the performance of the high-efficiency Research-Cottrell electrostatic precipitator (ESP) located at the Wood River Power Station in East Alton, Illinois. This precipitator is integrated with the flue gas output of the 100 MW Unit 4 steam generator to remove particulate matter from the flue gas stream prior to entering the Cat-Ox[®] sulfur dioxide control process.* The precipitator has a design efficiency of 99.6 percent and a design output grain loading of 0.005 grains/SCF, which satisfies Cat-Ox[®] maintenance requirements.

Although the test evaluation that was performed is pertinent to the future planned testing of the Cat-Ox[®] process, the primary objective of this program was to evaluate the electrostatic precipitator itself as a control device with regard to ESP performance characteristics that have not been extensively measured in the past. Of particular interest was the efficiency of the precipitator as a function of particle size over the range from 0.01 μm to 5 μm . In addition, precipitator parameters were measured in order to compare them with the results obtained for an idealized computer simulation model of an electrostatic precipitator that had been developed by the Southern Research Institute (SRI) for the Environmental Protection Agency (EPA) under a separate contract.

The test program was a joint effort among The MITRE Corporation, the Southern Research Institute, the Midwest Research Institute (MRI), and the Industrial Environmental Research Laboratory (Research Triangle Park) of the Environmental Protection Agency. In addition, the Illinois Power Company cooperated throughout the

* Cat-Ox[®] is a proprietary term and registered trademark of Monsanto Enviro-Chem Systems, Inc.

program by making facilities available and by operating the steam generator at specific test conditions. MITRE was responsible for the overall test program, with subcontractor effort provided by SRI. Test support provided by MRI was under a separate Task Order contract currently in effect with EPA.

MEASUREMENT PROGRAM

The test program as it was actually carried out is shown in Table 1. Fifteen tests were performed under various test conditions over a period of approximately three weeks. The objectives of the tests were to determine the performance of the ESP as a function of steam generator load, coal sulfur content, soot blowing, and ESP current density. A separate test was performed with the last section of the ESP turned off. The first test performed was for equipment checkout and calibration. As can be seen in Table 1, some of the tests were conducted out of sequence from the original plan, due to the following reasons:

- a. Additional test time was required to obtain a reliable particle count in the diffusional particle size range at the inlet to the electrostatic precipitator. Therefore, an additional test day was added on Saturday, 15 September 1973, and the test was identified as Test 15 as an add-on to the original 14 scheduled tests.
- b. Unit 4 developed a series of problems starting Sunday night, 16 September 1973, and was not back on-line until Wednesday, 19 September 1973. In order to make up the lost test days, two tests were conducted on 19 September, and the test originally scheduled for Friday of that week was performed on Saturday. Table 2 outlines the difficulties encountered with the Unit 4 steam generator and the subsequent scheduling of load.

TEST CONDITIONS

Tests were conducted at several operating conditions of the steam generator and ESP (see Table 1). For each test, the steam generator was operated at one of three loads, 103 MW, 85 MW, and 70 MW. The majority of the tests were conducted at 103 MW and 70 MW, with a single test at 85 MW. With a few exceptions, each test consisted of two runs under identical operating conditions of approximately four hours duration per run. The purpose of the second run was to indicate reproducibility of test results and to provide data redundancy when required. For those tests that required measurements

TABLE 1. ELECTROSTATIC PRECIPITATOR TEST PROGRAM

TEST NO.	RUN NO.	DATE (1973)	WEEK	STEAM GENERATOR OPERATING CONDITIONS			ESP OPERATING CONDITIONS*		TEST OBJECTIVES
				LOAD	COAL	SOOT BLOWING	PLATE CURRENT	TRANSFORMER SETS	
1	1	Sept. 11	1st	103	High Sulfur	None	Automatic	Normal	Calibration of gas volume flow
	2	(Night)		85			(55 $\mu\text{A}/\text{ft}^2$)		
	3			70					
		12							MRI checkout equipment; SRI install voltage dividers
2	1	13		103	High Sulfur	Retractable Wall	Automatic	Normal	ESP performance with soot blowing
	2	(Day)							
3	1	14		103	High Sulfur	None	Automatic	4th Sect. Off	ESP performance with last section off
	2	(Day)							
15	1	15		103	High Sulfur	None	---	---	Characterization of EPS inlet for diffusional Particle size range (0.01-0.15 μm)
		(Day)							
		16-19	2nd						Steam generator under repair
8	1	19		103	High Sulfur	None	---	---	Characterization of ESP inlet for diffusional Particle Size Range (0.01-0.15 μm)
		(Day)							
4	1	19		103	High Sulfur	None	Automatic	Normal	ESP performance under normal operation
	2	(Day)							
5	1	20		103	High Sulfur	None	20 $\mu\text{A}/\text{ft}^2$	Normal	ESP performance at lower current density
	2	(Day)							
6	1	21		103	High Sulfur	None	10 $\mu\text{A}/\text{ft}^2$	Normal	ESP performance at lower current density
	2	(Day)							
7	1	22		103	High Sulfur	None	30 $\mu\text{A}/\text{ft}^2$	Normal	ESP performance at lower current density
	2	(Day)							
9	1	24-25	3rd	85	High Sulfur	None	Automatic	Normal	ESP performance at intermediate load
	2	(Night)							
10	1	25-26		70	High Sulfur	None	Automatic	Normal	ESP performance at low load
	2	(Night)							
11	1	26-27		70	High Sulfur	None	30 $\mu\text{A}/\text{ft}^2$	Normal	ESP performance at low load and current density
	2	(Night)							
12	1	27-28		70	High Sulfur	None	20 $\mu\text{A}/\text{ft}^2$	Normal	ESP performance at low load and current density
	2	(Night)							
13	1	28-29		70	High Sulfur	None	10 $\mu\text{A}/\text{ft}^2$	Normal	ESP performance at low load and current density
	2	(Night)							
		29							Conversion to low-sulfur coal
14	1	Oct. 1	4th	103	Low Sulfur	None	Automatic	Normal	ESP performance with low-sulfur coal
	2	(Day)							

*Collecting plate rapping conditions and discharge wipe vibration conditions constant throughout test program.

TABLE 2. BREAKDOWN AND REPAIR OF UNIT 4 STEAM GENERATOR

DATE	DAY	STATUS
9/16/73	Sunday	Superheaters on unit 4 fail Unit 4 taken down for repair
9/17/73	Monday	Unit 4 under repair
9/18/73	Tuesday	Additional trouble developed with oil feed pump which controls boiler feed pump as Unit 4 load was brought up 10:09 PM: Load raised to 10 megawatts 10:14 PM: Load reached 50 megawatts 11:05 PM: Precipitator turned on
9/19/73	Wednesday	12:00 AM: Load held at 50 megawatts 6:00 AM: Load at 90 megawatts 6:30 AM: Load at 103 megawatts 6:45 AM: Coal mill 4C sheared pin Load dropped to 81 megawatts 7:15 AM: Load at 88 megawatts with mills 4A, B, D operational 7:45 AM: 150,000 CFM of gas added to raise load to 100 megawatts 8:00 AM: Work commenced to fix mill 4C 8:15 AM: Load at 100 megawatts with mixture of coal and gas 10:25 AM: Gas cut off and mill 4C brought on line 10:50 AM: Unit 4 on line at 103 mega- watts burning coal only

at the output of the precipitator, the steam generator was brought to the specified load condition approximately four hours prior to the start of measurements in order to allow the ESP to stabilize at the required test conditions. In most cases, the four-hour pre-soak condition was satisfied except for some of the low-load tests, where load demands on Illinois Power prevented dropping of the load at the specified time of 8:00 p.m. so that measurements could be started at midnight and ended at 7:00 a.m. when the load had to be brought back up again in order to meet the increased daytime demand. The test could not be slipped to satisfy the four-hour pre-soak condition because of the fixed end time.

For all tests except one, the coal burned was obtained from the Arch Minerals Company out of mines located in southwestern Illinois. The sulfur content of the Arch Minerals coal was approximately 3.6 percent sulfur (by weight). One low-sulfur test was conducted with a special episode coal that had a sulfur content of approximately 1.1 percent. The changeover to low-sulfur coal was initiated on Saturday, 29 September, to assure that the bunkers were purged of the higher sulfur coal and that the ESP would have ample time (more than 24 hours) to stabilize to low-sulfur conditions.

Finally, with regard to boiler operating conditions, a single test was performed with the soot blowers on. Two types of soot blowers are utilized on Unit 4; wall blowers located on the boiler walls and retractable blowers used to clean the superheaters. During the first run of this particular test, the retractable blowers were cycled continuously and during the second run, the wall blowers were cycled continuously. Therefore, the two soot blowing runs were conducted under different operating conditions and were not repeatability runs.

The precipitator consists of two identical units in parallel, each of which has four sections in series. During Test 3, the fourth section of each of the parallel units was de-energized, providing the equivalent of a shorter length precipitator.

The ESP was operated at four average current densities: $55 \mu\text{A}/\text{ft}^2$, $30 \mu\text{A}/\text{ft}^2$, $20 \mu\text{A}/\text{ft}^2$, and $10 \mu\text{A}/\text{ft}^2$. The first of these current densities is the average value for normal automatic operation of the ESP at which it has been set to achieve the design goal performance. For this case, the current density is not identical between all plates of the precipitator; however, for the three other current densities, the plate voltages were set to achieve uniform current density between all plates of the precipitator. The ESP was operated at each of these four current densities for both the 103 MW and 70 MW loads.

PARAMETERS AND MEASUREMENT METHODS

Table 3 shows the parameters that were measured during each of the tests and identifies the contractor responsible for each type of measurement. MITRE measured flue gas concentrations and gas volume flow, collected coal samples, and recorded gauge board readings and secondary voltage during some of the tests when SRI was not present. SRI measured in situ resistivity, particle size distribution in the diffusional and optical regions, ESP volt-ampere characteristics, and secondary voltage. MRI performed the mass loading measurements, impactor measurements, and gaseous SO_3 measurements and analyzed the ash samples.

Table 4 shows the measurement methods employed, the sampling frequency, the sampling locations, and the purpose of each type of measurement. The measurements of primary interest were the mass loading and particle sizing measurements. Mass loading was measured

TABLE 3. PARAMETERS MEASURED DURING TEST PROGRAM																					
TEST NO.	RUN NO.	DATE (1973)	WEEK	MITRE										SRI				MRI			
				GAS CONCENTRATION				GAS VOL. FLOW			MANUAL			MANUAL				MANUAL			
				SO ₂	CO ₂	O ₂	H ₂ O	ΔP	SP	T	GB	CS	SV	SV	IR	CN	CL	ML	I	SO ₃	AS
1	1	Sept. 11	1st		X	X	X	X	X	X	X										
	2	(Night)			X	X	X	X	X	X	X										
	3				X	X	X	X	X	X	X										
		12																			
2	1	13		X	X	X	X	X	X	X	X	X	X					X	X	X	X
	2	(Day)		X	X	X	X	X	X	X	X	X	X					X	X	X	X
3	1	14		X	X	X	X	X	X	X	X	X	X					X	X	X	X
	2	(Day)		X	X	X	X	X	X	X	X	X	X			X	X	X	X	X	X
15	1	15		X	X	X	X	X	X	X	X										
		(Day)																X	X	(Inlet)	
		16-19	2nd																		
8	1	19		(Day)	X	X	X	X	X	X	X	X							X	X	(Inlet)
4	1	19		X	X	X	X	X	X	X	X	X		X	X			X	X	X	X
	2	(Day)		X	X	X	X	X	X	X	X	X		X	X	(Outlet)		X	X	X	X
5	1	20		X	X	X	X	X	X	X	X	X		X	X			X	X	X	X
	2	(Day)		X	X	X	X	X	X	X	X	X		X	X	(Outlet)		X	X	X	X
6	1	21		X	X	X	X	X	X	X	X	X		X	X			X	X	X	X
	2	(Day)		X	X	X	X	X	X	X	X	X		X	X	(Outlet)		X	X	X	X
7	1	22		X	X	X	X	X	X	X	X	X		X	X			X	X	X	X
	2	(Day)		X	X	X	X	X	X	X	X	X		X	X	(Outlet)		X	X	X	X
9	1	24-25	3rd	X	X	X	X	X	X	X	X	X	X					X	X	X	X
	2	(Night)		X	X	X	X	X	X	X	X	X	X					X	X	X	X
10	1	25-26		X	X	X	X	X	X	X	X	X	X					X	X	X	X
	2	(Night)		X	X	X	X	X	X	X	X	X	X					X	X	X	X
11	1	26-27		X	X	X	X	X	X	X	X	X	X					X	X	X	X
	2	(Night)		X	X	X	X	X	X	X	X	X	X					X	X	X	X
12	1	27-28		X	X	X	X	X	X	X	X	X	X					X	X	X	X
	2	(Night)		X	X	X	X	X	X	X	X	X	X					X	X	X	X
13	1	28-29		X	X	X	X	X	X	X	X	X	X					X	X	X	X
	2	(Night)		X	X	X	X	X	X	X	X	X	X					X	X	X	X
		29																			
14	1	Oct. 1	4th	X	X	X	X	X	X	X	X	X		X	X			X	X	X	X
	2	(Day)		X	X	X	X	X	X	X	X	X		X	X			X	X	X	X

LEGEND

ΔP Differential Pressure
SP Static Pressure
T Gas Temperature
GB Gauge Board Readings
CS Coal Samples
SV Secondary Voltage
IR In-Situ Resistivity
CN Condensation Nuclei
CL Climet Counter
ML Mass Loading
I Impactor
AS Ash Samples
SO₃ Gaseous SO₃

TABLE 4. MEASUREMENT METHODS

ITEM	MEASURED VARIABLE	SAMPLING METHOD	FREQUENCY	LOCATION	PURPOSE
1	Gas Concentrations	Time-Shared Gas Meas. Subsystem DuPont SO ₂ Analyzer Bendix CO ₂ Analyzer Beckman O ₂ Analyzer MSA H ₂ O Vapor Analyzer H ₂ O vapor by Silica Gel Method (Obtained during Mass Loading)	Continuous One/Run/Location	Time Shared: Economizer Input ESP Output ESP Input ESP Output ESP	Determine molecular weight of gas; correlation of SO ₂ and SO ₃ concentrations; H ₂ O vapor concentration and conditioning of fly ash resistivity
2	Gas Volume Flow	Flow Measurement Subsystem with Temp./Pres. Rakes Manual Traverse (Obtained during Mass Loading)	Continuous/Location One/Run/Location	Economizer Stack Input ESP Output ESP	Determine mass flow of particulates and flue gases
3	Gauge Board Readings	Manual Recording of IP Instrumentation	Two/Run		Control and measurement of steam generator and ESP operating conditions
4	Coal Samples	Cyclone Collector	One/Run	Outputs of each Coal Mill (A, B, C, D)	Ultimate and proximate analysis to determine constituents including sulfur content
5	Secondary Voltage	Voltage Dividers and Precision Voltmeter	One/Hr.	Secondary of High Voltage Transformers	Measurement of Voltage-Current relationship
6	Fly Ash Resistivity	In-Situ Point-to-Plane Resistivity Probe	Two/Run	Input ESP	Effect of resistivity on ESP performance
7	Diffusional Particle Sizing (.01 μ m-.15 μ m)	Diffusion Battery and Condensation Nuclei Counter	One/Test	Input ESP Output ESP	Distribution and ESP efficiency versus particle size
8	Submicron Particle Sizing (0.4 μ m-1.5 μ m)	Climet Optical Particle Counter	One/Test	Input ESP Output ESP	Distribution and ESP efficiency versus particle size
9	Submicron Particle Sizing (0.3 μ m- 5 μ m)	Brinks Impactor Andersen Model III Impactor	One/Run One/Run	Inlet ESP Outlet ESP	Mass distribution and ESP efficiency versus particle size
10	Mass Loading	Modified EPA Train In-Stack Thimble	One/Run One/Run	Inlet ESP Outlet ESP	Mass loading and overall ESP efficiency
11	Gaseous SO ₃	Controlled Condensation with Adapted EPA SO ₂ Train	One/Run/Location	Inlet ESP Outlet ESP	Measurement of SO ₃ concentration and conditioning of fly ash resistivity
12	Ash Samples	Fly Ash obtained during Mass Loading	One/Run	Inlet ESP	Analysis of fly ash chemical composition; correlation with resistivity measurements

at the inlet and outlet of the precipitator using a modified EPA train at the inlet and an in-stack filter at the outlet. In order to obtain two runs during a single test day, only half of the available ports could be sampled during each run. Therefore, alternate ports were sampled during each run at the inlet. The same procedure was not possible at the outlet, because one of the ports had to be dedicated to the condensation nuclei (CN) equipment, which was too bulky and heavy to move around. The mass sample was integrated over either 21 or 18 points at the inlet, depending on the particular run, and over 12 points at the outlet during each run (see Appendix III).

Particle size measurements were made using three different methods covering the 0.01 μm to 5 μm size range. The Brinks impactor was used for measurements at the inlet of the precipitator over the 0.4 μm to 5 μm size range. The sample was collected at a single port by inserting the impactor in the duct and allowing it to reach the flue gas temperature before a sample was drawn. Sampling was anisokinetic, as the particles of interest were less than 5 μm in size. The sampling time for most cases was approximately 20 minutes.

The Andersen Model III impactor was used at the precipitator outlet over the 0.3 μm to 5 μm size range because of the lower particle density and, consequently, longer integration time required. The integration time for most tests was approximately 180 minutes. As was the case with the Brinks impactor, the Andersen impactor was inserted in the duct and allowed to reach the gas temperature prior to sampling. One Brinks and one Andersen sample were taken for each run.

A diffusion battery and CN counter were used for particle size distribution measurements in the 0.01 μm to 0.15 μm range. As the equipment for CN measurements is bulky and not readily moved and measurements are time consuming, it was possible to sample only the inlet or the outlet during any particular test. CN measurements were only performed for the 103 MW load condition, as shown in Table 3. Table 3 also identifies the tests performed to characterize the ESP inlet and outlet.

In conjunction with the CN measurements and, therefore, for the same tests, particle size distributions were obtained over the 0.4 μm to 1.5 μm range using the Climet optical counter. The optical counter provided a data overlap with the impactor measurements.

High fly ash resistivities can cause excessive sparking or reverse corona, thereby limiting precipitator performance. Therefore, an in situ point-to-plane resistivity probe was used to measure resistivity at the ESP inlet. The point-to-plane probe is designed to collect the fly ash electrostatically in the duct and, to measure the fly ash resistivity in the duct under actual flue gas conditions. Since both temperature and composition of the flue gas can have significant influence on the fly ash resistivity, depending on the conductivity mechanism, an in-the-duct measurement of this type, which measures resistivity under actual flue gas conditions, has advantages over a method that depends on laboratory analysis of the sample.

The flue gas constituents that may influence fly ash resistivity are water vapor and SO_3 . Therefore, as shown in Table 4, these gases were measured, as well as SO_2 , CO_2 , and O_2 . Gaseous SO_3 was manually measured at the inlet and outlet of the ESP using the

method of controlled condensation, and water vapor was measured manually using the technique associated with "Method 5 - Determination of Particulate Emissions from Stationary Sources " (Federal Register, Vol. 36, No. 27, December 1971). The other gases, including water vapor, were measured by a continuous measurement system that was sequentially time-shared during each run among the economizer, the ESP inlet, and the ESP outlet.

The fly ash collected during the mass loading measurements at the inlet to the precipitator was retained for chemical analysis. The purpose of the analysis was to correlate the chemical composition of the fly ash to the resistivity.

Gas volume flow was measured manually at the inlet and outlet of the ESP while making the mass loading measurements. In addition, a check was made of the gas volume flow by measurements at the economizer and the stack using a continuously recording flow measurement system.

Gauge board readings of the steam generator and ESP operating conditions were recorded periodically. Examples of the parameters recorded are generator load, steam flow, coal flow, barometric pressure, and ESP plate currents. The continuous gas measurement system measured the excess air by recording O_2 content of the flue gas at the economizer. The precipitator plate voltages were measured by means of a precision voltmeter and voltage dividers that were installed across the secondary of the transformer prior to the test program.

Coal samples were obtained by a cyclone collector at the outlet of each of the four pulverizer mills. Samples collected during each run were subsequently combined by riffing and were packaged into moisture-proof bags for ultimate and proximate analysis.

TEST RESULTS

The detailed results of the test measurements are reported in Appendices I and II, and in the MRI data report.* Appendix I includes a report on the work performed by SRI and Appendix II incorporates the data collected by MITRE. The significant results from these sources are reported in the following sections.

MASS LOADING AND PRECIPITATOR EFFICIENCY

The Cat-Ox[®] electrostatic precipitator has been designed to operate under normal operating conditions for the Unit 4 steam generator with an efficiency of 99.6 percent. Deviations from normal operating conditions will affect the ESP efficiency and, as discussed previously, many of these conditions were investigated. Table 5 shows the results of the measurements for the various test conditions in terms of the mass loadings, mass flow, and ESP efficiency. Four of the data points out of the 24 measured are erroneous and are so indicated in Table 5. In one case, the sampling probe was leaky; in the second case, sampling was anisokinetic; and in the third and fourth cases, water apparently contaminated the filter used in the thimble.

In the normal mode of operation for the Unit 4 steam generator (i.e., 103 MW load, high-sulfur coal, and the ESP functioning automatically), the efficiency was measured to be 99.70 percent in the second run. These two measurements indicate that the ESP was operating either at the design efficiency or close to it.

*Tussey, R. C., Jr. and W. H. Maxwell, "Cat-Ox Demonstration Particulate Study, Electrostatic Precipitator Evaluation, Manual gas, Mass Sampling Analysis," MRI Project No 3585-C, EPA Contract No. 68-02-0228, Task 35.

TABLE 5. ESP MASS LOADING AND EFFICIENCY AT VARIOUS OPERATING CONDITIONS

TEST RUN #	OPERATING CONDITIONS				LOCATION	MASS LOADING			EFFICIENCY
	LOAD	FUEL*	PLATE CURRENT	SPECIAL		GR/DSCF	GR/ACF	lb/HR	
2-1	103	HIGH SULFUR 3.56% wt.	AUTOMATIC (55 $\mu\text{A}/\text{ft}^2$)	SOOT BLOW	INLET OUTLET	1.6406 0.0148	0.9870 0.0092	3629.11 36.79	99.10
2-2					INLET OUTLET	1.6459 0.0089	0.9950 0.0054	4031.30 21.88	99.46
3-1	103	HIGH SULFUR 3.48% wt.	AUTOMATIC	4TH SECTION OFF	INLET OUTLET	1.3025 0.0208	0.8127 0.0128	2989.71 51.80	98.40
3-2					INLET OUTLET	1.2929 0.0159	0.8230 0.0098	2998.22 40.27	98.77
4-1	103	HIGH SULFUR 3.38% wt.	AUTOMATIC		INLET OUTLET	1.4312 0.0081	0.9118 0.0051	3247.51 20.14	99.43
4-2					INLET OUTLET	1.4748 0.0045	0.9168 0.0028	3333.57 11.54	99.70
5-1	103	HIGH SULFUR 3.44% wt.	20 $\mu\text{A}/\text{ft}^2$		INLET OUTLET	1.2860 0.0125	0.7987 0.0077	3085.08 31.37	99.03
5-2					INLET OUTLET	1.3086 0.0150	0.8057 0.0093	3061.56 38.25	98.85
6-1	103	HIGH SULFUR 3.46% wt.	10 $\mu\text{A}/\text{ft}^2$		INLET OUTLET	1.4489 0.0554	0.9033 0.0351	3246.70 141.91	96.18
6-2					INLET OUTLET	1.3277 0.0357	0.8179 0.0226	3118.33 94.23	97.31
7-1	103	HIGH SULFUR 3.67% wt.	30 $\mu\text{A}/\text{ft}^2$		INLET OUTLET	1.4020 0.0031	0.8649 0.0020	3106.46 8.08	99.78
7-2					INLET OUTLET	1.3687 0.0023	0.8226 0.0015	3056.38 6.23	99.83
9-1	85	HIGH SULFUR 3.56% wt.	AUTOMATIC		INLET OUTLET	2.3658 ---	1.4689 ---	4356.20 ---	(Leaky Probe)
9-2					INLET OUTLET	1.4372 0.0140	0.9163 0.0087	2708.30 30.32	99.03 (88% Isokinetic)
10-1	70	HIGH SULFUR 3.68% wt.	AUTOMATIC		INLET OUTLET	1.2311 0.0101	0.7600 0.0061	1931.38 15.48	99.18
10-2					INLET OUTLET	1.0265 0.0302	0.6426 0.0183	1626.41 47.48	97.06 (Green Filter)
11-1	70	HIGH SULFUR 3.81% wt.	30 $\mu\text{A}/\text{ft}^2$		INLET OUTLET	1.1870 0.0088	0.7057 0.0054	1731.44 14.86	99.26
11-2					INLET OUTLET	1.2843 0.0351	0.7580 0.0216	1915.80 58.18	97.27 (Green Filter)
12-1	70	HIGH SULFUR 3.75% wt.	20 $\mu\text{A}/\text{ft}^2$		INLET OUTLET	1.3063 0.0121	0.8049 0.0075	2089.63 20.11	99.07
12-2					INLET OUTLET	1.3465 0.0123	0.8096 0.0076	2130.74 19.91	99.09
13-1	70	HIGH SULFUR 3.60% wt.	10 $\mu\text{A}/\text{ft}^2$		INLET OUTLET	1.2982 0.0211	0.7706 0.0133	2038.85 34.73	98.38
13-2					INLET OUTLET	1.2161 0.0277	0.7190 0.0173	1812.58 47.70	97.72
14-1	103	LOW SULFUR 1.11% wt	AUTOMATIC		INLET OUTLET	0.9030 0.0038	0.5504 0.0023	2008.13 9.48	99.58
14-2					INLET OUTLET	0.8444 0.0049	0.5114 0.0030	1911.69 12.41	99.42

* Percentage of sulfur is shown on an as received basis. For coal analysis, see Table 12 and 13.

Figures 1 through 6 present plots of the ESP collection efficiency and penetration as a function of the steam generator and ESP operating conditions. Where available, both the first and second runs at each test condition are plotted to show the spread in the data. Figure 1 shows the collection efficiency and penetration versus current density at the 103 MW load for the high-sulfur coal. The average sulfur content of the coal was measured to be 3.58 percent. The average gas volume flow at 103 MW was approximately 308,000 SCFM. The data show that the collection efficiency remains nearly constant from a current density of $55 \mu\text{A}/\text{ft}^2$ to $30 \mu\text{A}/\text{ft}^2$, and then begins dropping at some point after $30 \mu\text{A}/\text{ft}^2$. At the lowest current density of $10 \mu\text{A}/\text{ft}^2$, the efficiency ranged from 96.18 percent to 97.31 percent. Conversely, the penetration, which is $1 - \text{collection efficiency}$, increased to values in the range of 2.69 to 3.82 percent at $10 \mu\text{A}/\text{ft}^2$ from values in the range of 0.17 to 0.22 percent at $30 \mu\text{A}/\text{ft}^2$. Therefore, on the average, the penetration increased by a factor of approximately 16 for a factor of 3 decrease in current density.

Figure 2 shows the ESP efficiency versus current density at the 70 MW load. The curve is similar to that obtained for the 103 MW load; however, as discussed previously, two of the data points at the higher current densities were lost, so the spread in the data is not indicated. At this lower load, the average gas volume flow is approximately 203,750 SCFM, which should theoretically result in a precipitator efficiency equal to or higher than that of the 103 MW case (see discussion in Section 4.0). This expected increased efficiency was not observed at the higher current densities, but was observed at the $20 \mu\text{A}/\text{ft}^2$ and $10 \mu\text{A}/\text{ft}^2$ current densities. The anticipated results may have been obscured by the loss of data points and the need to obtain sufficient data to indicate a statistical trend. Conversely, existing analytical expressions do not define all of the significant phenomena occurring in commercial precipitators.

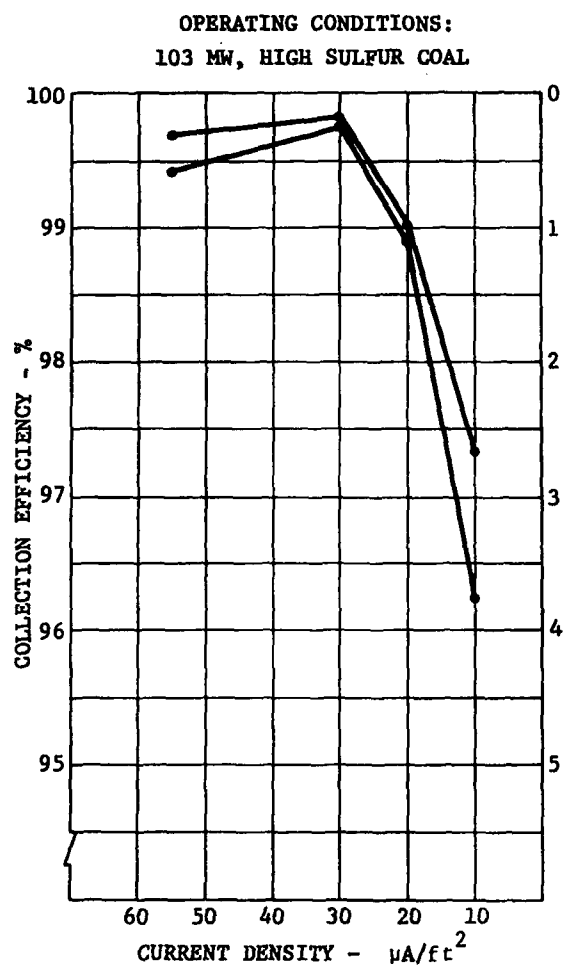


FIGURE 1
ESP EFFICIENCY VS.
CURRENT DENSITY

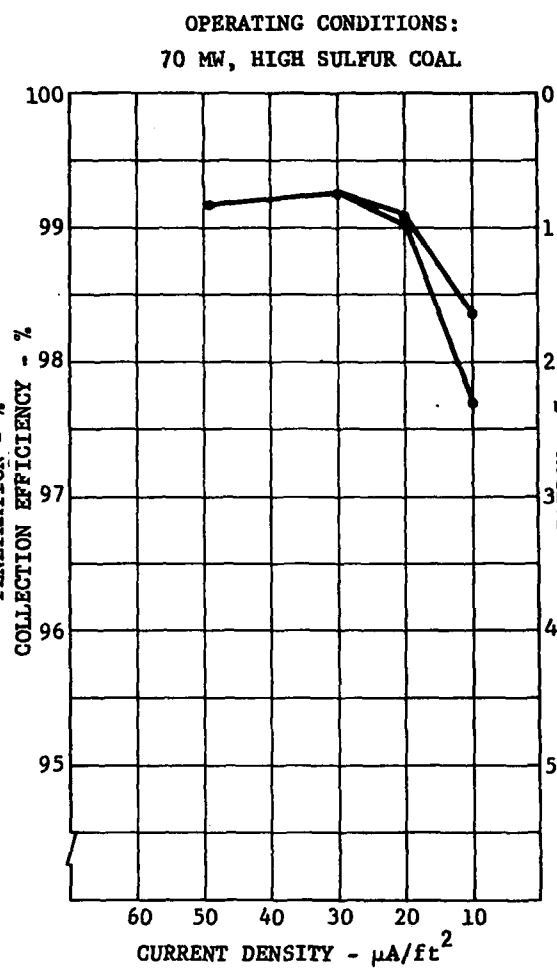


FIGURE 2
ESP EFFICIENCY VS.
CURRENT DENSITY

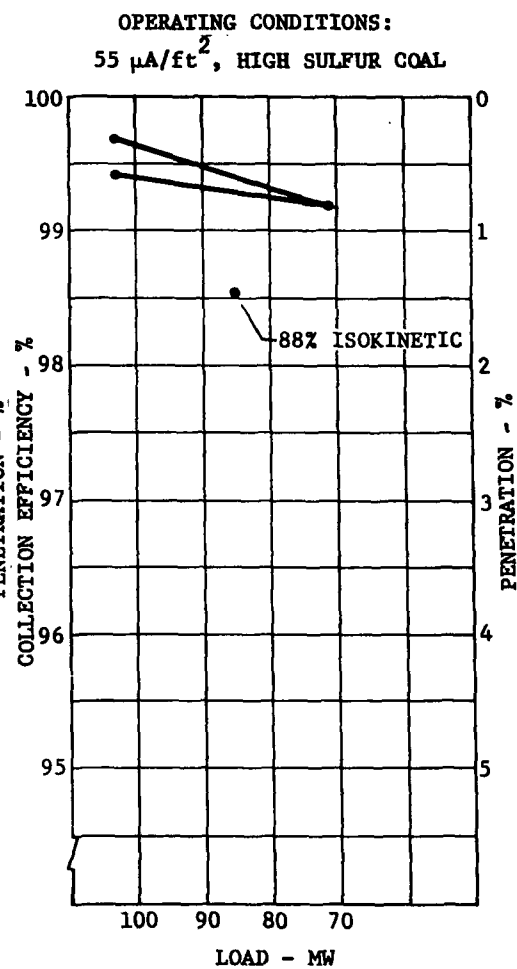


FIGURE 3
ESP EFFICIENCY
VS. LOAD

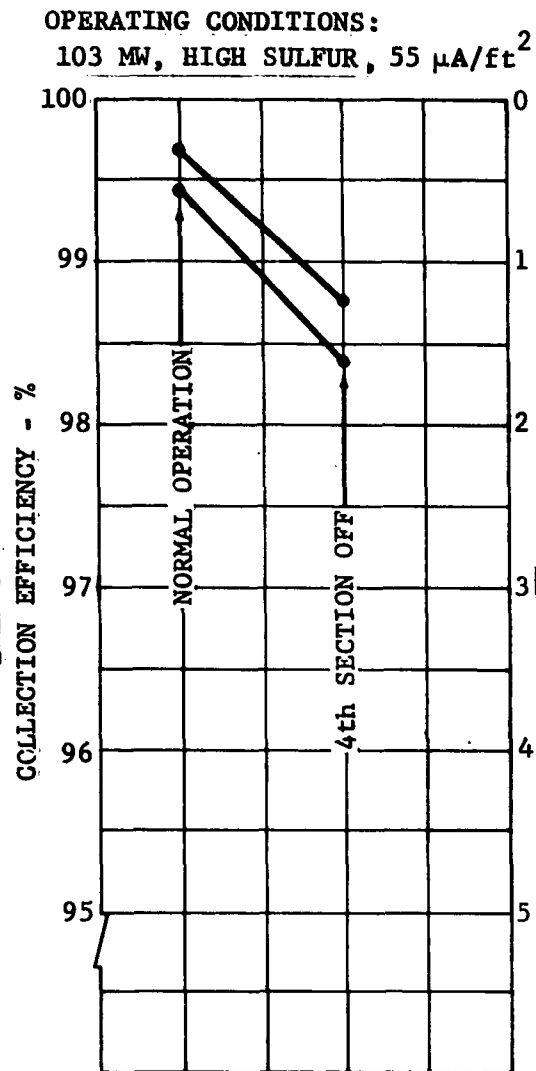


FIGURE 4
ESP EFFICIENCY WITH
4TH SECTION OFF

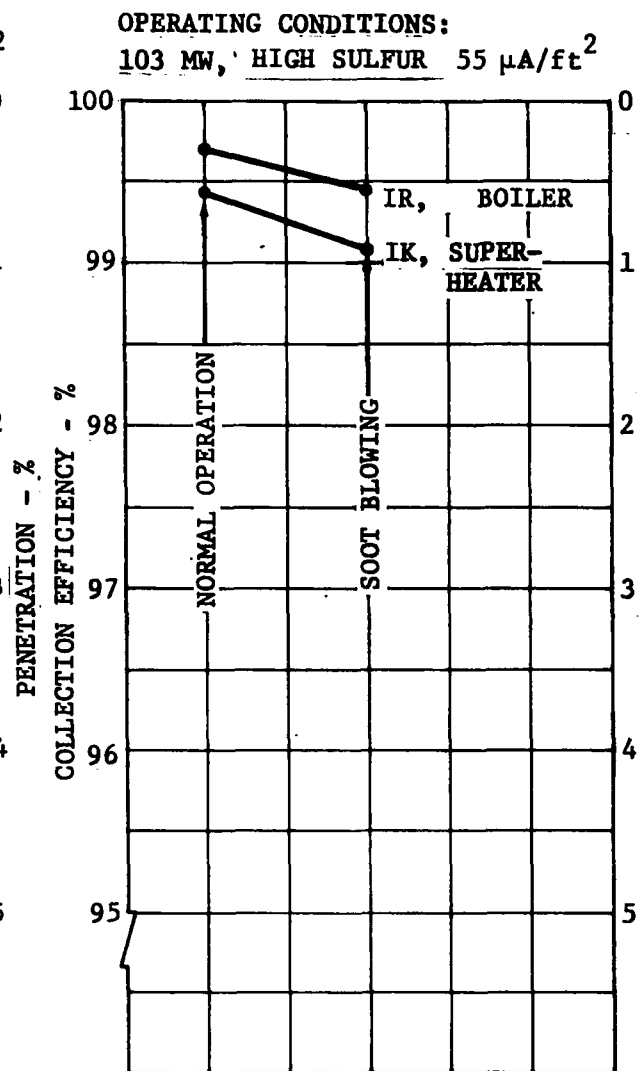


FIGURE 5
ESP EFFICIENCY DURING
SOOT BLOWING

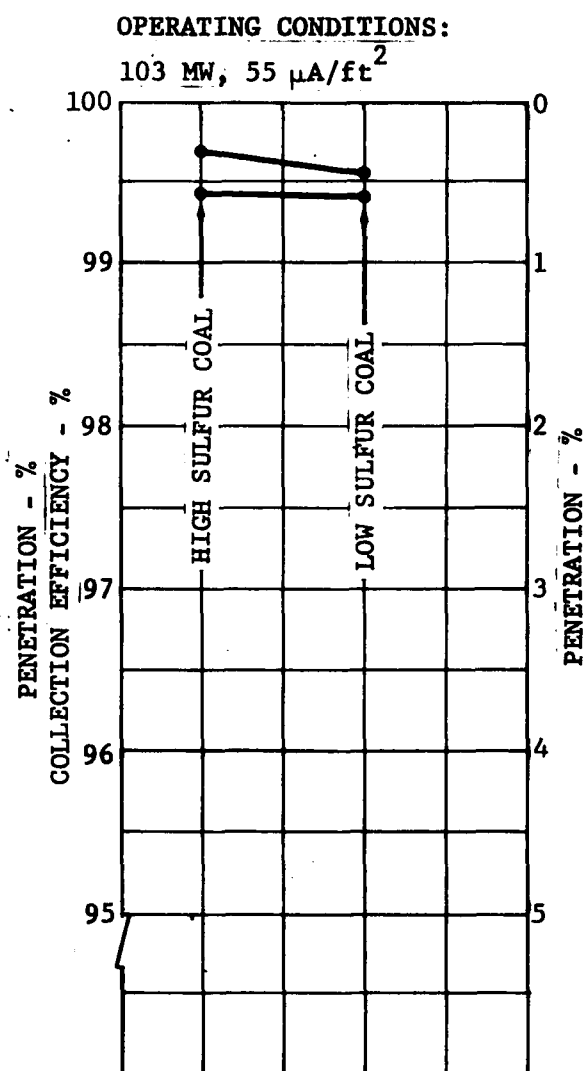


FIGURE 6
ESP EFFICIENCY FOR
LOW SULFUR COAL

Figure 3 demonstrates the slight drop in efficiency at the 70 MW load. The 85 MW load point is not reliable because it was sampled anisokinetically.

Figure 4 shows the effect of shutting off the fourth section of the ESP, which is equivalent to a precipitator approximately ten feet shorter (25 percent of total length). The results indicated a loss in ESP efficiency of approximately 1 percent, with a corresponding tripling of the fly ash penetration.

Figure 5 shows the effect of soot blowing on precipitator efficiency. During the first run, the retractables on the superheater were energized and, during the second run, the wall blowers on the boiler were energized. The wall blowers had no discernible effect on the precipitator efficiency or on the grain loading; however, the retractables dropped the efficiency 0.3 to 0.6 percent and caused approximately a doubling of the fly ash penetration. This may represent a worse than normal case for soot blowing because the blowers were cycled continuously during the sampling.

Figure 6 shows a comparison of the precipitator efficiency for the low-sulfur and high-sulfur coals. The low-sulfur coal, as discussed earlier, was approximately one percent by weight. As can be seen, there was no significant loss in efficiency for the low-sulfur coal. The resistivity measurements showed no significant increase in fly ash resistivity, substantiating the results obtained for efficiency.

PARTICLE SIZE DISTRIBUTION AND FRACTIONAL EFFICIENCY

As shown in Table 4, measurements were performed using cascade impactors, a Climet optical particle counter, and diffusion batteries with CN counters to obtain particle size distributions. For the majority of the tests (see Table 3), the impactor measurements were

performed by MRI and the optical and CN counter measurements by SRI. Impactor measurements on Tests 3 and 4 were repeated because initial results were unsatisfactory. The makeup tests were performed by SRI.

Due to the concentration limits for operating optical counters and CN counters and problems with condensation and coagulation in the sampling lines and diffusion batteries, it is necessary to dry and dilute the sample aerosol before it reaches these areas. Because of the difference in particle concentration at the inlet and outlet of emission control devices, the required dilution factor at the outlet is normally much smaller than at the inlet. During these particular tests, the outlet data were influenced by condensation of H_2SO_4 in the sampling systems. The number of particles counted by the CN counters included macro-molecular droplets of H_2SO_4 , as did the mass accumulated on the outlet impactor stages. There was no evidence that the optical counter data were affected because the H_2SO_4 droplets were far too small ($0.002\ \mu\text{m}$) to be detected optically.

Sufficient data were obtained to permit calculation of lower limits for the fractional efficiencies in the size ranges covered by diffusional methods (CN counting). This was accomplished by assuming that all the particles counted at the outlet were of uniform size and dividing those by the number of particles of that size at the inlet to yield the maximum penetration for that size.

Table 6 and Figure 7 show the fractional efficiency calculated from the optical and diffusional data. The part of the curve calculated using diffusional data (0.01 to $0.15\ \mu\text{m}$ diameter) is a lower limit of efficiency. The efficiency calculated from the optical data (0.4 to $1.5\ \mu\text{m}$ diameter) represents an accurate measure of precipitator performance.

TABLE 6. FRACTIONAL EFFICIENCY FROM SRI DIFFUSIONAL AND OPTICAL DATA*

<u>Test No.</u>	<u>3</u>	<u>4</u>	<u>5</u>	<u>6</u>	<u>7</u>
Date	9/14	9/19	9/20	9/21	9/22
Power Supply Settings	Automatic 4th Section Off	Automatic	20 $\mu\text{A}/\text{ft}^2$	10 $\mu\text{A}/\text{ft}^2$	30 $\mu\text{A}/\text{ft}^2$
<u>Size (μm)**</u>	<u>Efficiency %</u>				
0.015	95	97.9	90	82	98.5
0.037	97.7	99.1	95.5	92.3	99.35
0.078	96.8	98.6	93.5	88	99
0.11	93.2	97.1	87	76	98
0.135	94	97.5	88	78	98.2
0.46	97.8	96.8	96.3	91.3	98.1
0.68	98.8	98.6	98.6	96.2	99.4
1.0	98.7	98.9	99.3	98.2	99.6
1.25	99.2	99.55	99.65	98.8	99.83
1.4	99.75	99.55	99.8	99.4	99.8
1.5	99	99.85	99.7	99.4	99.85

* Operating conditions: 103 MW, high-sulfur coal (3.49% weight average, as received, for tests indicated).

** Efficiency data in the size range 0.01 - 0.15 μm (diffusional data) are lower limits.

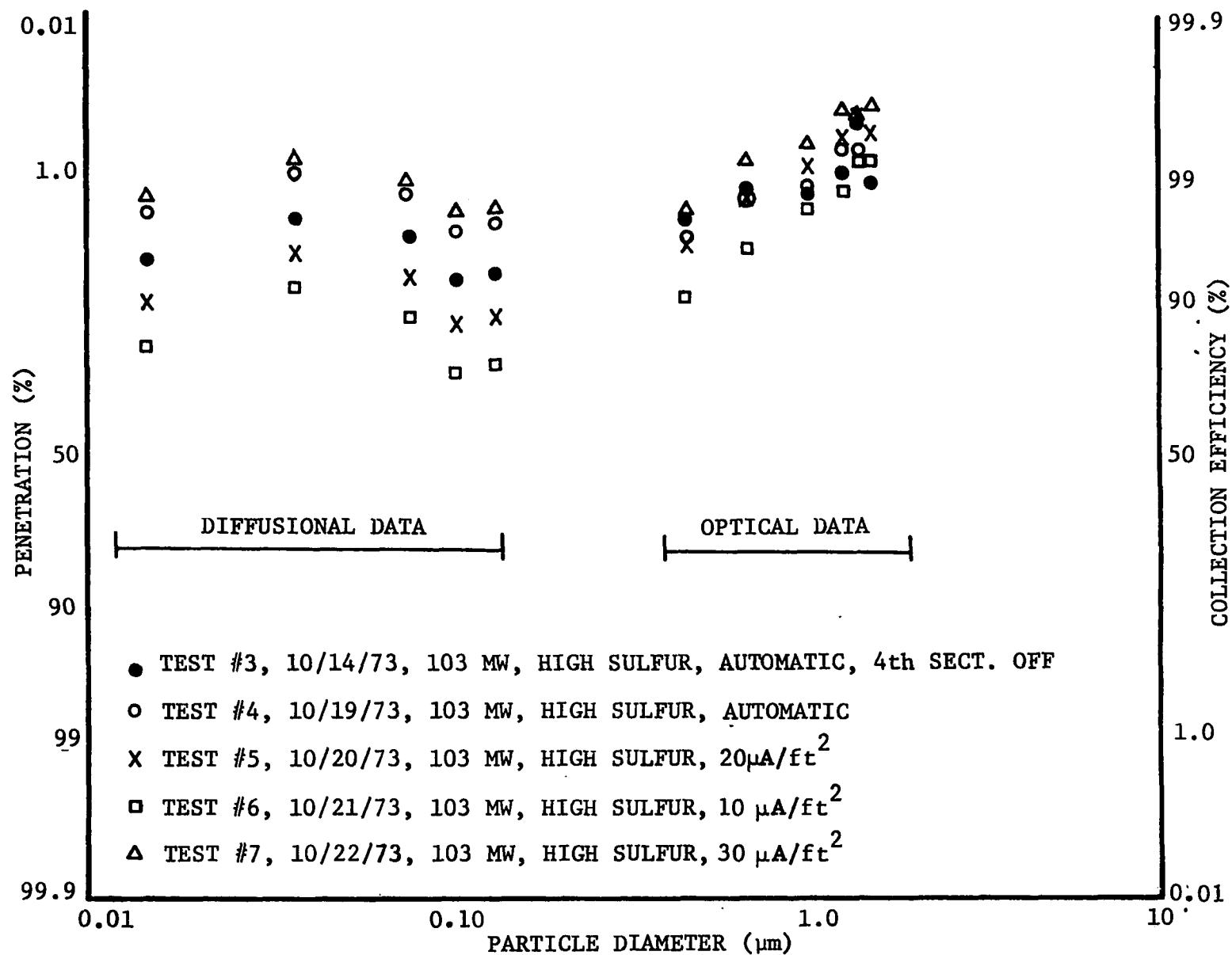


FIGURE 7
FRACTIONAL EFFICIENCIES FOR THE CAT-OX PRECIPITATOR

Precipitator efficiency versus particle size, based on the impactor data obtained by MRI, are shown in Table 7. In general, the efficiencies calculated are lower than would have been expected, verifying SRI's conclusion that the impactor measurements at the precipitator outlet had been contaminated by the presence of H_2SO_4 . However, the mechanism by which the contamination occurred has not been determined. The impactor had been given adequate soaking in the flue gas prior to initiation of sampling to bring the impactor up to flue gas temperature. The flue gas temperature was at approximately 325°F, which is above the dew point for the concentrations of SO_3 measured, indicating that the H_2SO_4 probably did not exist in the duct as a mist.

Figure 8 shows a comparison of the optical data and the impactor data for those tests where both measurements were taken. The optical data show much higher ESP efficiencies for the three current densities at which the precipitator was operated. Assuming that the optical data are accurate, this comparison graphically demonstrates the likely contamination of the impactor data.

The particle size distribution obtained by MRI at the inlet and outlet of the precipitator from the impactors are shown in Figures 9, 10, and 11. The outlet data appear to have been contaminated by H_2SO_4 condensation. The data has been cut off at 5 μm because sampling was not performed isokinetically. The mass distribution at the precipitator inlet for the makeup tests performed by SRI are shown in Figure 12.

IN SITU RESISTIVITY MEASUREMENTS

Both the parallel-disc measurement technique and the electric field-current density technique were used to measure in situ resistivity. The procedures and advantages of these techniques are discussed in

TABLE 7. FRACTIONAL EFFICIENCIES FROM MRI IMPACTOR DATA*

Test No.	Date	Load (MW)	Coal	Plate Current ($\mu\text{A}/\text{ft}^2$)	Particle Diameter, Geometric Mean (μm)**				
					4	2	1	0.8	0.4
5	9/20	103	High sulfur	20	97.05	96.08	91.89	90.03	85.44
6	9/21	103	High sulfur	10	87.91	89.92	85.73	84.44	85.61
7	9/22	103	High sulfur	30	98.89	97.97	96.90	95.80	91.73
9	9/25	85	High sulfur	Automatic	99.61	99.65	99.30	98.93	97.32
10	9/26	70	High sulfur	Automatic	99.04	98.02	96.39	95.11	89.33
11	9/27	70	High sulfur	30	97.96	97.75	94.78	92.67	82.67
12	9/28	70	High sulfur	20	99.28	97.95	97.08	95.71	88.65
13	9/29	70	High sulfur	10	99.24	98.26	94.51	93.14	98.66
14	10/1	103	Low sulfur	Automatic	98.79	98.19	95.79	95.15	94.33

* Data reduction for particle size distribution was performed by EPA.

** Efficiencies generally lower due to contamination of impactor stages by H_2SO_4 condensation.

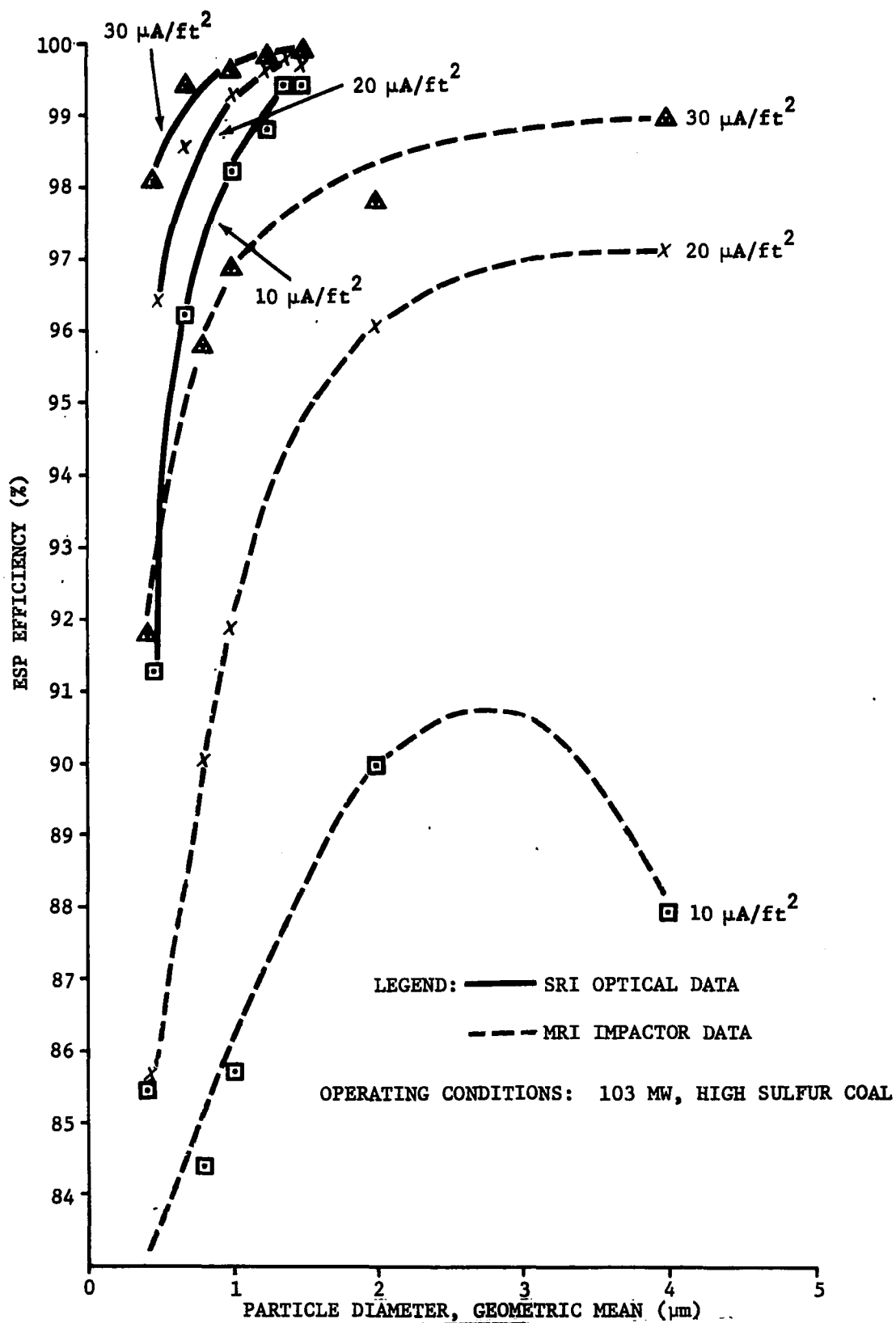


FIGURE 8
COMPARISON OF OPTICAL AND IMPACTOR DATA

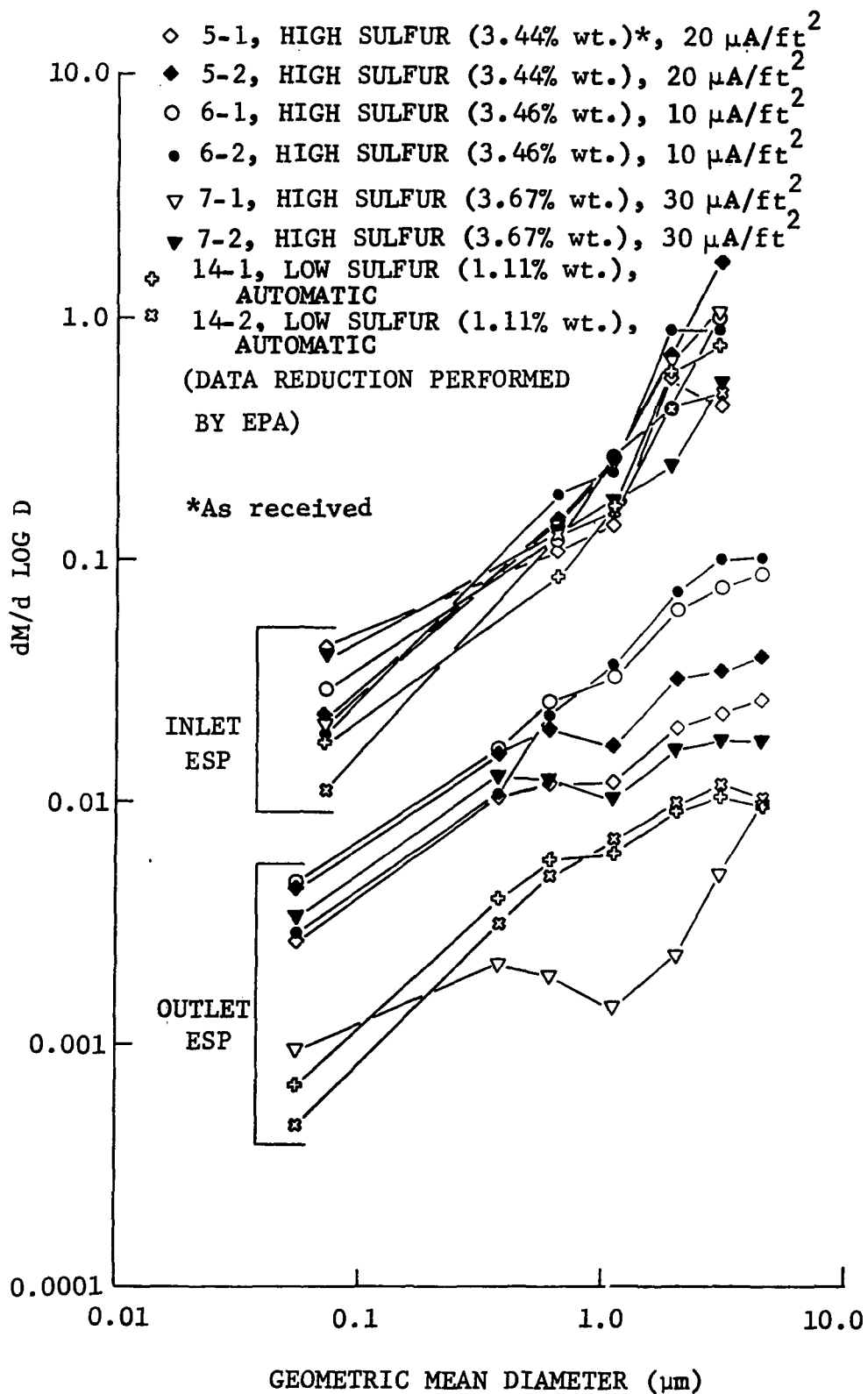


FIGURE 9
 $dM/d \text{ LOG } D$ VERSUS GEOMETRIC MEAN DIAMETER FOR 103 MW LOAD TESTS

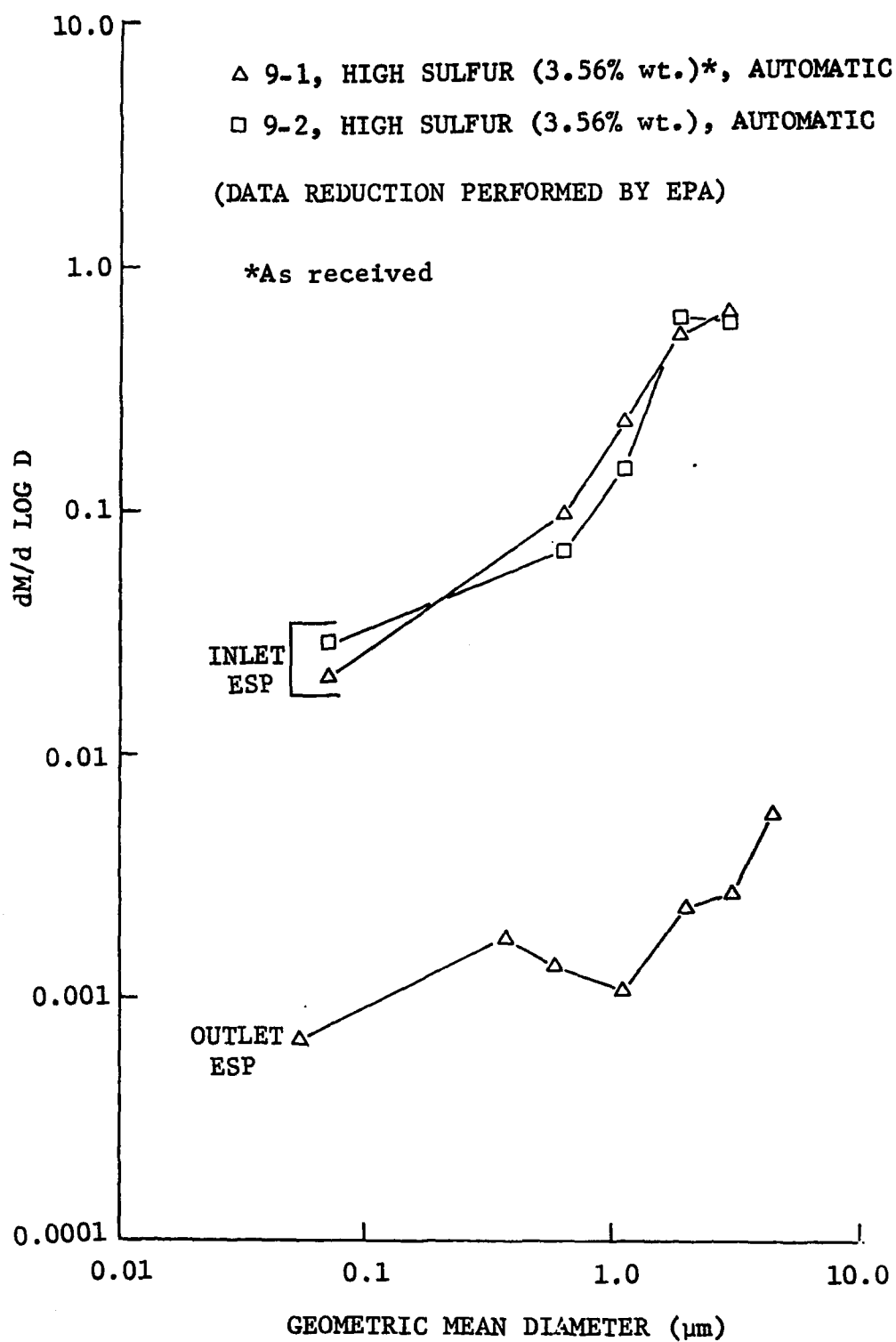


FIGURE 10
 $dM/d \text{ LOG } D$ VERSUS GEOMETRIC MEAN DIAMETER FOR 85 MW LOAD TESTS

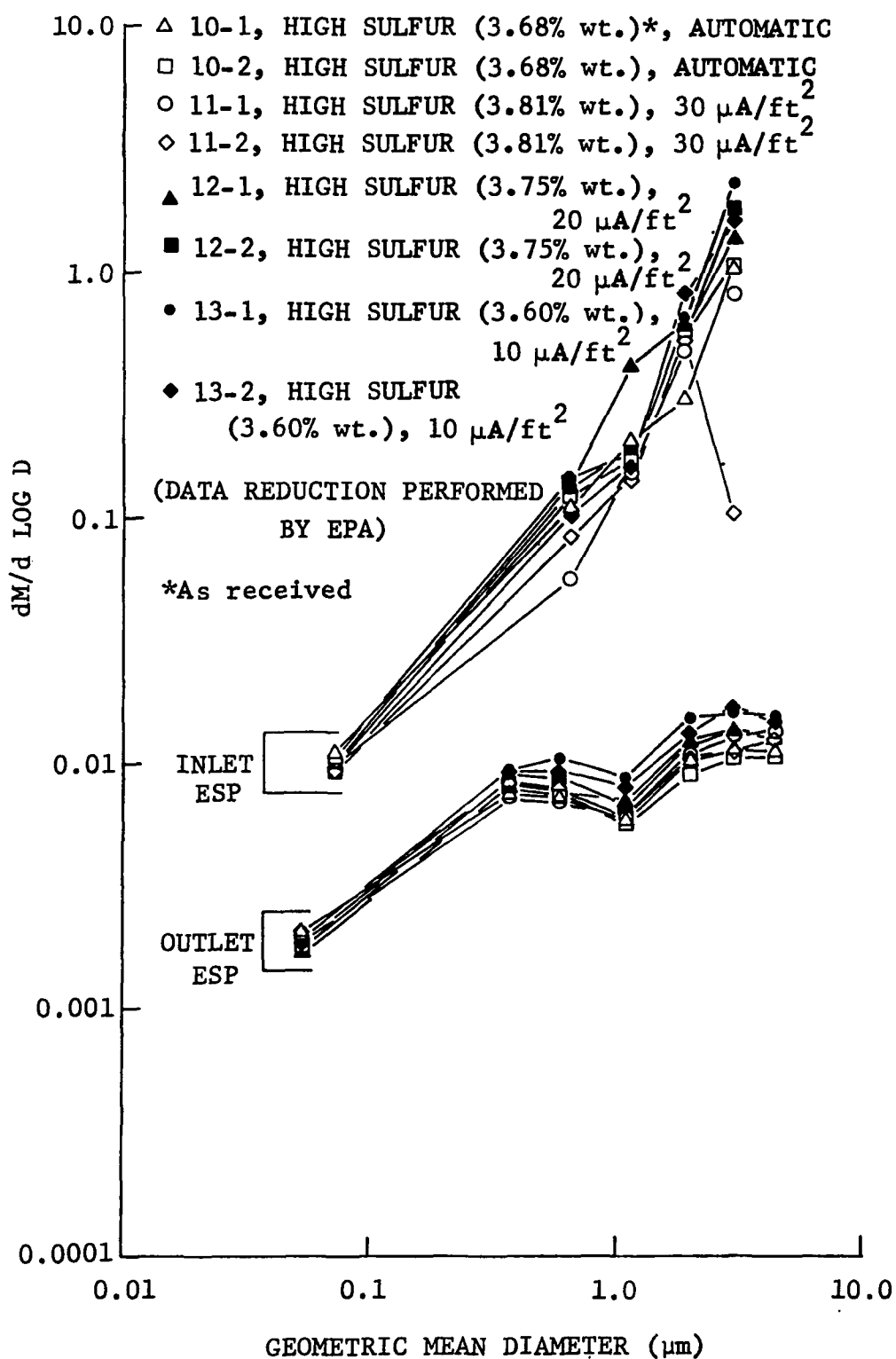


FIGURE 11
 $dM/d \text{ LOG } D$ VERSUS GEOMETRIC MEAN DIAMETER FOR 70 MW LOAD TESTS

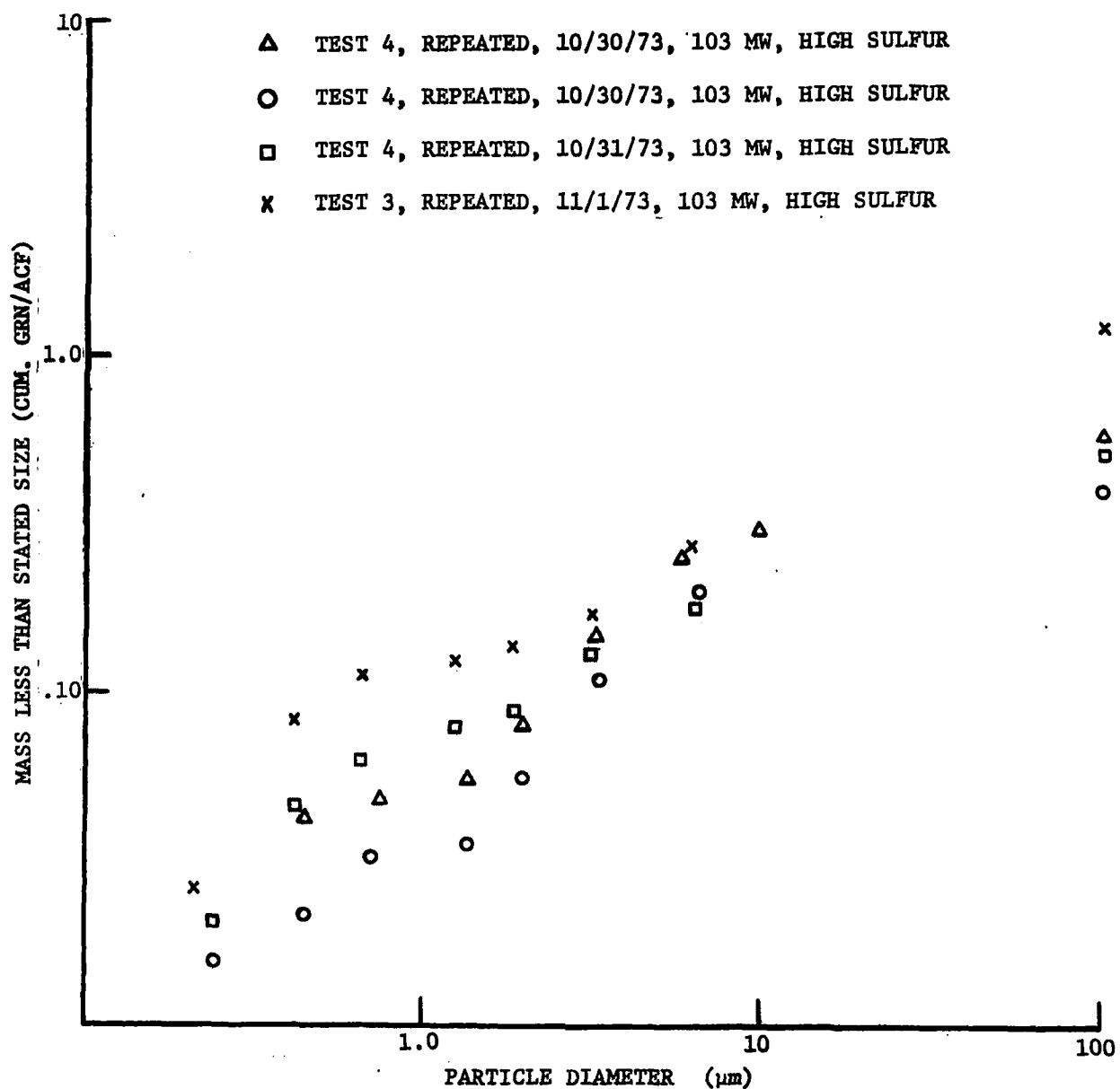


FIGURE 12
INLET MASS DISTRIBUTION CALCULATED FROM CASCADE IMPACTOR DATA

Appendix I. The test conditions at the Cat-Ox[®] precipitator were such that the parallel-disc method did not provide useful data for the high-sulfur coal tests, but did provide good data for the low-sulfur test. Therefore, only the electric field-current density data could be used to compare the resistivities of the high-sulfur and low-sulfur coals. These results are shown in Figure 13 as a function of measurement temperature. Resistivity was only measured during the 103 MW load tests. The results show that the resistivity of the low-sulfur coal was approximately the same as that of the higher sulfur coal. As a result, the low-sulfur coal did not have a significant effect on the precipitator efficiency.

SULFUR TRIOXIDE, SULFUR DIOXIDE, AND WATER VAPOR MEASUREMENTS

Table 8 shows the SO₃ concentrations and mass flow for each test run at both the inlet and outlet of the precipitator. The values in Table 8 that are identified with asterisks are lower in value than the detectable limit of the analytical technique that was employed. In the majority of the cases, the SO₃ concentrations at the outlet of the precipitator were lower than at the input, indicating that the SO₃ was being removed by some mechanism. This is verified by Table 9, which shows the average values of the SO₃ concentrations and mass flow for the 103 MW and 70 MW loads and the high- and low-sulfur coals. All values greater than the detectable limit are averaged. The results show that, on the average, the SO₃ concentrations were two to five times lower at the outlet of the precipitator. Possible speculation is that the SO₃ was removed by absorption on the fly ash.

A comparison of the SO₃ and SO₂ concentrations is shown in Table 10. The SO₂ measurements are discussed further in Appendix II. For the high-sulfur tests, the SO₂ concentrations averaged 2267 ppm and,

for the low-sulfur test, the average SO_2 concentration was 424 ppm. The SO_3 concentration on the average was 0.7 percent of the SO_2 concentration at the ESP inlet and 0.3 percent of the SO_2 concentration at the ESP outlet.

The water vapor measurements for each test using two different techniques are shown in Table 11. MRI used silica gel in a midget impinger to absorb the water vapor as part of the mass sampling train (Method 5, Federal Register, Vol. 36, No. 247, Dec. 1971). The moisture was determined from the change in weight of the impinger and the quantity of gas passed through the impinger. In the technique used by MITRE, the flue gas was pumped through a heated line approximately 100 feet in length to an MSA water vapor analyzer that measured the amount of moisture by spectral photometric absorption with continuous strip chart recording. The MRI measurements average 9.2 percent by volume at the ESP inlet and 8.1 percent by volume at the outlet. MITRE's readings were generally lower, averaging 73 percent of the MRI readings. The reasons for this difference are not understood at this time. However, this was the first use of the MSA instrument by MITRE, so more operational experience is required to determine its accuracy. The MRI measurements using the standard method should be regarded as the reference data.

COAL AND FLY ASH ANALYSIS

The results of the coal analyses for each test are shown in Table 12 on an "as received basis" and in Table 13, on a "dry basis." Both ultimate and proximate analyses were performed. The sulfur content on an "as received basis" averaged 3.58 percent, varying from 3.38 to 3.81 percent for the high-sulfur coal. The corresponding value for the single low-sulfur test was 1.11 percent sulfur by weight. The ash content was 10.64 percent for the high-sulfur coal and 6.45 percent for the single low-sulfur test. The sulfur and

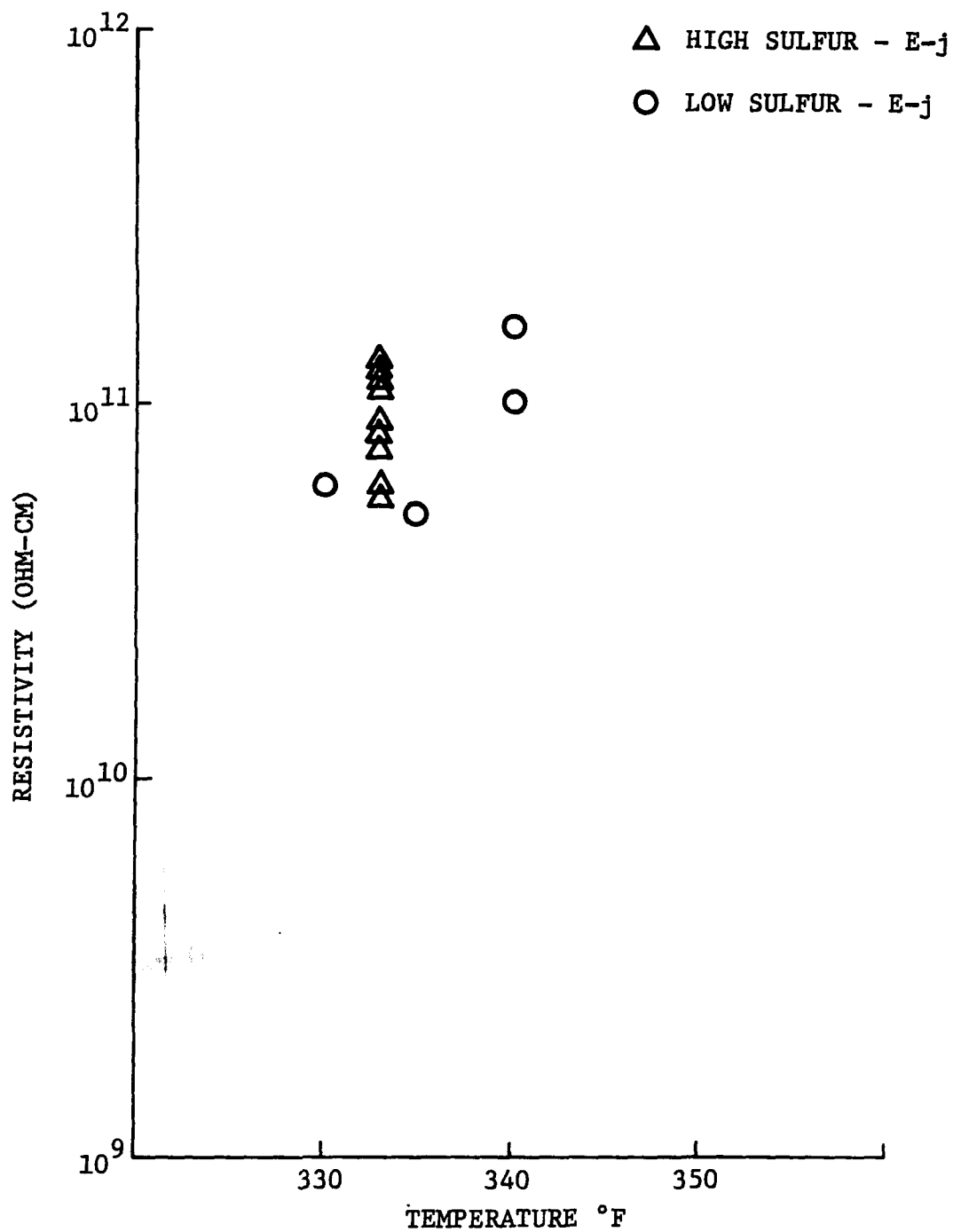


FIGURE 13
RESISTIVITY AS A FUNCTION OF TEMPERATURE BY
THE ELECTRIC FIELD-CURRENT DENSITY METHOD

TABLE 8. MEASURED SO₃ CONCENTRATIONS AND MASS FLOW

TEST NO.	LOCATION	OPERATING CONDITIONS				SO ₃ CONCENTRATION		MASS FLOW (lb/Hr.)
		LOAD	COAL	SPECIAL	PLATE CURRENT	(PPM)	(lb/DSCF)	
2-1	INLET	103	HIGH SULFUR	SOOT BLOWING	AUTOMATIC	9.1	1.89×10^{-6}	29.27
	OUTLET			RETRACTABLES		5.0*	1.02×10^{-6} *	17.72 *
2-2	INLET	103	HIGH SULFUR	WALL BLOWERS	AUTOMATIC	--	--	--
	OUTLET					5.1*	1.05×10^{-6} *	18.14 *
3-1	INLET	103	HIGH SULFUR	4th SECTION OFF	AUTOMATIC	27.9	5.78×10^{-6}	92.88
	OUTLET					5.6	1.16×10^{-6}	20.25
3-2	INLET	103	HIGH SULFUR	4th SECTION OFF	AUTOMATIC	47.7	9.86×10^{-6}	160.08
	OUTLET					3.5	$.71 \times 10^{-6}$	12.61
4-1	INLET	103	HIGH SULFUR	--	AUTOMATIC	21.1	4.36×10^{-6}	69.27
	OUTLET					8.1	1.68×10^{-6}	29.21
4-2	INLET	103	HIGH SULFUR	--	AUTOMATIC	15.8	3.27×10^{-6}	51.75
	OUTLET					.9	$.19 \times 10^{-6}$	3.91
5-1	INLET	103	HIGH SULFUR	--	20 $\mu\text{A}/\text{ft}^2$	2.9	$.59 \times 10^{-6}$	9.91
	OUTLET					15.4	3.18×10^{-6}	55.97
5-2	INLET	103	HIGH SULFUR	--	20 $\mu\text{A}/\text{ft}^2$	6.0	1.24×10^{-6}	20.31
	OUTLET					5.9*	1.23×10^{-6} *	21.90 *
6-1	INLET	103	HIGH SULFUR	--	10 $\mu\text{A}/\text{ft}^2$	9.8	2.02×10^{-6}	31.69
	OUTLET					23.7	4.89×10^{-6}	87.76
6-2	INLET	103	HIGH SULFUR	--	10 $\mu\text{A}/\text{ft}^2$	13.0	2.70×10^{-6}	44.40
	OUTLET					1.7	$.35 \times 10^{-6}$	6.47
7-1	INLET	103	HIGH SULFUR	--	30 $\mu\text{A}/\text{ft}^2$	17.9	3.69×10^{-6}	57.24
	OUTLET					6.8*	1.4×10^{-6} *	25.79 *
7-2	INLET	103	HIGH SULFUR	--	30 $\mu\text{A}/\text{ft}^2$	10.7	2.21×10^{-6}	34.40
	OUTLET					5.3	1.09×10^{-6}	20.51
9-1	INLET	85	HIGH SULFUR	--	AUTOMATIC	5.9*	1.21×10^{-6} *	15.60 *
	OUTLET					4.7	$.98 \times 10^{-6}$	12.63
9-2	INLET	85	HIGH SULFUR	--	AUTOMATIC	4.7	$.97 \times 10^{-6}$	12.80
	OUTLET					6.4*	1.31×10^{-6} *	19.83 *
10-1	INLET	70	HIGH SULFUR	--	AUTOMATIC	5.9*	1.23×10^{-6} *	13.51 *
	OUTLET					5.1*	1.05×10^{-6} *	11.27 *
10-2	INLET	70	HIGH SULFUR	--	AUTOMATIC	25.1	5.18×10^{-6}	57.46
	OUTLET					1.6	$.33 \times 10^{-6}$	3.63
11-1	INLET	70	HIGH SULFUR	--	30 $\mu\text{A}/\text{ft}^2$	18.5	3.83×10^{-6}	39.12
	OUTLET					6.1	1.26×10^{-6}	14.82
11-2	INLET	70	HIGH SULFUR	--	30 $\mu\text{A}/\text{ft}^2$	5.0	1.04×10^{-6}	10.86
	OUTLET					5.8*	1.20×10^{-6} *	13.92 *
12-1	INLET	70	HIGH SULFUR	--	20 $\mu\text{A}/\text{ft}^2$	21.5	4.44×10^{-6}	49.73
	OUTLET					1.8	$.38 \times 10^{-6}$	4.44
12-2	INLET	70	HIGH SULFUR	--	20 $\mu\text{A}/\text{ft}^2$	8.7	1.81×10^{-6}	20.05
	OUTLET					5.6	1.16×10^{-6} *	13.11 *
13-1	INLET	70	HIGH SULFUR	--	10 $\mu\text{A}/\text{ft}^2$	19.5	4.04×10^{-6}	44.42
	OUTLET					1.9	$.38 \times 10^{-6}$	4.37
13-2	INLET	70	HIGH SULFUR	--	10 $\mu\text{A}/\text{ft}^2$	7.8*	1.61×10^{-6} *	16.80 *
	OUTLET					1.4	$.28 \times 10^{-6}$	3.37
14-1	INLET	103	LOW SULFUR	--	AUTOMATIC	4.4*	$.90 \times 10^{-6}$ *	14.01
	OUTLET					5.4*	1.12×10^{-6} *	19.65 *
14-2	INLET	103	LOW SULFUR	--	AUTOMATIC	9.3	1.93×10^{-6}	30.59
	OUTLET					2.9	$.60 \times 10^{-6}$	10.61

NOTE:

*At detectable limit of analytical method.

TABLE 9. AVERAGE SO₃ CONCENTRATIONS AND MASS FLOW

LOAD	COAL	LOCATION	SO ₃ CONCENTRATION		SO ₃ MASS FLOW (lb/Hr.)
			(PPM)	(lb/DSCF)	
103	HIGH SULFUR	INLET	16.5	3.4×10^{-6}	54.7
		OUTLET	8.0	1.7×10^{-6}	29.5
103	LOW SULFUR	INLET	9.3	1.9×10^{-6}	30.6
		OUTLET	2.9	0.6×10^{-6}	10.6
70	HIGH SULFUR	INLET	14.7	3.4×10^{-6}	36.9
		OUTLET	2.9	0.5×10^{-6}	6.1

TABLE 10. COMPARISON OF SO ₃ AND SO ₂ CONCENTRATIONS				
TEST NO.	LOCATION	SO ₃ CONCENTRATION (PPM)	SO ₂ CONCENTRATION (PPM)	SO ₃ /SO ₂ (Percent)
2-1	INLET	9.1	2405	0.4
	OUTLET	5.0*	—	—
2-2	INLET	—	2280	—
	OUTLET	5.1*	—	—
3-1	INLET	27.9	2229	1.3
	OUTLET	5.6	—	—
3-2	INLET	47.7	2235	2.1
	OUTLET	3.5	—	—
4-1	INLET	21.1	2310	0.9
	OUTLET	8.1	2274	0.4
4-2	INLET	15.8	2235	0.7
	OUTLET	0.9	2235	0.0
5-1	INLET	2.9	2190	0.1
	OUTLET	15.4	2220	0.7
5-2	INLET	6.0	2025	0.3
	OUTLET	5.9*	2138	—
6-1	INLET	9.8	2190	0.5
	OUTLET	23.7	2190	1.1
6-2	INLET	13.0	2175	0.6
	OUTLET	1.7	2280	0.1
7-1	INLET	17.9	2250	0.8
	OUTLET	6.8*	2250	—
7-2	INLET	10.7	2235	0.5
	OUTLET	5.3	2235	0.2
9-1	INLET	5.9*	2280	—
	OUTLET	4.7	2235	0.2
9-2	INLET	4.7	2295	0.2
	OUTLET	6.4*	2295	—
10-1	INLET	5.9*	2265	—
	OUTLET	5.1*	2325	—
10-2	INLET	25.1	2305	1.1
	OUTLET	1.6	2325	0.1
11-1	INLET	18.5	2370	0.8
	OUTLET	6.1	2385	0.3
11-2	INLET	5.0	2400	0.2
	OUTLET	5.8*	—	—
12-1	INLET	21.5	2400	0.9
	OUTLET	1.8	2355	0.1
12-2	INLET	8.7	2400	0.4
	OUTLET	5.6*	2400	—
13-1	INLET	19.5	—	—
	OUTLET	1.9	2250	0.1
13-2	INLET	7.8*	2115	—
	OUTLET	1.4	2175	0.1
14-1	INLET	4.4*	—	—
	OUTLET	5.4*	458	—
14-2	INLET	9.3	390	2.4
	OUTLET	2.9	—	—

TABLE 11. WATER VAPOR MEASUREMENTS				
TEST NO.	LOCATION	H ₂ O VAPOR		COMPARISON MITRE/MRI
		MRI (% Vol.)	MITRE (% Vol.)	
2-1	INLET	12.4	--	--
	OUTLET	7.9	--	--
2-2	INLET	10.5	--	--
	OUTLET	8.0	--	--
3-1	INLET	8.1	--	--
	OUTLET	8.4	--	--
3-2	INLET	8.6	--	--
	OUTLET	8.1	--	--
4-1	INLET	7.9	--	--
	OUTLET	8.1	--	--
4-2	INLET	9.1	--	--
	OUTLET	8.4	--	--
5-1	INLET	8.3	--	--
	OUTLET	8.8	--	--
5-2	INLET	8.7	--	--
	OUTLET	9.5	--	--
6-1	INLET	8.3	--	--
	OUTLET	6.5	5.1	0.78
6-2	INLET	8.7	5.0	0.57
	OUTLET	6.0	5.5	0.91
7-1	INLET	10.1	5.6	0.60
	OUTLET	6.4	--	--
7-2	INLET	13.1	5.2	0.39
	OUTLET	3.4	5.6	1.64
9-1	INLET	9.6	5.3	0.55
	OUTLET	--	6.8	--
9-2	INLET	6.7	--	--
	OUTLET	7.8	5.8	0.74
10-1	INLET	6.7	4.9	0.73
	OUTLET	9.5	5.1	0.53
10-2	INLET	5.4	6.5	1.20
	OUTLET	9.0	6.1	0.67
11-1	INLET	10.6	6.3	0.59
	OUTLET	10.0	6.6	0.66
11-2	INLET	11.0	6.1	0.55
	OUTLET	9.4	5.7	0.60
12-1	INLET	9.3	6.5	0.69
	OUTLET	8.8	6.5	0.73
12-2	INLET	9.3	6.8	0.73
	OUTLET	9.2	6.9	0.75
13-1	INLET	10.0	--	--
	OUTLET	7.4	7.2	0.97
13-2	INLET	10.0	6.6	0.66
	OUTLET	8.2	--	--
14-1	INLET	8.8	6.1	0.69
	OUTLET	8.8	5.3	0.60
14-2	INLET	9.1	6.4	0.70
	OUTLET	8.6	6.8	0.79
AVERAGE	INLET	9.2	5.9	0.73
	OUTLET	8.1	6.1	

TABLE 12. PROXIMATE AND ULTIMATE ANALYSIS OF COAL - AS RECEIVED BASIS

Test Number	ULTIMATE ANALYSIS					PROXIMATE ANALYSIS				
	Carbon (% Wt.)	Hydrogen (% Wt.)	Nitrogen (% Wt.)	Sulfur (% Wt.)	Oxygen (% Wt.)	Moisture (% Wt.)	Ash (% Wt.)	Volatile Matter (% Wt.)	Fixed Carbon (% Wt.)	Heat of Combustion (Btu/lb)
2	66.23	5.12	0.99	3.54	13.26	3.62	10.86	37.56	47.96	12,114
3	67.96	4.67	1.06	3.48	12.76	3.65	10.07	37.86	48.42	12,096
4	66.90	5.24	1.02	3.38	12.32	3.69	11.14	37.73	47.44	12,113
5	66.36	5.04	1.03	3.44	13.03	3.77	11.10	37.54	47.59	12,006
6	66.83	5.18	1.02	3.46	12.95	4.02	10.56	37.84	47.58	12,077
7	66.24	5.19	1.09	3.67	13.34	4.21	10.47	38.20	47.12	12,136
8	66.11	5.13	0.99	3.62	12.76	3.61	11.39	37.49	47.51	11,991
9	66.84	5.21	0.95	3.56	13.13	4.10	10.31	38.35	47.24	12,088
10	66.87	5.26	0.99	3.68	12.83	3.60	10.37	38.19	47.84	12,202
11	67.05	5.26	0.89	3.81	12.59	3.61	10.40	38.01	47.98	12,211
12	66.54	5.23	0.99	3.75	12.59	3.50	10.90	37.82	47.78	12,065
13	67.05	5.11	1.00	3.60	12.84	3.55	10.40	37.91	48.14	12,210
14	72.71	5.48	1.21	1.11	13.04	4.19	6.45	34.48	54.88	12,813
15	67.25	5.16	0.99	3.51	12.73	3.65	10.36	38.06	47.93	12,066

Average High Sulfur = 3.58% by weight

Average High Sulfur Ash = 10.64% by weight

TABLE 13. PROXIMATE AND ULTIMATE ANALYSIS OF COAL - DRY BASIS

Test Number	ULTIMATE ANALYSIS					PROXIMATE ANALYSIS			
	Carbon (% Wt.)	Hydrogen (% Wt.)	Nitrogen (% Wt.)	Sulfur (% Wt.)	Oxygen (% Wt.)	Ash (% Wt.)	Volatile Matter (% Wt.)	Fixed Carbon (% Wt.)	Heat of Combustion (Btu/lb)
2	68.72	4.90	1.03	3.67	10.41	11.27	38.97	49.76	12,569
3	70.53	4.43	1.10	3.61	9.88	10.45	39.29	50.26	12,554
4	69.46	5.02	1.06	3.51	9.38	11.57	39.18	49.25	12,577
5	68.96	4.80	1.07	3.57	10.05	11.55	39.01	49.44	12,476
6	69.63	4.93	1.06	3.60	9.78	11.00	39.42	49.58	12,583
7	69.15	4.93	1.14	3.83	10.02	10.93	39.88	49.19	12,669
8	68.59	4.91	1.03	3.76	9.89	11.82	38.89	49.29	12,440
9	69.70	4.96	0.99	3.71	9.89	10.75	39.99	49.26	12,605
10	69.37	5.04	1.03	3.82	9.98	10.76	39.62	49.62	12,658
11	69.56	5.04	0.92	3.95	9.74	10.79	39.43	49.78	12,668
12	68.95	5.02	1.03	3.89	9.81	11.30	39.19	49.51	12,502
13	69.52	4.89	1.04	3.73	10.04	10.78	39.31	49.91	12,659
14	75.89	5.23	1.26	1.16	9.73	6.73	35.99	57.28	13,373
15	69.80	4.93	1.03	3.64	9.85	10.75	39.50	49.75	12,523

Average High Sulfur = 3.72% by weight

Average High Sulfur Ash = 11.06% by weight

ash content on a "dry basis" were approximately four percent higher than on the "as received basis," in accordance with the moisture content of the coal.

The chemical content of the fly ash for certain critical elements and for total sulfates for samples collected at the ESP inlet are shown in Table 14. The fly ash consisted of three components from the sampling train: (1) the dry catch in the cyclone, (2) the fly ash collected on the fibreglass filter, from which it was carefully removed for analysis; and (3) the acetone rinse of the sampling probe. The sampling probe, the cyclone, and the filter were heated to approximately 350 F. The total sulfate content was determined to average 3.8 percent for the high-sulfur coal tests and 1.7 percent for the single low-sulfur coal test.

TABLE 14. CHEMICAL CONTENT OF FLY-ASH SAMPLED AT ESP INLET

Test Number	C (% Wt)	H (% Wt)	N (% Wt)	Al (% Wt)	Ca (% Wt)	Fe (% Wt)	Li (% Wt)	Mg (% Wt)	K (% Wt)	Si (% Wt)	Na (% Wt)	Sulfate (% Wt)
2	2.76	0.39	0	6.7	1.73	9.0	0.0071	0.045	1.22	11.6	0.29	3.2
3	2.21	0.12	0	6.5	1.76	8.3	0.0071	0.029	0.99	11.4	0.39	1.7
4	1.63	0.70	0	6.4	1.90	8.2	0.0077	0.038	1.22	12.0	0.52	2.8
5	1.28	0.51	0	8.2	2.46	7.9	0.0074	0.062	1.29	12.6	0.48	2.8
6	3.09	0.36	0	8.2	2.29	8.0	0.0063	0.052	1.21	12.7	0.39	3.7
7	1.14	0.40	0	10.4	0.58	8.1	-----	0.049	1.15	15.1	0.65	---
9	1.94	0.60	0	8.4	2.15	9.5	0.0070	0.053	1.36	13.6	0.42	3.0
10	2.20	0.70	0	8.5	2.23	9.7	0.0075	0.058	1.44	13.1	0.41	5.2
11	1.06	0.46	0	6.6	1.80	9.3	0.0074	0.043	1.13	12.2	0.37	3.7
12	0.75	0.61	0	6.8	1.72	9.6	0.0068	0.046	1.30	13.5	0.37	4.6
13	1.50	0.35	0	7.9	1.82	9.0	0.0054	0.043	1.19	12.9	0.29	7.1
14	3.74	0.47	0	9.5	1.42	4.7	0.0086	0.041	1.37	12.6	0.27	1.7

COMPARISON OF RESULTS OF COMPUTER SIMULATION

The SRI ESP computer systems model was utilized to project the variation in efficiency expected for a variation in volume flow rate. The results of the computer simulation with the experimental data superimposed are shown in Figure 14 for the four levels of current density employed in the test program. The computer simulation curves are based on the Deutsch exponential collection efficiency equation, which has been substantiated experimentally for ideal operating conditions. The field measured data for the $10 \mu\text{A}/\text{ft}^2$ current density approximates the theoretical curve; however, as the current density is increased, the field measured data systematically deviate from the theoretical curves such that the efficiencies at the larger gas volume flow rates become higher than at the smaller gas volume flow rates. The implication is that the computer simulation program does not account for some of the phenomena that can cause slight changes in efficiency at the high levels of performance being obtained. These phenomena are complex and may possibly be related to the effect of ion density on the electric field, diffusion charging, and non-uniform gas flow.

The computer model does not include factors to account for particle re-entrainment. Therefore, the model is primarily useful for extrapolating the gross behavior of precipitators, rather than the absolute efficiency of a particular ESP unit. The result of neglecting re-entrainment primarily influences the computed versus measured performance in the particle sizes greater than $1 \mu\text{m}$. Therefore, the computer simulation for 10, 20, and 30 microamperes per square foot was run for size-fractional efficiencies in this range. The results of this simulation are shown, together with the size-fractional efficiency as determined by measurement, in Figures 15, 16, and 17. The break in the predicted simulation curve results from the unavailability of a suitable theory to explain the transition from the region where field charging dominates to the region where diffusional

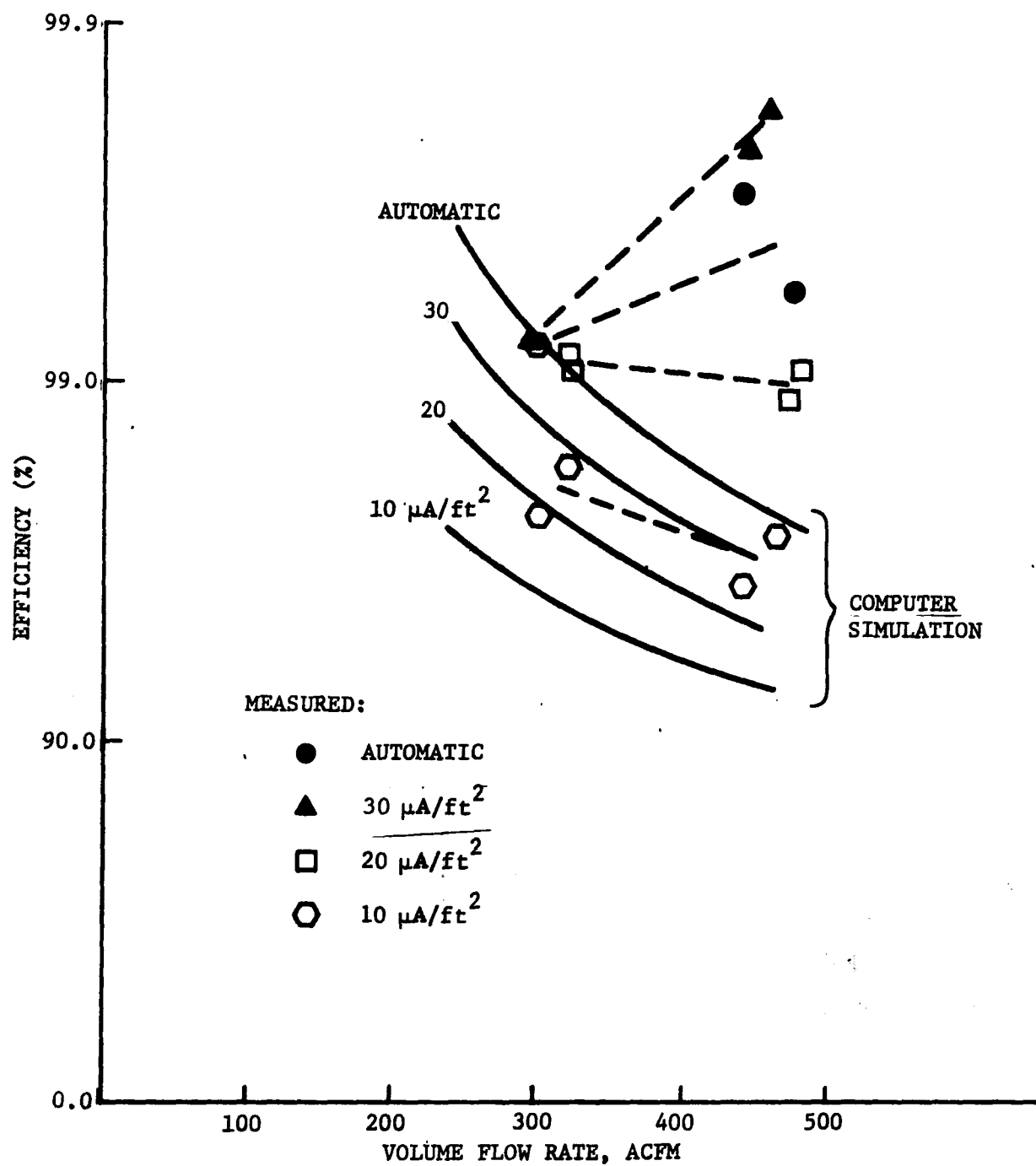


FIGURE 14
COMPARISON OF COMPUTER SIMULATED AND MEASURED ESP EFFICIENCIES

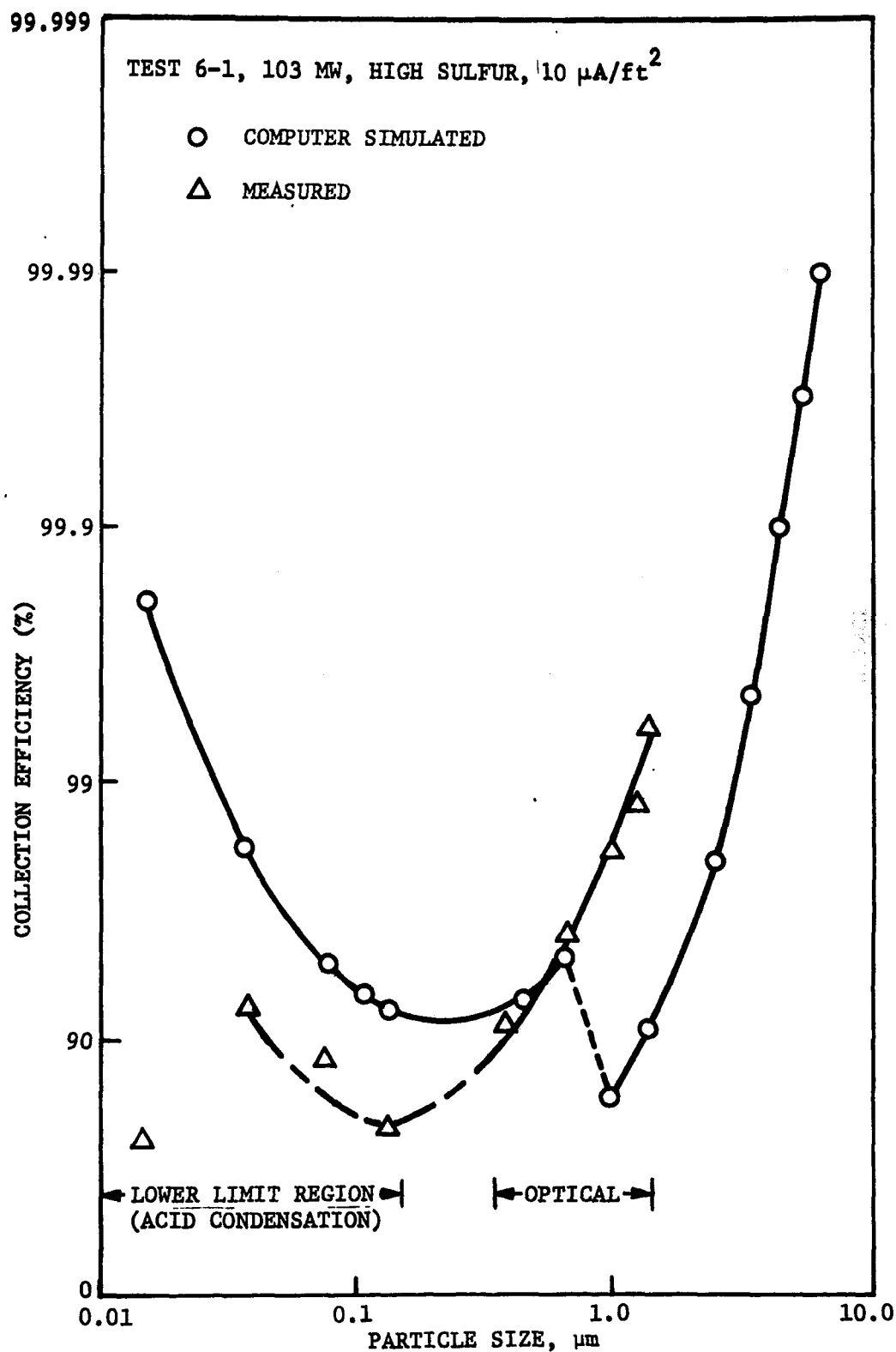


FIGURE 15
COMPARISON OF COMPUTED AND MEASURED SIZE FRACTIONAL EFFICIENCIES
FOR 10 MICROAMPERES PER SQUARE FOOT CURRENT DENSITY

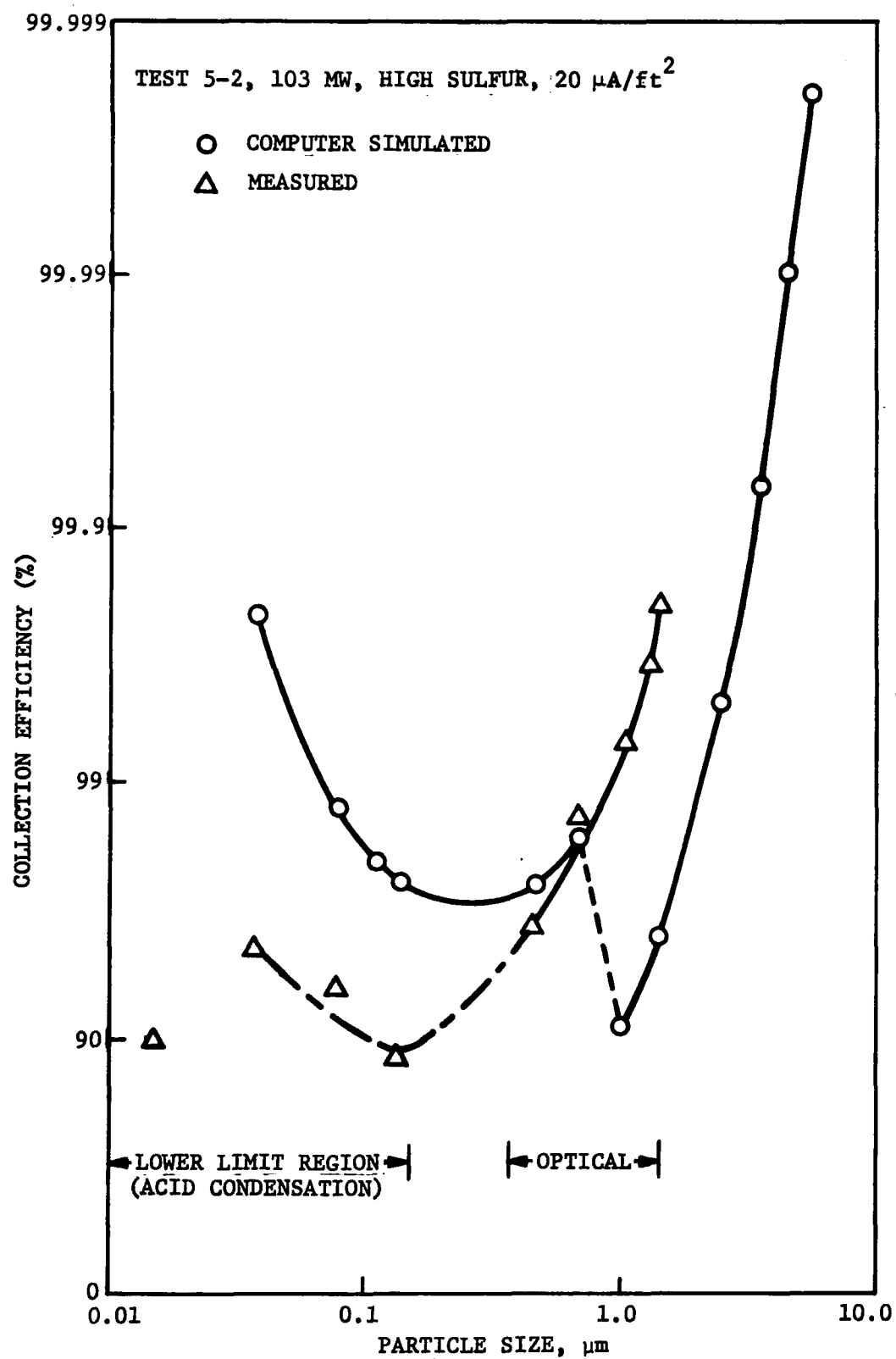


FIGURE 16
COMPARISON OF COMPUTED AND MEASURED SIZE FRACTIONAL EFFICIENCIES
FOR 20 MICROAMPERES PER SQUARE FOOT CURRENT DENSITY

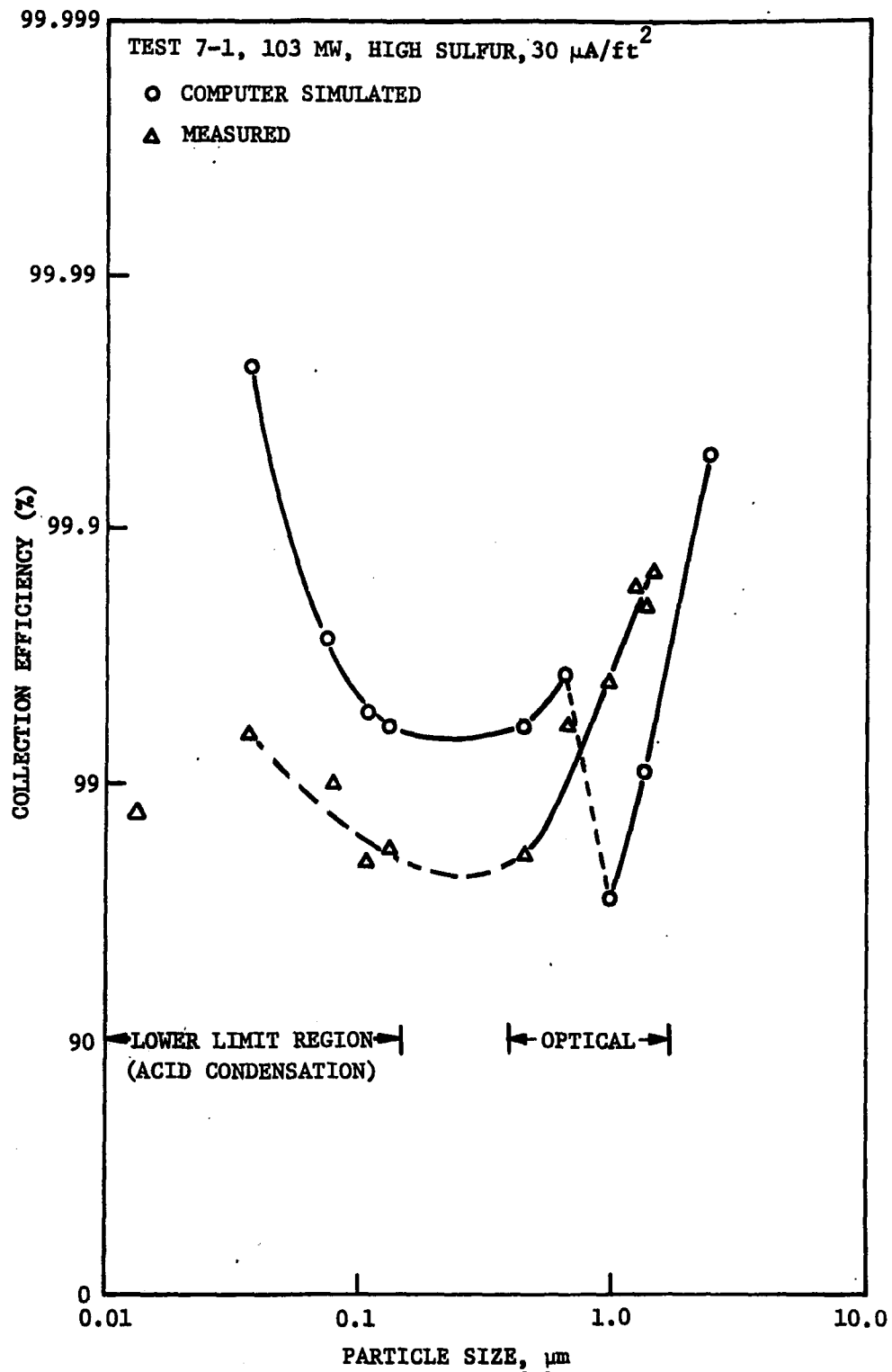


FIGURE 17
COMPARISON OF COMPUTED AND MEASURED SIZE FRACTIONAL
EFFICIENCIES FOR 30 MICROAMPERES PER SQUARE FOOT
CURRENT DENSITY

charging dominates. In the lower limit region of the measured data, the experimental points represent the lowest possible level of efficiency. Consequently, the measured data in this region are not a true measure of the efficiency and have been connected to the optically measured data to show, in general, that the form of the curve agrees with theory.

APPENDIX I

CATALYTIC OXIDATION PRECIPITATOR PERFORMANCE
AT THE WOOD RIVER POWER STATION

Final Report
to
THE MITRE CORPORATION
McLean, Virginia

SOUTHERN RESEARCH INSTITUTE
2000 Ninth Avenue South
Birmingham, Alabama 35205
May 14, 1974

SORI-EAS-74-009
3155-IF-A

PROGRAM SCOPE

This report describes the results of a test program conducted jointly with The MITRE Corporation, Midwest Research Institute, and The Southern Research Institute to evaluate the performance of an electrostatic precipitator that removes fly ash from the flue gas prior to entering the Cat-Ox[®] process for removal of sulfur dioxide. The Southern Research Institute conducted the particle size distribution tests in the submicron size range, rechecked the supermicron particle size distribution with impactors at one test condition, conducted resistivity tests, and measured the precipitator secondary voltage and current characteristics. SRI also utilized the precipitator computer systems model to predict the precipitator performance based on the inlet particle size distribution and the electrical conditions determined for the installed precipitator. Midwest Research and MITRE conducted the remainder of the tests.

TEST RESULTS

The results of the SRI tests are discussed individually in the following sections of this report, together with a short discussion of the test procedures.

PARTICLE SIZE DISTRIBUTION MEASUREMENTS

Tests were performed, using cascade impactors, a Climet optical particle counter, and diffusion batteries with condensation nuclei (CN) counters, to measure particle size distributions and fractional efficiencies at different precipitator operating conditions.

A Brink six-stage impactor with precollector cyclone and backup filter was used to measure mass distributions at the inlet. Greased, prebaked foils were used as impaction substrates. An Andersen Model III stack sampler with backup filter was used at the outlet. Glass fiber "bullseye" substrates were used with the Andersen. The outlet data were obscured by the condensation of H_2SO_4 upon the impaction substrates.

Due to the concentration limits for operating optical counters and CN counters and problems with condensation and coagulation in the sampling lines and diffusion batteries, it is necessary to dry and dilute the sample aerosol before it reaches these areas. Because of the difference in particle concentration at the inlet and outlet of emission control devices, the dilution factor at the outlet is normally much smaller than that at the inlet. At this installation, the outlet data were influenced by condensation of H_2SO_4 in the sampling systems. The number of particles counted by the CN counters included macro-molecular droplets of H_2SO_4 , as did the mass accumulated on the outlet impactor stages. There was no evidence that the optical counter data were affected.

Sufficient data were obtained to permit calculation of lower limits for the fractional efficiencies in the range of sizes covered by diffusional methods. This was done by assuming that all the particles counted at the outlet were of uniform size and that dividing by the number of particles of the size at the inlet yields the maximum penetration for that size.

Figure 18 summarizes the inlet mass distribution data as calculated using the Brink impactors. Figure 19 shows the inlet particle size distribution expressed on a cumulative basis.

Table 15 and Figure 20 show the fractional efficiency calculated from the optical and diffusional data. The part of the curve calculated using the diffusional data (0.01 to 0.15 μm diameter), is a lower limit as described above. The efficiency calculated from the optical data (0.4 to 1.5 μm diameter) represents actual precipitator performance.

IN SITU RESISTIVITY MEASUREMENTS

The resistivity of the fly ash was determined by measurements made with the SRI point-to-plane in situ resistivity instrumentation. This device is used to electrostatically collect a dust layer while the dust is maintained at flue gas conditions.

The point-to-plane probe lends itself to two types of measurement, commonly referred to as the parallel-disc method and the electric field-current density methods. The parallel-disc measurement is very similar to that described in the A.S.M.E. Power Test Code Number 28. After the dust-laden electrode volt-ampere characteristic is recorded, a measurement disc is lowered to contact the dust layer. A pressure on the order of ten grams per square

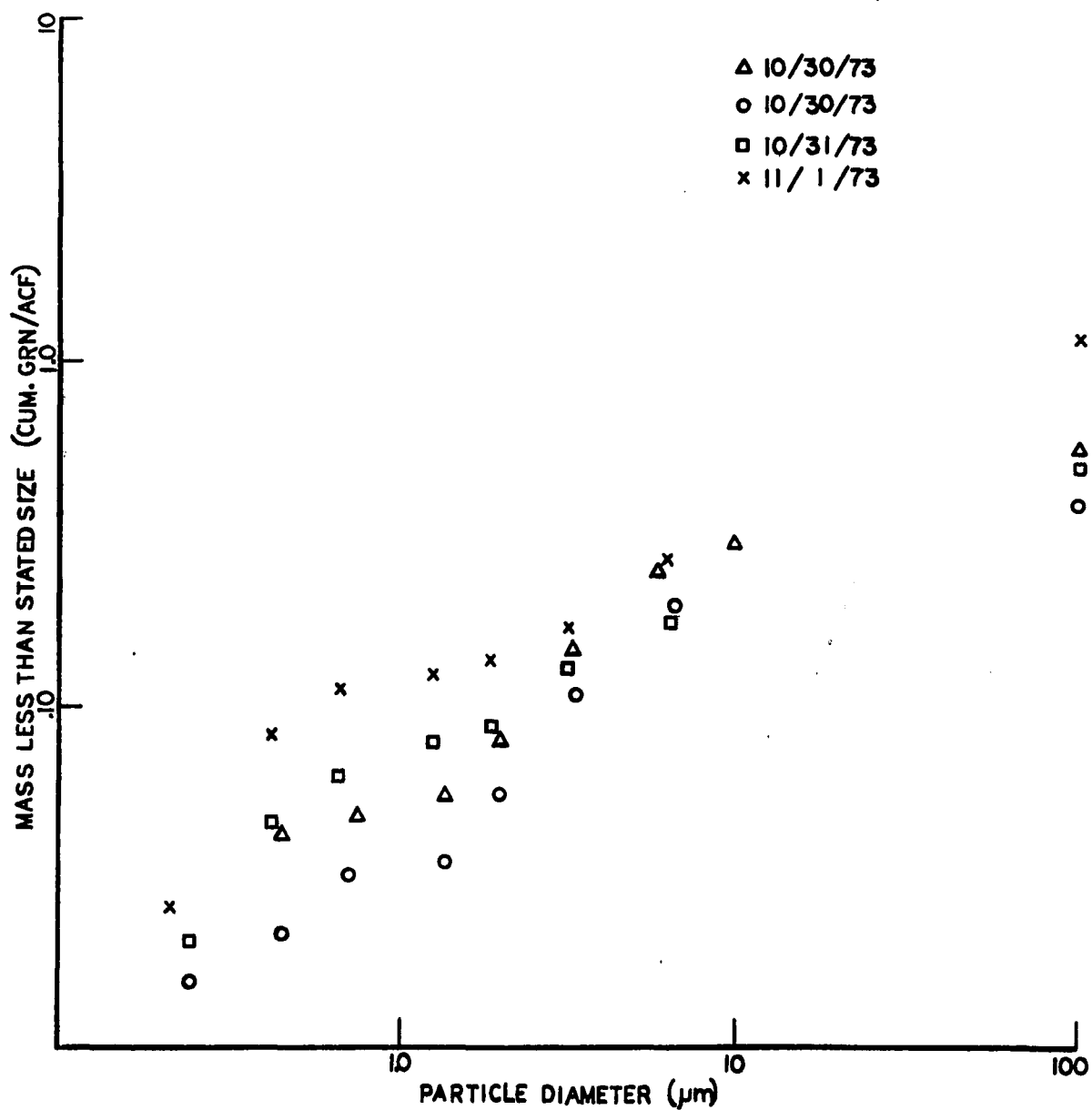


Figure 18 Inlet Mass Distribution Calculated from Cascade Impactor Data

SOUTHERN RESEARCH INSTITUTE

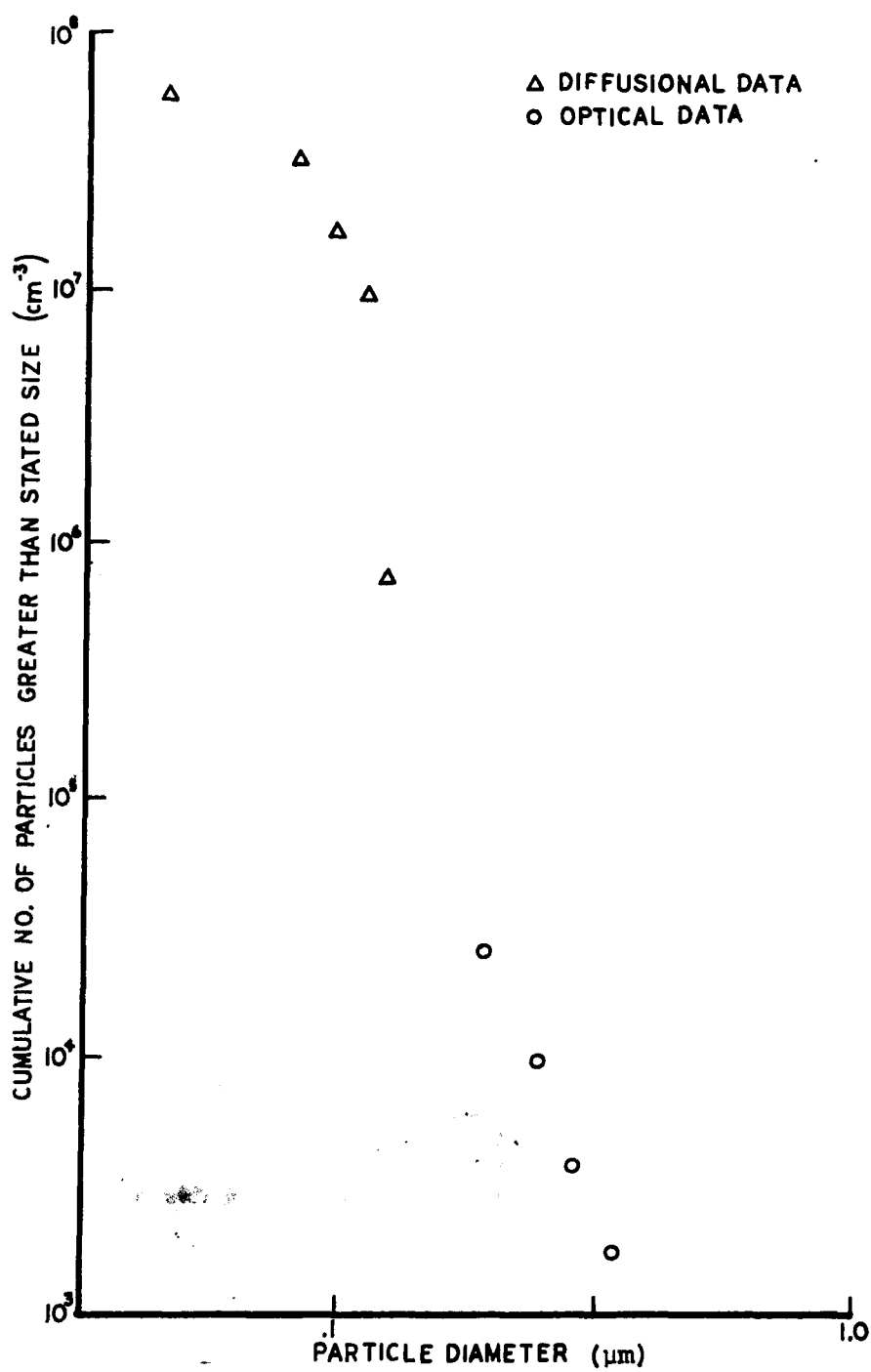


Figure 19 Inlet Particle-Size Distribution

SOUTHERN RESEARCH INSTITUTE

TABLE 15 FRACTIONAL EFFICIENCY DATA

<u>Power Supply Settings</u>	<u>Automatic 4th Section Off</u>	<u>Automatic</u>	<u>20 $\mu\text{A}/\text{ft}^2$</u>	<u>10 $\mu\text{A}/\text{ft}^2$</u>	<u>30 $\mu\text{A}/\text{ft}^2$</u>
<u>Date</u>	<u>9/14</u>	<u>9/19</u>	<u>9/20</u>	<u>9/21</u>	<u>9/22</u>
<u>Size (μm)</u>	<u>Efficiency %</u>				
0.015 ¹	95	97.9	90	82	98.5
0.037	97.7	99.1	95.5	92.3	99.35
0.078	96.8	98.6	93.5	88	99
0.11	93.2	97.1	87	76	98
0.135	94	97.5	88	78	98.2
0.46	97.8	96.8	96.3	91.3	98.1
0.68	98.8	98.6	98.6	96.2	99.4
1.0	98.7	98.9	99.3	98.2	99.6
1.25	99.2	99.55	99.65	98.8	99.83
1.4	99.75	99.55	99.8	99.4	99.8
1.5	99	99.85	99.7	99.4	99.85

1. Efficiency data in the size range 0.01-0.15 μm (diffusional data) are lower limits.

SOUTHERN RESEARCH INSTITUTE

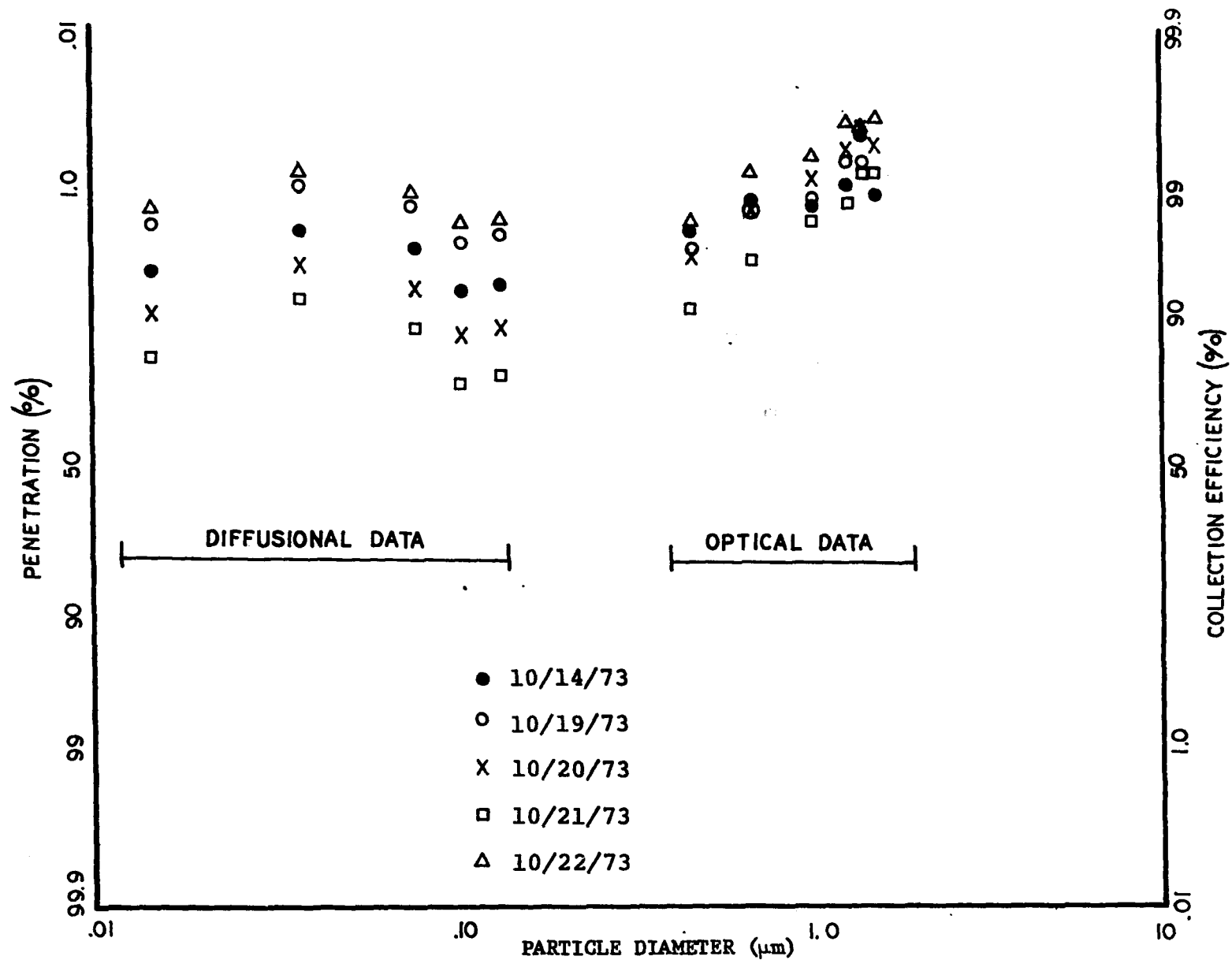


Figure 20 Fractional Efficiencies for the Wood River Precipitator

centimeter is supplied by a spring. The resistivity is determined by measuring the resistance of a known geometrical configuration of the dust (cylindrical solid). The resistivity is determined just prior to electrical flashover between the parallel discs.

The electric field-current density method is dependent upon the Ohms Law relationship that the electric field in a medium is proportional to the current density and the resistivity. The corona current from the point electrode flows through flue gas in the form of ions. If there were no dust deposit on the electrode system, the electrical conditions would be determined only by the flue gas constituents. However, if there were a dust layer on the collection electrode, the corona current flow through the layer would cause a voltage drop across the layer, which results in a shift in the electrical conditions. This shift in the voltage-current characteristics of the point-to-plane probe provides the data for the resistivity measurements.

Each method of measurement has potential problems. The parallel-disc measurement is made by contacting a metal electrode with the dust layer. This disturbs the surface and compresses the dust. Variation in contact area and compaction can lead to variations in the resistance of a given sample.

The electric field-current density (E vs j) measurement technique more nearly duplicates the behavior of a precipitator in that the dust layer is undisturbed and the electron transfer mechanism at the dust surface is duplicated. There is some problem with the dust thickness determination for the technique.

The conditions at the Wood River Plant were such that the parallel-disc method did not provide useful data for the high-sulfur coal tests. Therefore, only the electric field-current density (E-j) data are included. The low-sulfur tests did provide good parallel-disc measurements as well as E-j data. The relative values for the two methods for a current density of $0.2 \mu\text{A}$ per square centimeter are shown in Table 16.

The results of the electric field-current density resistivity measurements are plotted as a function of temperature in Figure 21.

PRECIPITATOR SECONDARY VOLTAGE AND CURRENT MEASUREMENTS

The operating voltage and current conditions were determined at regular intervals during the test program. A set of high megohm voltage dividers (10,000:1) was installed on selected power sets in the precipitator. These dividers were used to provide voltages proportional to the secondary voltage between the corona and collecting electrodes. Voltage-current curves are included in Figures 22 through 29 for the test conditions that were established at the Cat-Ox[®] test site.

The operating voltages and currents were set for each test condition and monitored at hourly intervals. These conditions remained constant during the test interval except for some minor variations when operating in the automatic mode.

TABLE 16. COMPARISON BETWEEN THE RESISTIVITY DETERMINED BY EACH METHOD AT
A CURRENT DENSITY OF 0.2 A/cm², TEST DATE 10/1/73

<u>Test Number</u>	<u>Temperature</u>	<u>Parallel Disc Resistivity</u>	<u>Electric Field-Current Density</u>
1	330	2.3x10 ¹⁰ ohm-cm	6.1x10 ¹⁰ ohm-cm
2	335	3.1x10 ¹⁰ ohm-cm	5.0x10 ¹⁰ ohm-cm
3	340	2.5x10 ¹⁰ ohm-cm	7.5x10 ¹⁰ ohm-cm
4	335	4.1x10 ¹⁰ ohm-cm	1.6x10 ¹⁰ ohm-cm

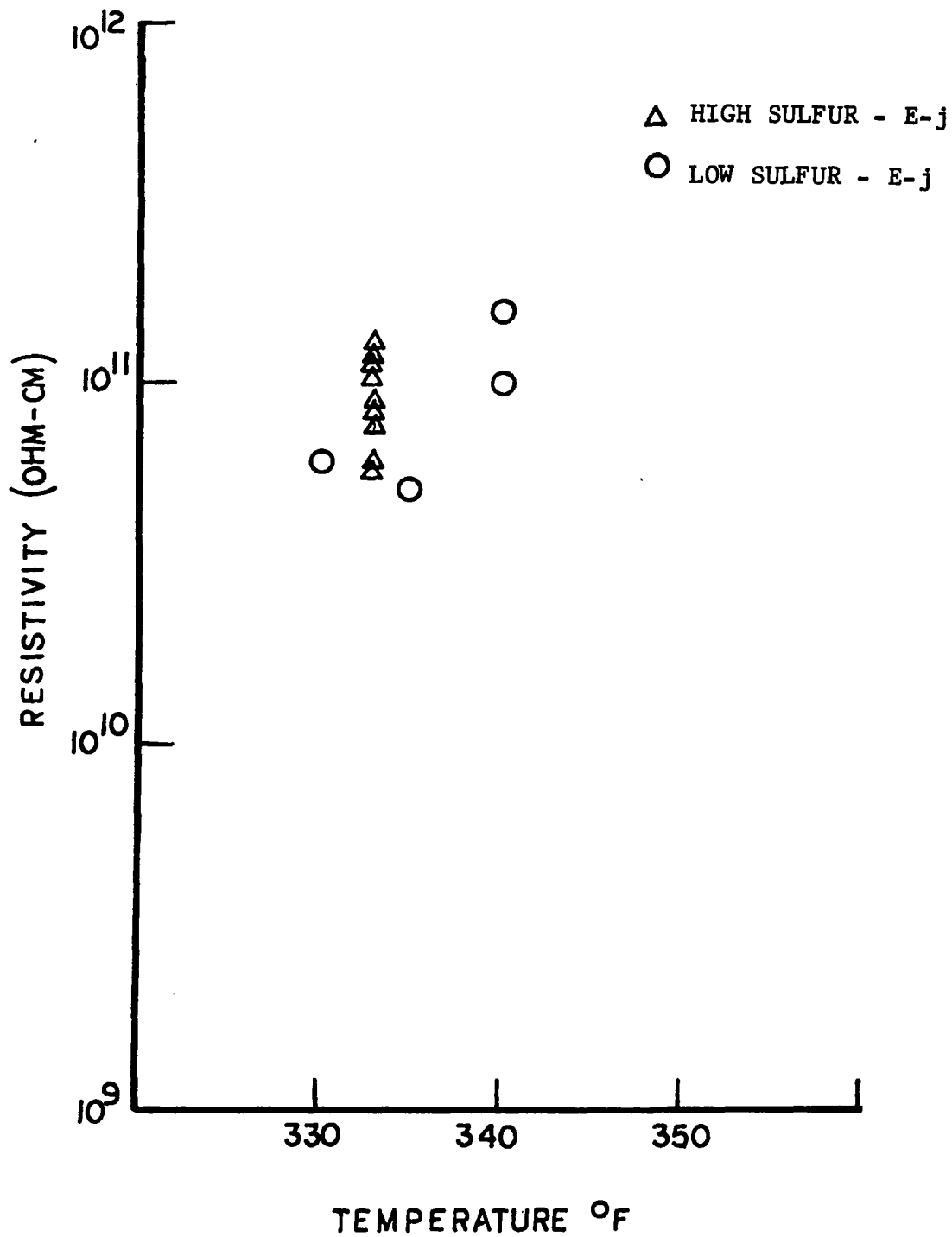


Figure 21 Resistivity as a Function of Temperature by the Electric Field-Current Density Method for the Wood River Catalytic Oxidation Project Tests.

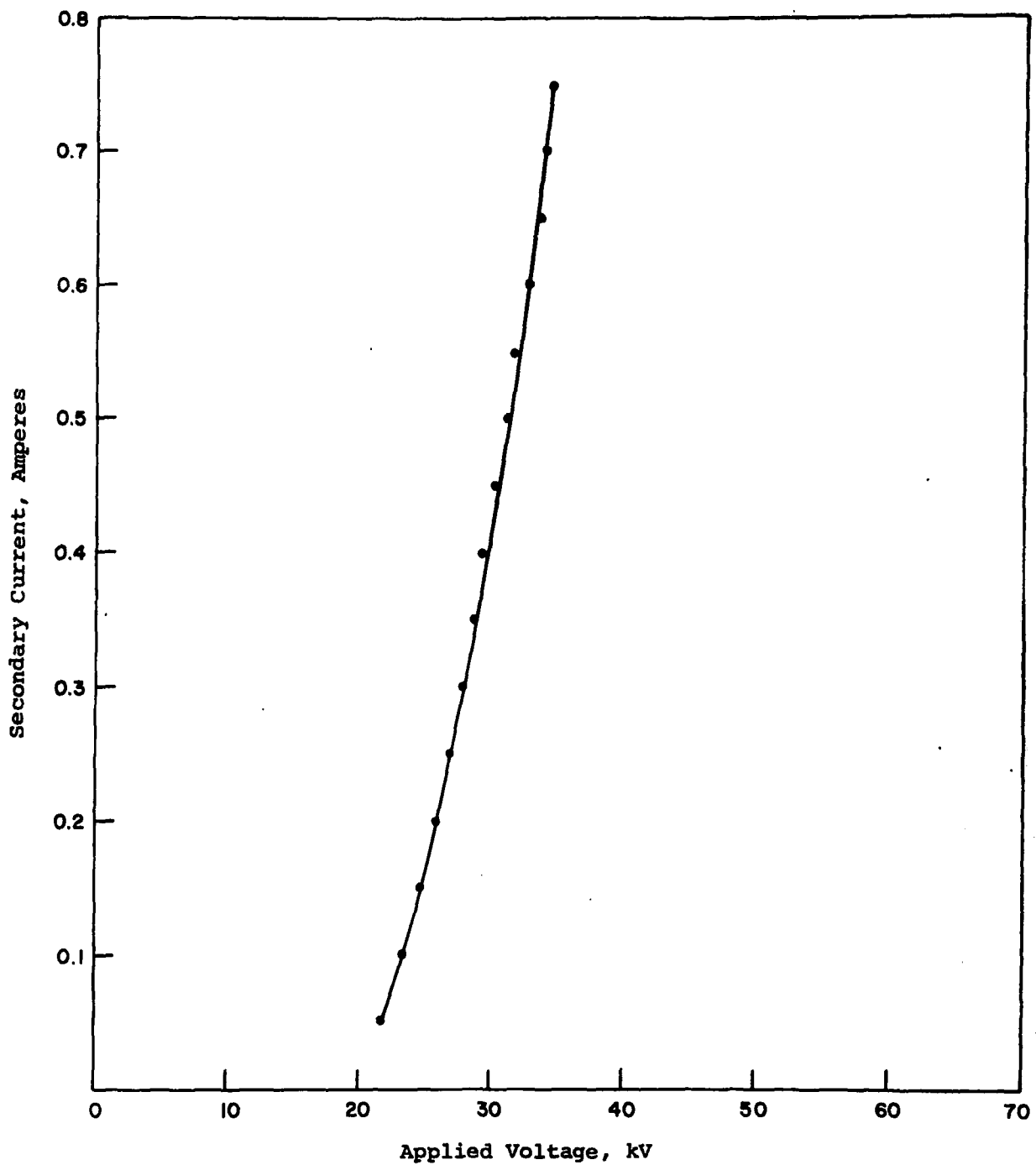


Figure 22 Voltage vs Current Characteristics for Power Supply No. 2 for the Low Sulfur Test Conditions

SOUTHERN RESEARCH INSTITUTE

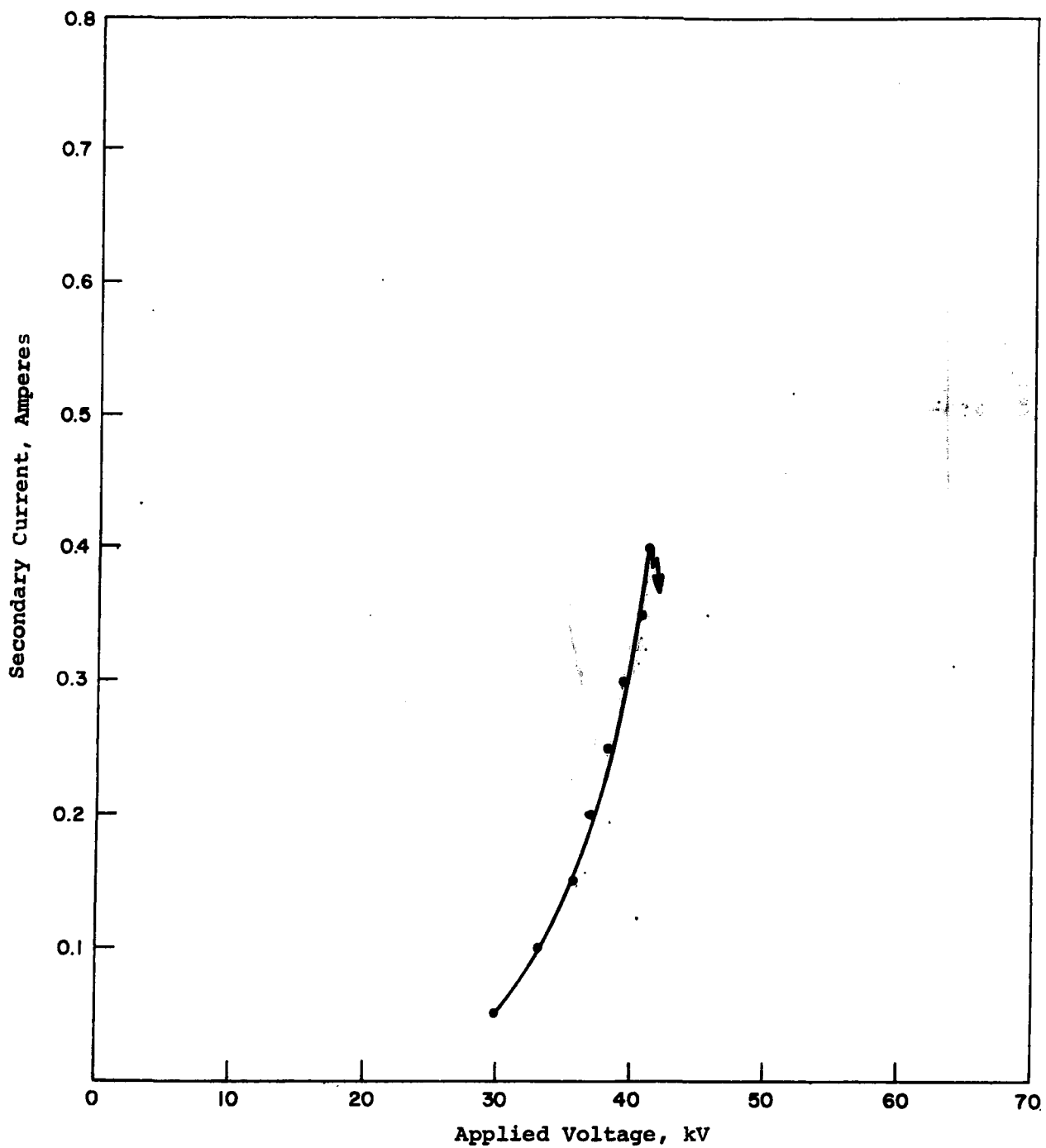


Figure 23 Voltage vs Current Characteristics for Power Supply No. 4 for the Low Sulfur Test Conditions

SOUTHERN RESEARCH INSTITUTE

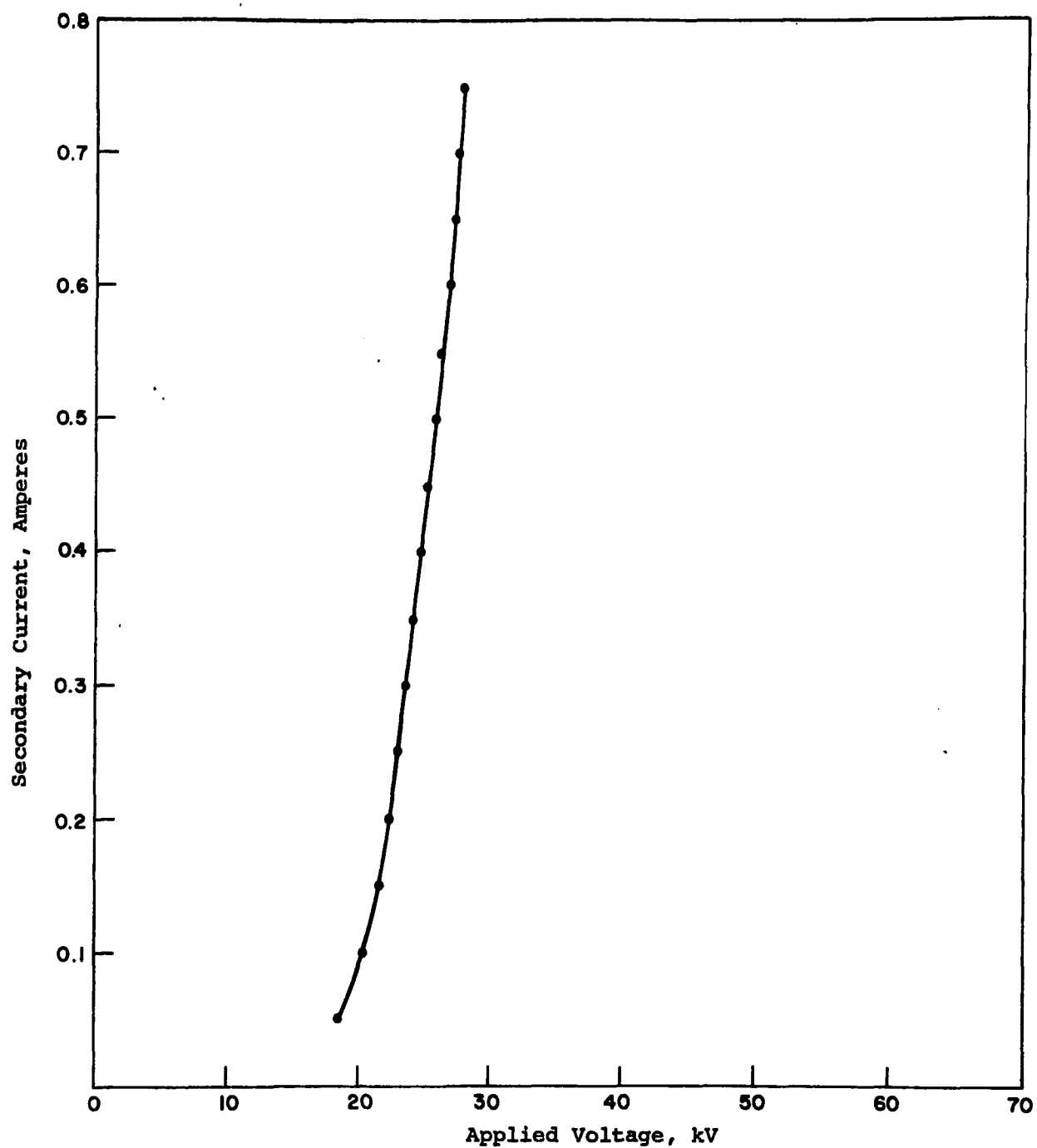


Figure 24 Voltage vs Current Characteristics for Power Supply No. 5 for the Low Sulfur Test Conditions

SOUTHERN RESEARCH INSTITUTE

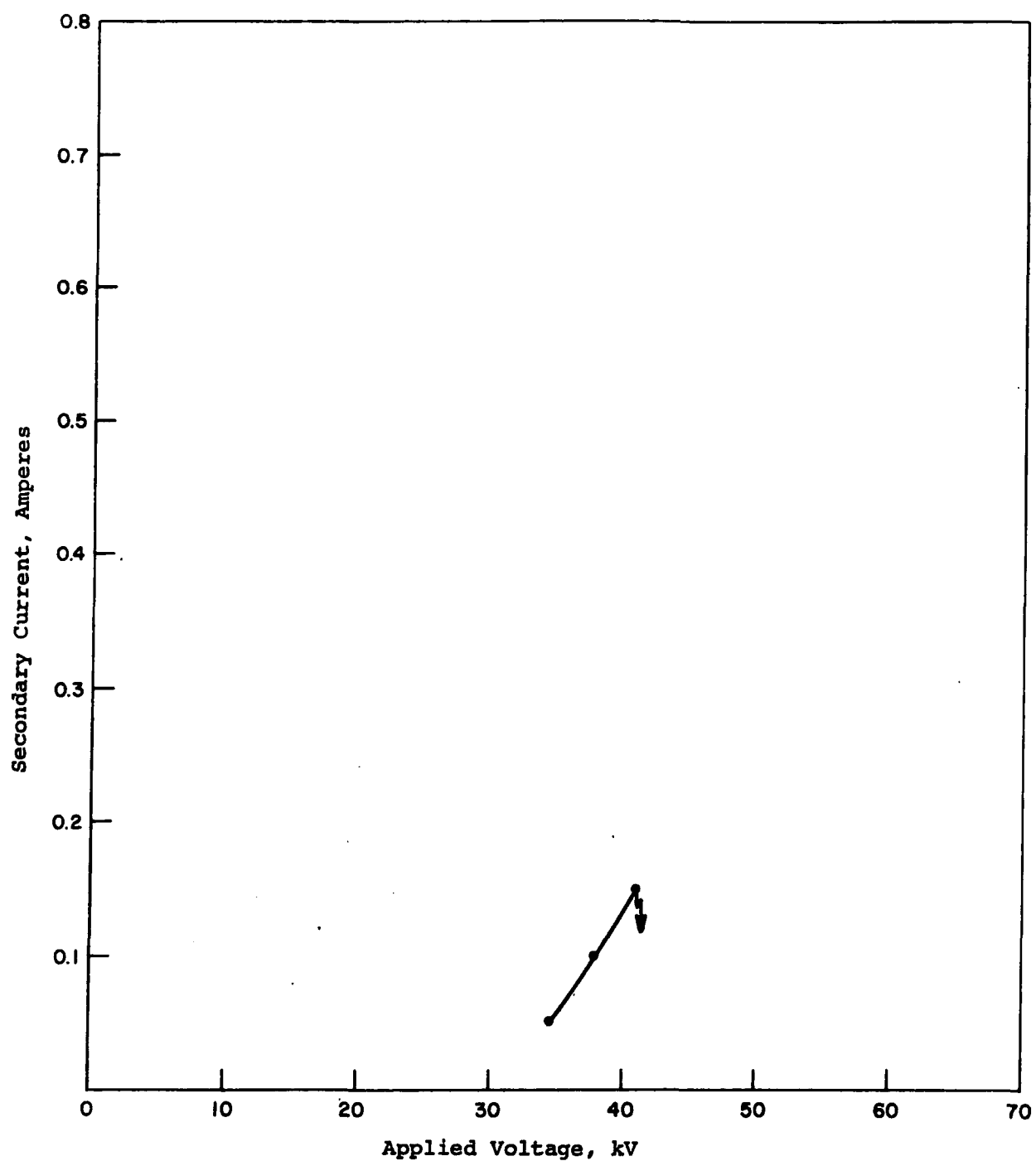


Figure 25 Voltage vs Current Characteristics for Power Supply No. 8 for the Low Sulfur Test Conditions

SOUTHERN RESEARCH INSTITUTE

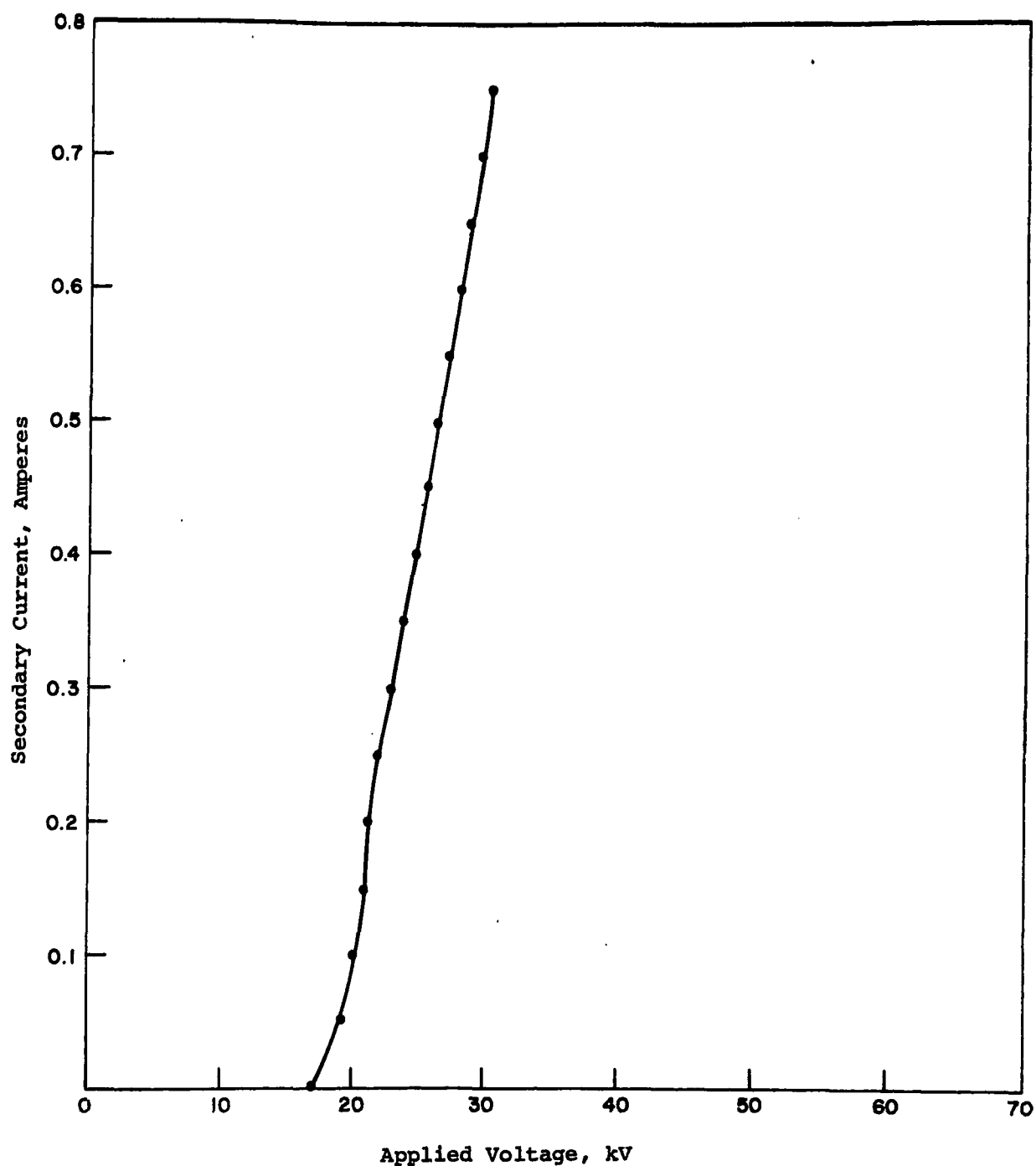


Figure 26 Voltage vs Current Characteristics for Power Supply No. 2 for the High Sulfur Test Conditions

SOUTHERN RESEARCH INSTITUTE

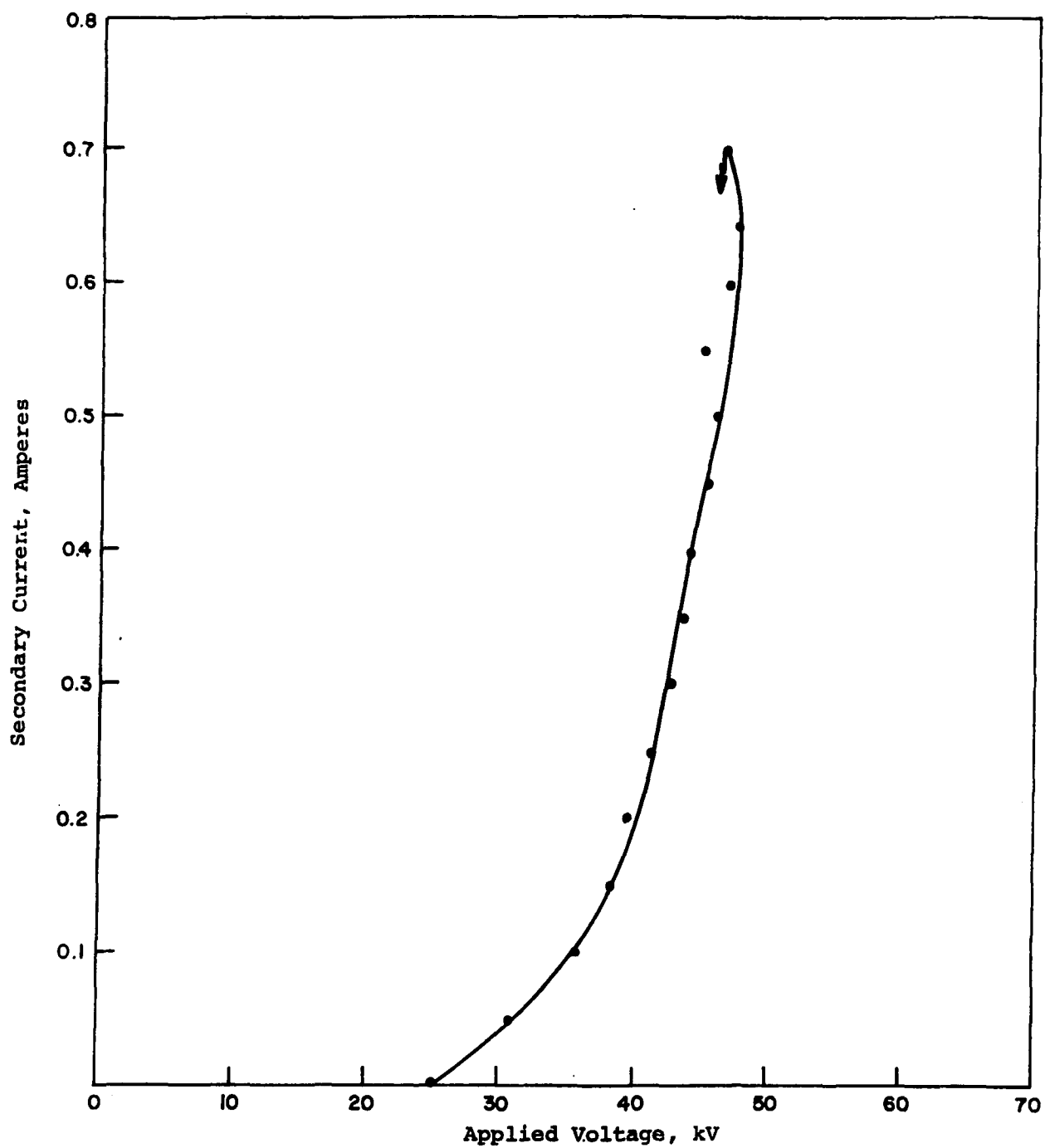


Figure 27 Voltage vs Current Characteristics for Power Supply No. 4 for the High Sulfur Test Conditions

SOUTHERN RESEARCH INSTITUTE

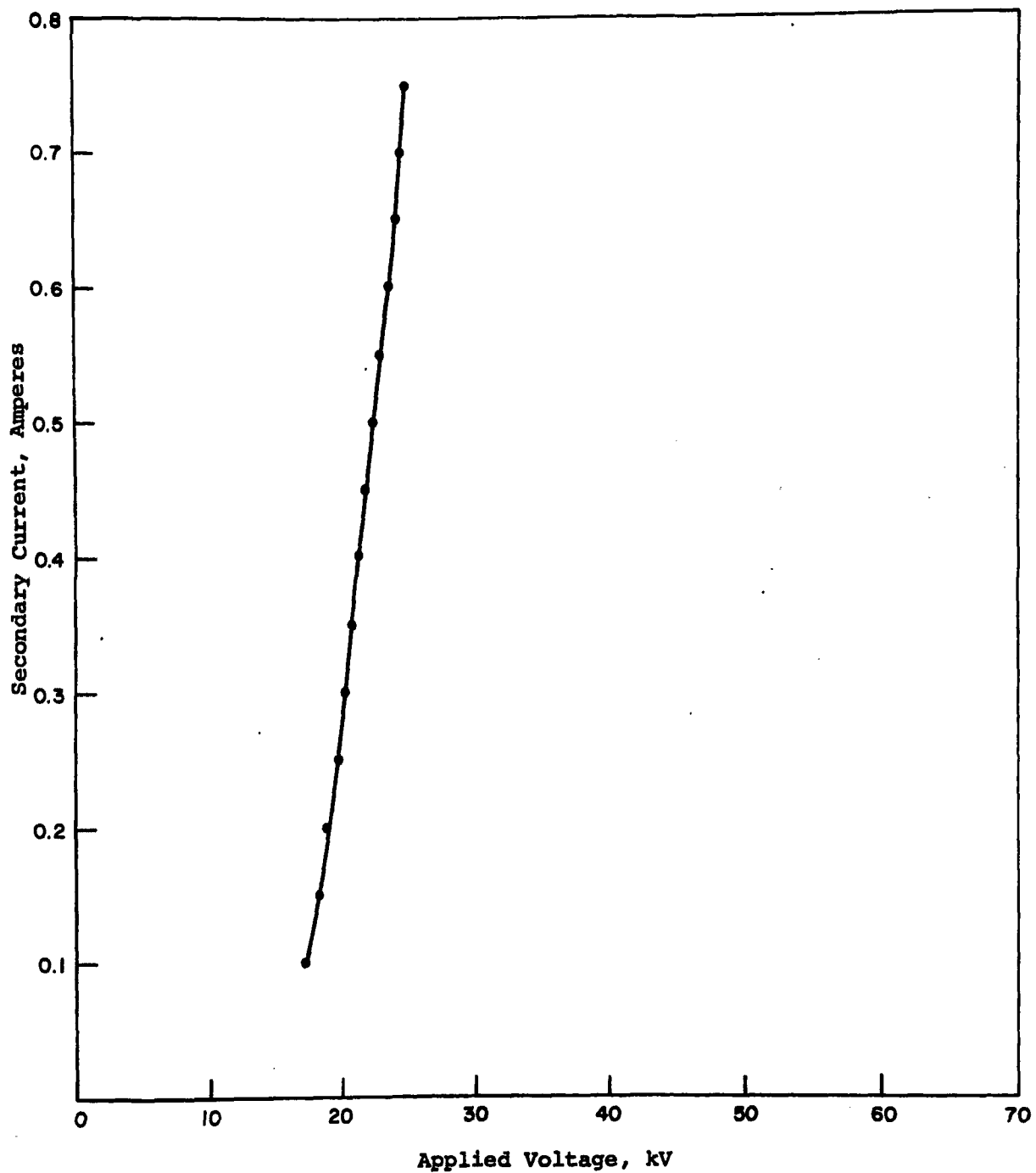


Figure 28 Voltage vs Current Characteristics for Power Supply No. 5 for the High Sulfur Test Conditions

SOUTHERN RESEARCH INSTITUTE

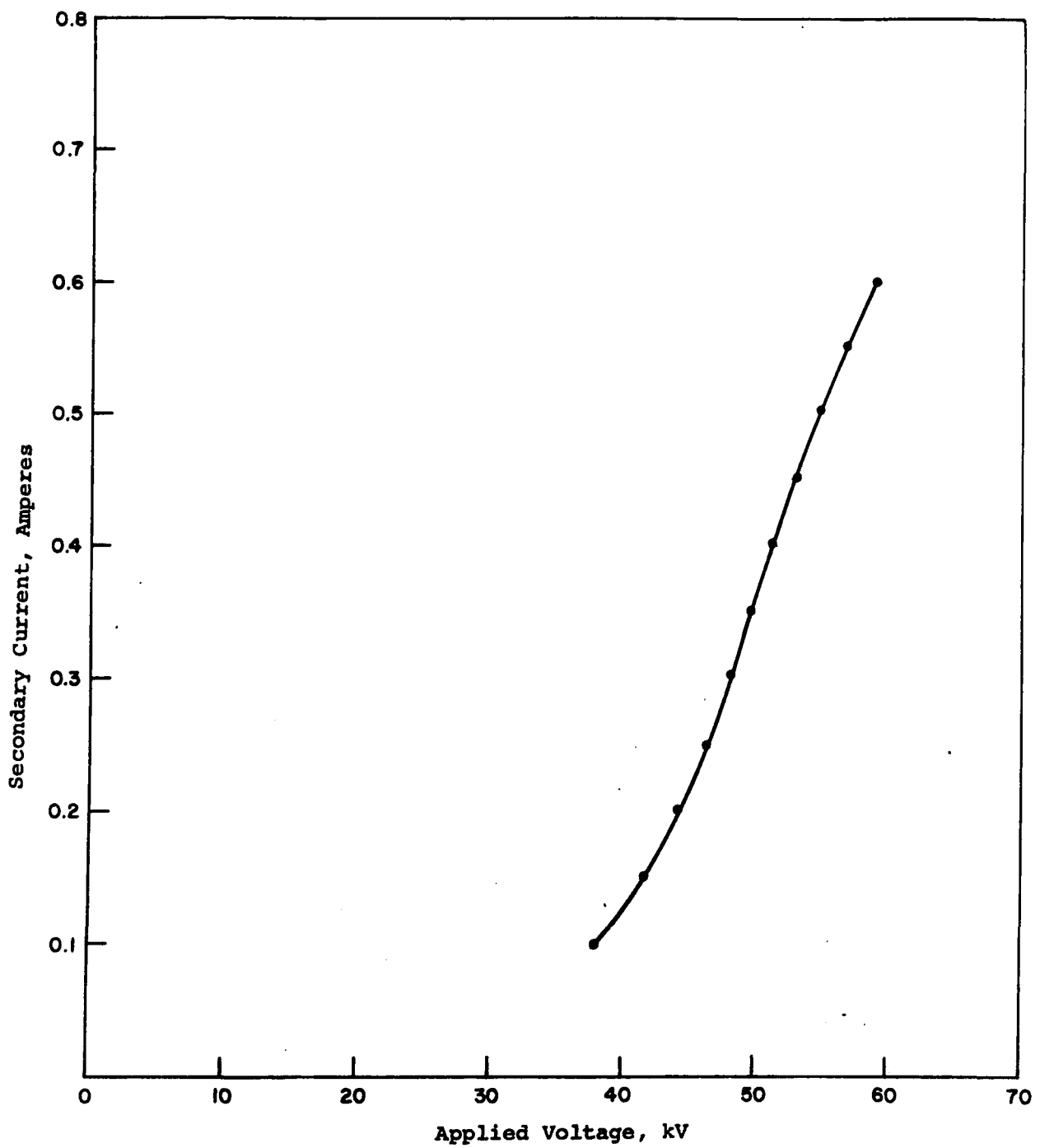


Figure 29 Voltage vs Current Characteristics for Power Supply No. 8 for the High Sulfur Test Conditions

SOUTHERN RESEARCH INSTITUTE

COMPUTER SYSTEMS ANALYSIS

The SRI electrostatic precipitator computer systems model was utilized to project the variation in efficiency that would be expected for a variation in volume flow rate. The electrical conditions utilized for this projection were for current densities of 10, 20, and 30 microamperes per square foot and automatic conditions. These results are shown, together with the reported efficiency data, in Figures 30 and 31.

The trend in efficiency as a function of volume flow rate as suggested by the computer projection is realistic even though the computer model does not include factors for particle re-entrainment. Therefore, at this time, the model is primarily useful for extrapolating the gross behavior of precipitators, rather than for definitively determining the overall efficiency of a unit.

Neglecting re-entrainment primarily influences the computed versus measured performance in the particle sizes greater than one micrometer ($1\text{ }\mu\text{m}$), since re-entrained particles are expected to occur in size bands $1\text{ }\mu\text{m}$ and larger. Therefore, the computer simulation for 10, 20, and 30 microamperes per square foot was run for size fractional efficiencies in this range. The results of this simulation are shown, together with the size fractional efficiency as determined by particle size instrumentation for this size band, in Figures 32, 33, and 34. The size measurements for $0.15\text{ }\mu\text{m}$ and smaller represent lower limit values and, therefore, are shown as dotted lines.

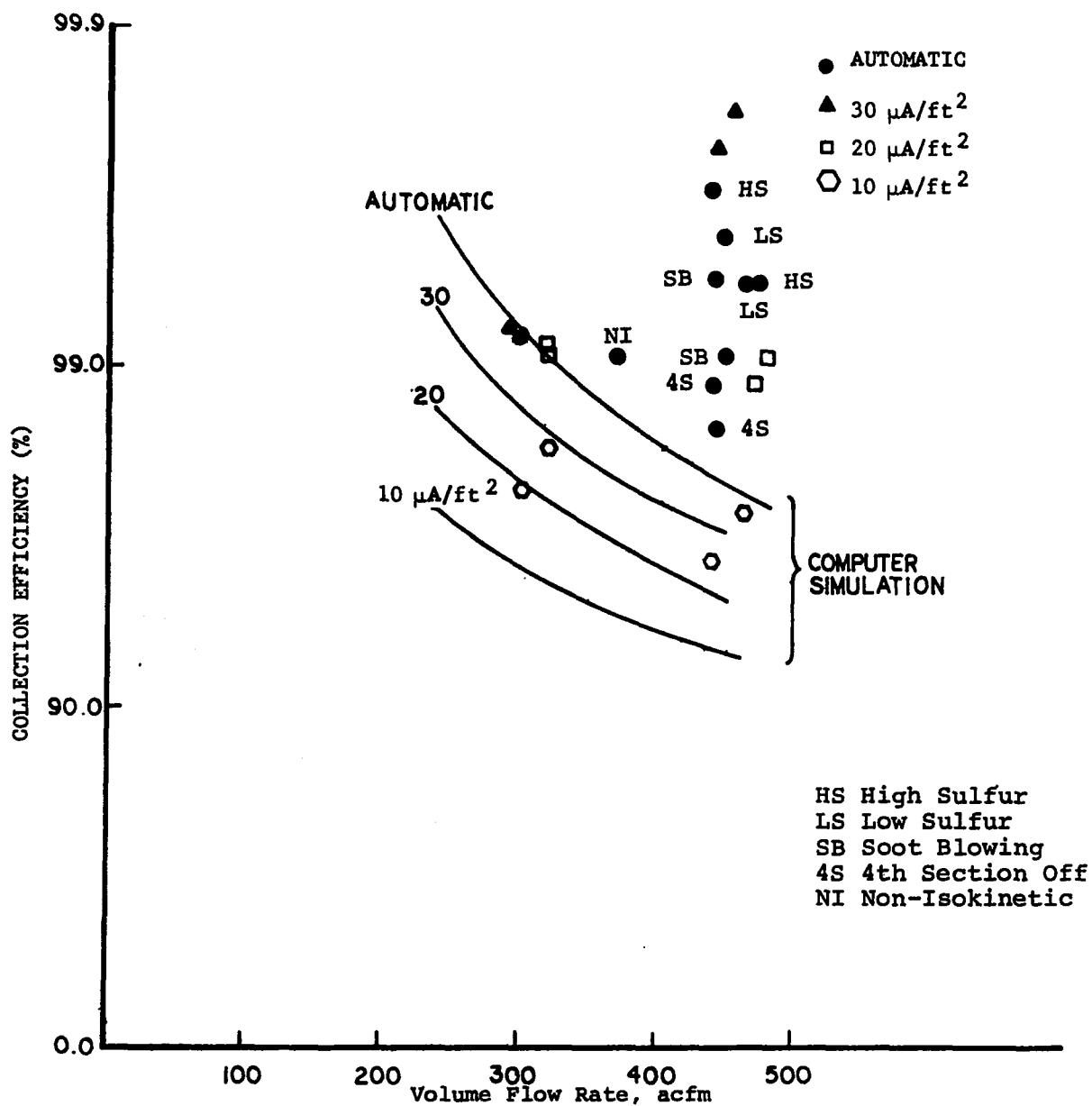


Figure 30 Actual Efficiency from Inlet and Outlet Dust Loading Measurements With All Data Points Included.

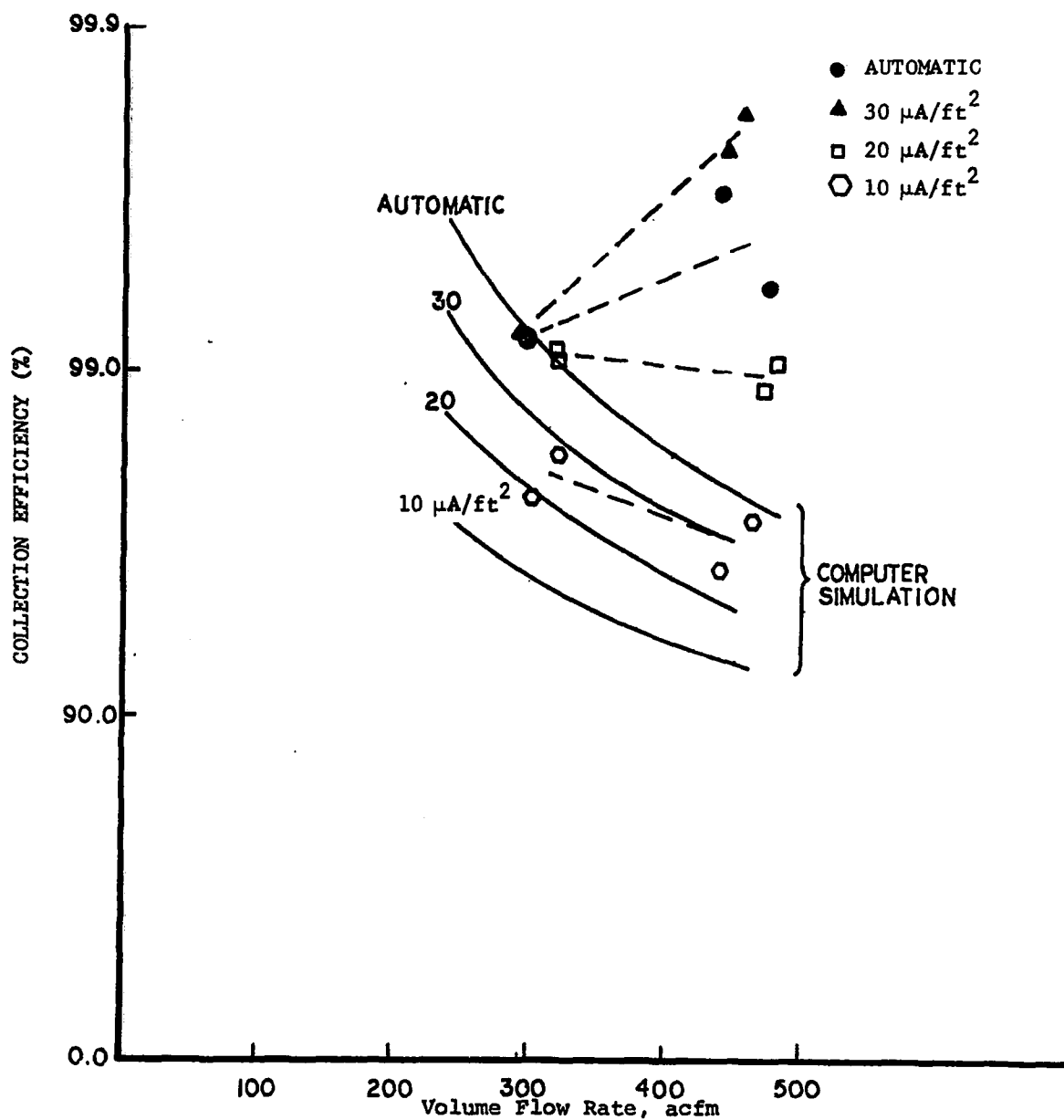


Figure 31 Actual Efficiency from Inlet and Outlet Dust Loading Measurements With Soot Blowing, Non-Isokinetic and Fourth Electrical Section Points Removed.

SOUTHERN RESEARCH INSTITUTE

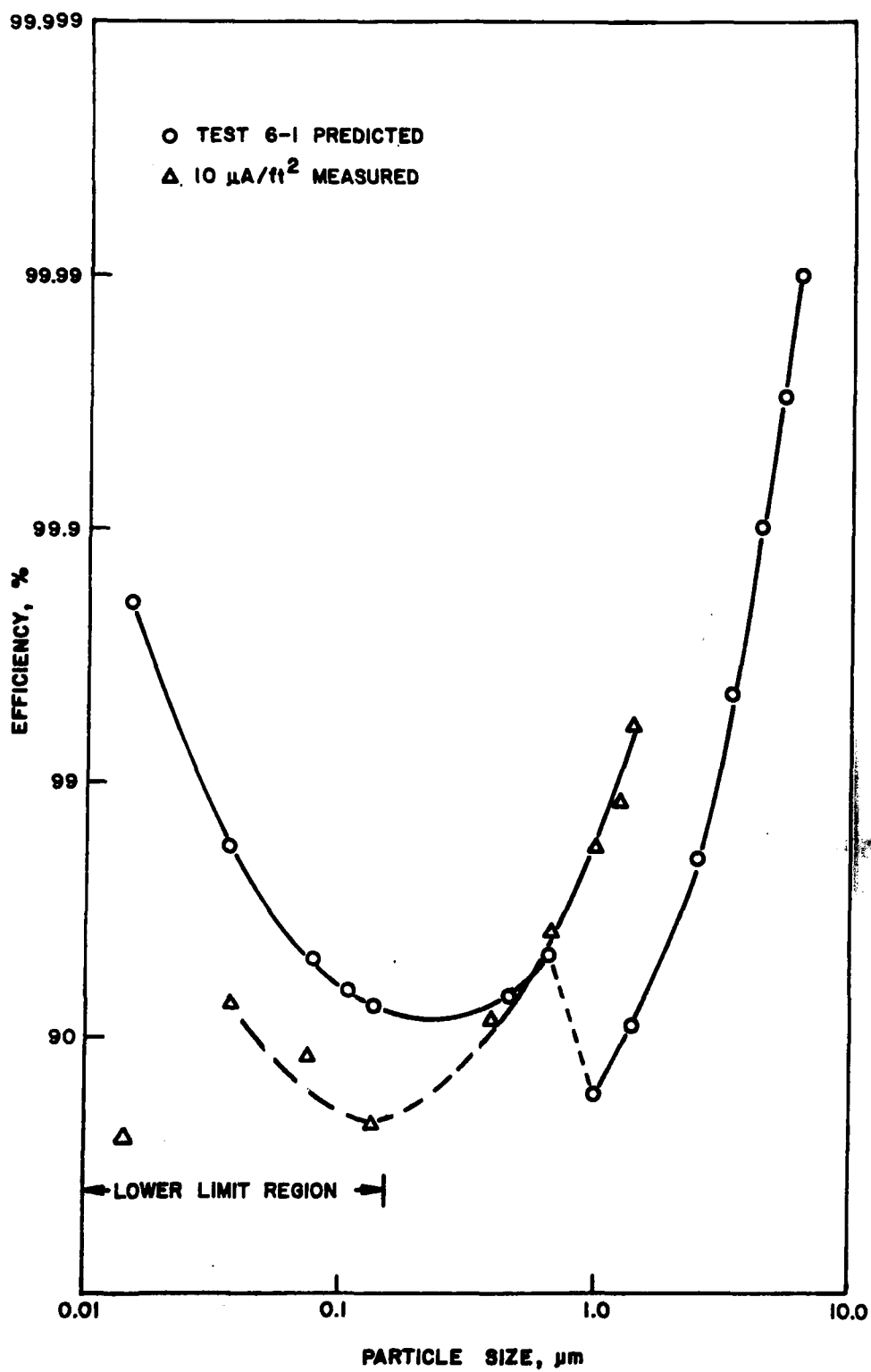


Figure 32 Computed and Measured Size Fractional Efficiencies for 10 Microamperes per Square Foot for the Cat-Ox[®] Tests. The region identified as lower limit region is that corresponding to acid condensation in the measurement system.

SOUTHERN RESEARCH INSTITUTE

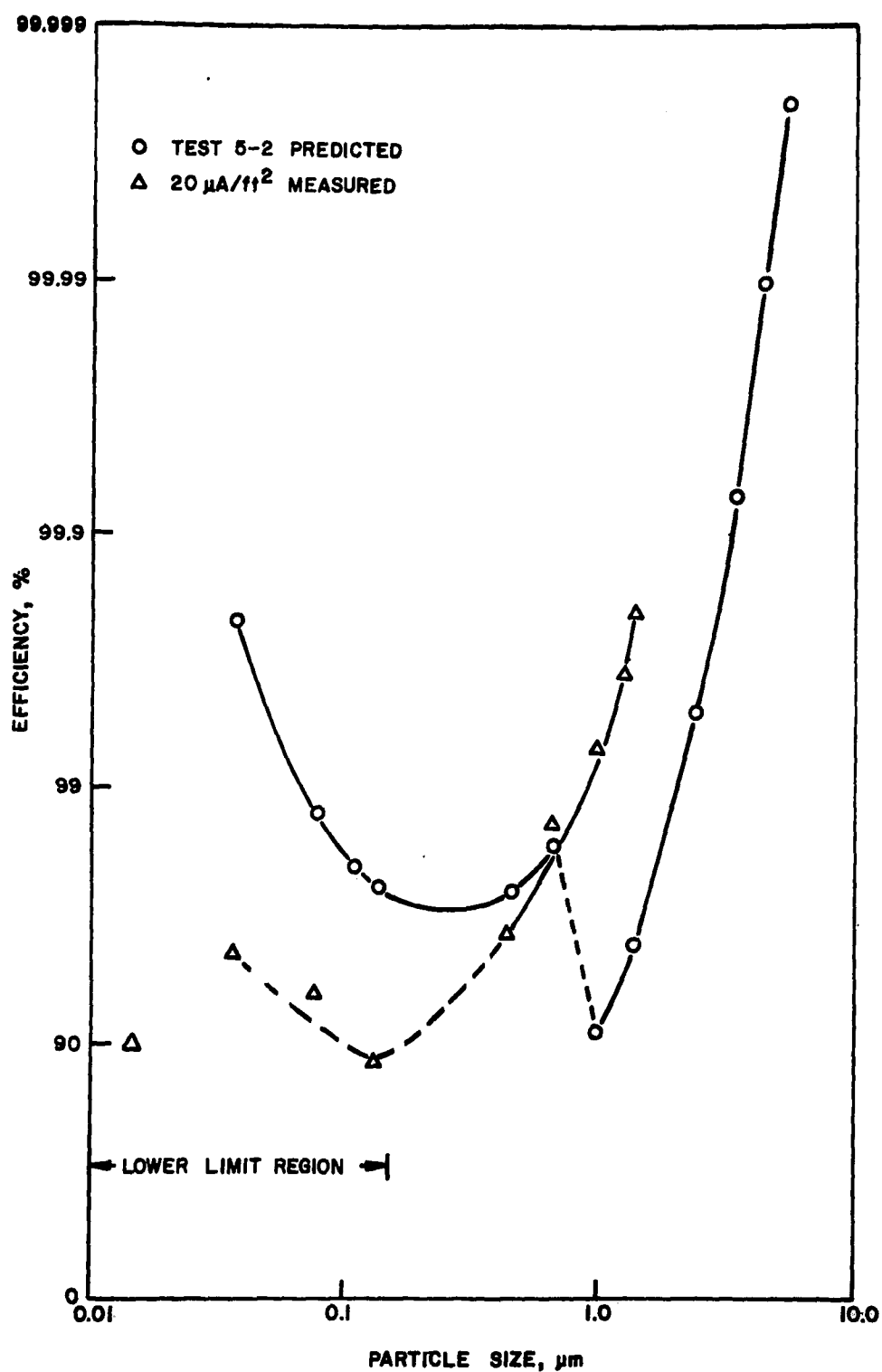


Figure 33 Computed and Measured Size Fractional Efficiencies for 20 Microamperes per Square Foot for the Cat-Ox[®] Tests. The region identified as lower limit region is that corresponding to acid condensation in the measurement system.

SOUTHERN RESEARCH INSTITUTE

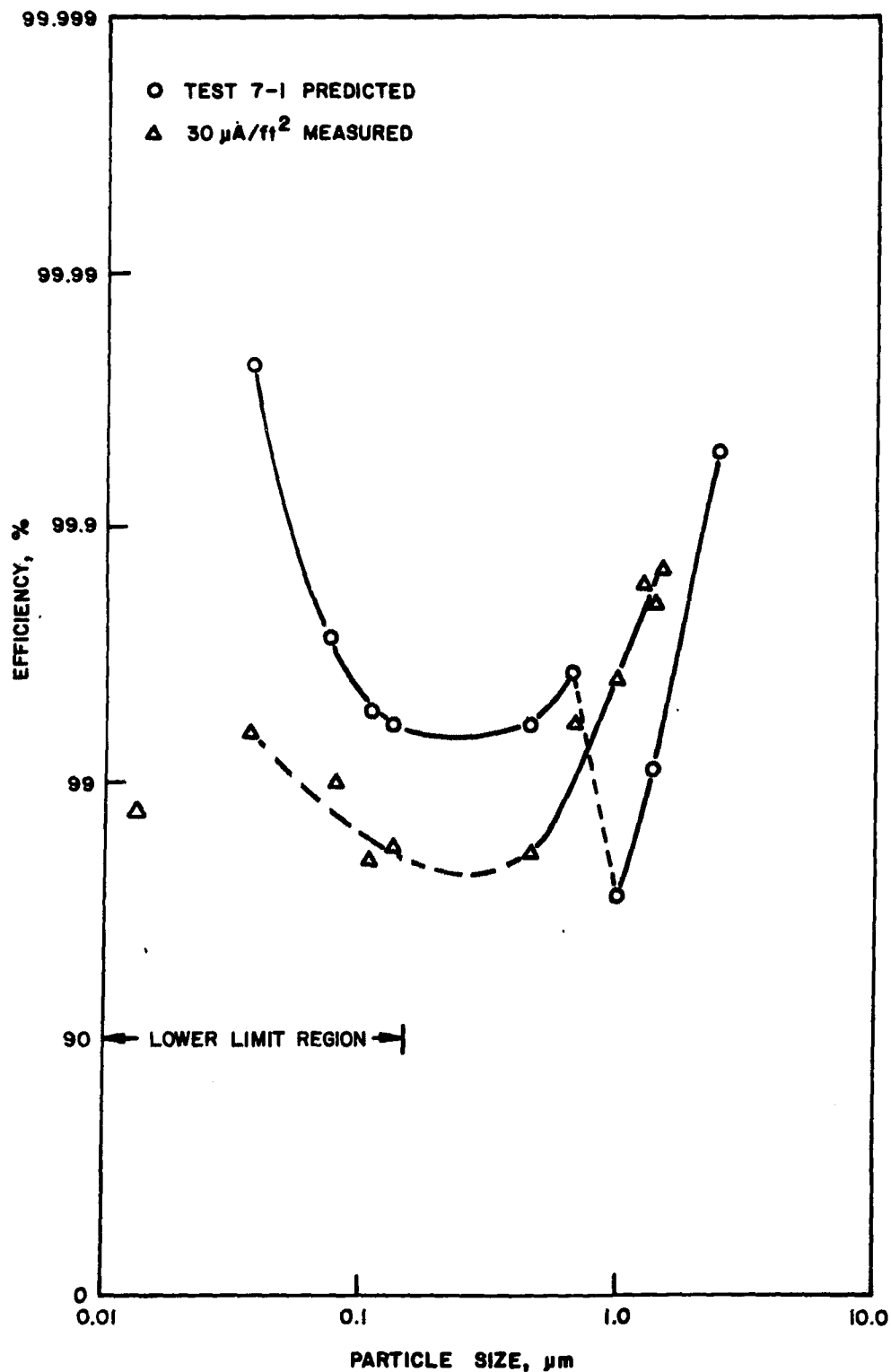


Figure 34 Computed and Measured Size Fractional Efficiencies for 30 Microamperes per Square Foot for the Cat-Ox[®] Tests. The region identified as lower limit region is that corresponding to acid condensation in the measurement system.

SOUTHERN RESEARCH INSTITUTE

DISCUSSION OF EFFICIENCY TESTS

The projections for the various current density conditions are shown with the complete test efficiencies in Figure 30. Each test condition is shown by each data point. Figure 31 is a repeat of Figure 30, with only selected data points shown. The soot blowing tests, with the fourth field deenergized, and those tests with isokinetic variations greater than 10 percent are removed.

The $10 \mu\text{A}/\text{ft}^2$ condition shows trends that are in agreement with theoretical expectations, but as the current density is increased, the trends are progressively at odds with theory. Theory predicts an increased collection efficiency with decreasing gas flow rate. We find no explanation for the observed behavior for the higher current density tests. Some possible explanations include:

- varying plant operating conditions
- varying coal characteristics
- insufficient stabilization time between test condition changes
- variation in test procedure

It is not possible to determine which of these factors may have contributed to the problem during this test program.

APPENDIX II

FLUE GAS COMPOSITION AND VOLUME FLOW MEASUREMENTS

FLUE GAS COMPOSITION

Flue gas concentrations were measured continuously and recorded on strip charts. The flue gas measurement system was time-shared between three locations--the economizer, the ESP input, and the ESP output. The gases measured were SO_2 , CO_2 , O_2 , and H_2O . The boiler excess air was set by measurement of O_2 at the economizer. Difficulties were experienced with the H_2O vapor analyzer during the initial tests so that good data were not obtained until Test 6.

The reduced results from the strip charts are summarized in Table 17 for the main part of the test program and in Table 18 for the repeat tests. Figure 35 shows a portion of the strip chart recording of the SO_2 concentration during the gradual conversion from low-sulfur coal to high-sulfur coal in Test 14.

TABLE 17. FLUE GAS COMPOSITION AT ECONOMIZER AND INPUT/OUTPUT OF ESP

Test Number ^a	Run Number	SO ₂			CO ₂			O ₂			H ₂ O		
		Economizer (ppm)	Input ESP (ppm)	Output ESP (ppm)	Economizer (%)	Input ESP (%)	Output ESP (%)	Economizer (%)	Input ESP (%)	Output ESP (%)	Economizer (%)	Input ESP (%)	Output ESP (%)
#2 9/13	#1 (10:03am-2:10pm)	2561	2405	1860	15.4	14.9	12.4	3.7	6.0	10.1	---	---	---
	#2 (3:30pm-7:45pm)	2535	2280	1725	15.2	14.3	11.9	3.7	5.6	10.3	---	---	---
#3 9/14	#1 (10:05am-3:13pm)	2276	2229	1525	15.1	13.9	11.4	4.3	6.2	11.7	---	---	---
	#2 (2:15pm-8:15pm)	2415	2235	1538	14.8	13.8	11.4	4.1	6.5	11.8	---	---	---
#15 9/15	Single Run (10:30am-5:30pm)	2370	2165	2250	15.7	14.0	11.0	3.8	5.7	10.8	---	---	---
#8 9/19	Single Run	2490	2340	2295	15.3	---	14.7	3.8	---	5.6	---	---	---
#4 9/19	#1 (1:00pm-5:00pm)	2469	2310	2274	15.5	14.8	14.8	3.7	5.2	5.5	---	---	---
	#2 (6:57pm-9:35am)	2445	2235	2235	15.5	14.8	14.7	3.5	5.6	5.6	---	---	---
#5 9/20	#1 (9:56am-1:20pm)	2385	2190	2220	14.6	14.6	14.6	3.2	4.4	5.5	---	---	---
	#2 (2:20pm-6:45pm)	2325	2025	2138	15.0	14.2	14.2	3.7	5.8	5.6	---	---	---
#6 9/21	#1 (10:05am-12:32pm)	2325	2190	2190	---	---	---	4.0	5.0	5.4	5.5	---	5.1
	#2 (1:35pm-5:00pm)	2400	2175	2280	15.2	14.8	14.6	3.9	5.4	5.5	5.9	5.0	5.5
#7 9/22	#1 (9:50am-1:00pm)	2430	2250	2250	15.3	14.5	14.6	4.1	5.8	5.8	4.8	5.6	---
	#2 (2:00pm-5:00pm)	2400	2235	2235	15.2	14.5	14.5	4.2	5.9	5.8	6.2	5.2	5.6
#9 9/24-25	#1 (12:26am-3:05am)	2468	2280	2235	14.6	14.1	14.2	4.7	6.1	6.2	6.7	5.3	6.8
	#2 (4:20am-6:58am)	2520	2295	2295	---	14.5	14.5	4.5	6.1	6.2	7.2	---	5.8
#10 9/25-26	#1 (12:00am-3:15am)	2430	2265	2325	14.5	14.7	14.6	4.2	5.7	5.6	5.2	4.9	5.1
	#2 (4:00am-7:02am)	2520	2305	2325	15.3	14.8	15.0	3.6	5.9	5.3	6.8	6.	6.1
#11 9/26-27	#1 (12:01am-4:00am)	2595	2370	2385	15.6	14.8	15.0	3.7	5.9	5.8	6.5	6.3	6.6
	#2 (4:15am-7:12am)	2655	2400	---	15.7	14.8	15.0	3.5	5.9	5.7	7.1	6.1	5.7
#12 9/27-28	#1 (12:00am-3:30am)	2665	2400	2355	14.3	14.7	14.2	3.6	5.7	6.0	8.2	6.5	6.5
	#2 (3:52am-6:55am)	2610	2400	2400	15.0	14.7	14.5	3.7	5.9	5.4	8.0	6.8	6.9
#13 9/28-29	#1 (12:00am-3:00am)	2505	---	2250	15.7	14.6	14.7	3.6	5.8	5.5	7.6	---	7.2
	#2 (3:55am-6:20am)	2385	2115	2175	15.5	14.7	14.9	3.6	5.8	5.6	7.9	6.6	---
#14 10/1	#1 (10:20am-1:20pm)	480	---	458	14.7	14.7	14.7	3.5	5.8	5.3	11.2	6.1	5.3
	#2 (1:55pm-3:57pm)**	420	390	---	14.9	14.5	14.2	4.0	5.5	5.8	7.3	6.4	6.8

^a Gas sampled at input to stack instead of ESP output during Tests 2, 3 and 15.

** SO₂ began increasing after 3:57 p.m. as shown in Figure 35.

TABLE 18. FLUE GAS COMPOSITION FOR REPEAT TESTS

Test Number	Run Number	SO ₂			CO ₂			O ₂			H ₂ O		
		Economizer (ppm)	Input ESP (ppm)	Output ESP (ppm)	Economizer (%)	Input ESP (%)	Output ESP (%)	Economizer (%)	Input ESP (%)	Output ESP (%)	Economizer (%)	Input ESP (%)	Output ESP (%)
#4 (R) 10/30	Single Run (1:15pm-4:15pm)	2618	2430	2400	15.5	14.8	14.8	3.5	5.5	5.6	6.7	7.1	7.0
#4 (R) 10/31	Single Run (10:00am-5:30pm)	2409	2205	2295	15.6	14.8	14.8	3.3	5.4	4.9	7.2	6.0	5.25
#3 (R) 11/1	Single Run (8:20am-12:35pm)	2559	2334	2175	15.6	14.6	14.4	3.3	5.4	5.0	7.1	7.7	7.8

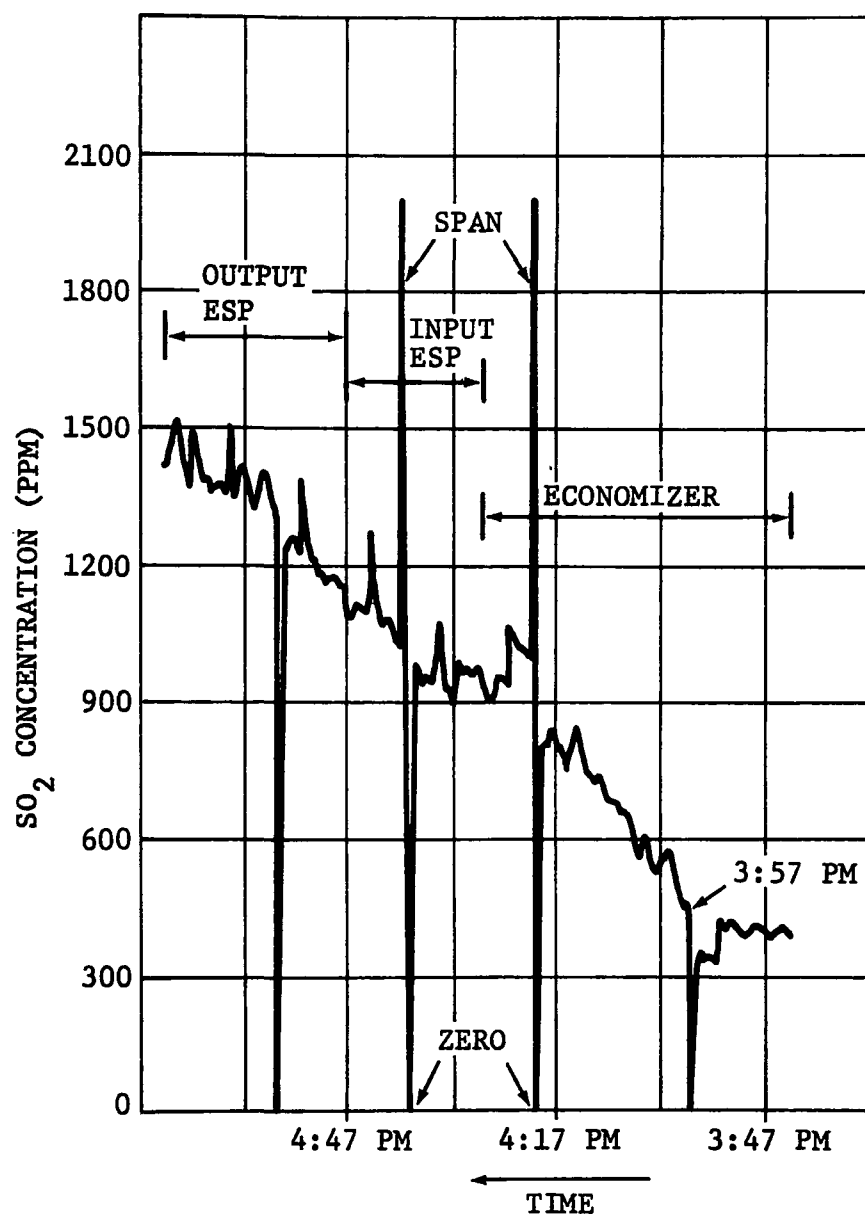


FIGURE 35
TEST #14 STRIP CHART SHOWING
TRANSITION FROM LOW SULFUR
TO HIGH SULFUR COAL

GAS VOLUME FLOW

The gas volume flow was measured at the economizer and stack, using a continuous measurement system consisting of pressure-temperature rakes and pressure sensors. The dynamic pressure, static pressure, and temperature were recorded continuously on strip charts and atmospheric pressure was recorded manually. The recorded data from the strip charts are shown in Table 19 and the reduced results, in Table 20.

Limited manual calibrations were performed during some of the tests. These consisted of traverses in the unoccupied ports and manometer measurements of the rake outputs. The results are summarized in Table 21.

The MRI manual gas volume flow measurements at the inlet and outlet of the precipitator are plotted in Figure 36 as a function of load. Also shown are the limited manual traverses obtained at the economizer and stack. The MRI measurements at the inlet and outlet of the precipitator were, on the average, higher than those obtained at the stack and economizer by MITRE. The discrepancy can be partially explained by the limited number of points traversed at all of the locations and the difference in instrumentation used.

Figure 37 shows the rake measurements of gas volume flow versus load at the economizer and stack. The rake measurements were generally lower than the calibration measurements, indicating again that full traverses are required in order to obtain good calibration data.

TABLE 19. PRESSURE AND TEMPERATURE MEASUREMENTS AT ECONOMIZER AND STACK USING RAKES

Test Number	Run Number	ECONOMIZER (511.14 ft ²)			STACK (444.66 ft ²)			
		Dynamic Pressure (in. H ₂ O)	Static Pressure (in. H ₂ O)	Temperature (°F)	Dynamic Pressure (in. H ₂ O)	Static Pressure (in. H ₂ O)	Temperature (°F)	Atmospheric Pressure (in. Hg)
2 9/13	1	----	----	711.2	----	----	311.7	29.56
	2	----	----	707.9	----	----	312.7	-----
3 9/14	1	----	----	738.4	----	----	315.7	29.67
	2	----	----	737.5	----	----	312.8	29.68
15 9/15	Single	----	----	698.9	----	----	318.9	29.74
8 9/19	Single	.067	-4.8	750.3	.045	-.82	299.0	29.71
4 9/19	1	.021	-5.3	759.7	.022	-.59	307.9	29.65
	2	.020	-5.2	757.8	.024	-.59	308.9	29.64
5 9/20	1	.033	-5.5	751.3	.021	-.50	308.9	29.75
	2	.038	-5.5	741.6	.024	-.51	311.0	29.73
6 9/21	1	.037	-5.4	754.1	.037	-.50	309.6	29.76
	2	.026	-5.4	748.1	.025	-.46	309.4	29.69
7 9/22	1	.023	-5.4	744.1	.027	-.49	312.4	29.78
	2	.024	-5.4	743.5	.020	-.48	314.3	29.77
9 9/24-25	1	.016	-3.5	710.5	.015	-.51	306.3	29.59
	2	.014	-3.5	702.5	.017	-.54	304.5	29.60
10 9/25-26	1	.008	-2.5	683.5	.014	-.50	301.2	29.73
	2	.007	-2.5	686.8	.016	-.52	297.8	29.73
11 9/26-27	1	.011	-2.6	681.7	.011	-.52	297.5	29.83
	2	.011	-2.6	688.7	.017	-.52	304.6	29.85
12 9/27-28	1	.005	-2.6	687.4	.014	-.51	304.4	29.80
	2	.006	-2.6	686.6	.015	-.50	303.5	29.75
13 9/28-29	1	.008	-2.6	679.9	.011	-.53	304.8	29.62
	2	.007	-2.6	686.7	.014	-.54	306.1	29.62
14 10/1	1	.015	-5.3	755.7	.022	-.55	308.2	29.68
	2	.018	-5.3	760.8	.021	-.44	312.4	29.62

TABLE 20. GAS VOLUME FLOW AT ECONOMIZER AND STACK USING RAKES

Test	Load (mw)	ECONOMIZER			STACK		
		Velocity (fpm)	Volume Flow (acfm)	Volume Flow (scfm)	Velocity (fpm)	Volume Flow (acfm)	Volume Flow (scfm)
4-1	103 ↓	872.14	445,783.84	189,429.28	704.36	313,200.08	213,903.70
4-2		850.61	434,778.85	185,024.52	736.43	327,460.44	223,276.68
5-1		1090.91	557,605.24	239,284.45	687.74	305,811.23	209,337.06
5-2		1164.70	595,325.82	257,358.22	737.22	327,814.20	223,631.37
6-1		1153.46	589,581.43	252,572.32	912.75	405,864.59	277,667.33
6-2		966.39	493,958.43	212,152.09	751.48	334,152.44	228,149.93
7-1		904.01	462,076.07	199,729.89	781.30	347,412.33	236,981.55
7-2		925.72	473,172.00	204,558.37	673.55	299,498.94	203,733.45
8	85 ↓	1549.95	792,239.74	340,388.53	1000.85	445,039.76	307,956.24
9-1		747.09	381,867.80	169,510.20	583.55	259,482.92	177,262.44
9-2	70 ↓	697.01	356,267.04	159,288.69	618.90	275,198.06	188,490.34
10-1		519.54	265,557.63	121,543.05	558.59	248,383.44	171,630.31
10-2		487.14	248,997.35	113,635.63	596.32	265,157.82	184,034.14
11-1		607.52	310,527.48	142,795.63	493.84	219,590.93	152,982.07
11-2		609.70	311,643.20	142,531.51	615.60	273,733.52	189,057.50
12-1		413.46	211,335.94	96,601.88	560.87	249,396.56	172,009.23
12-2		452.11	231,091.79	105,527.50	580.85	258,280.93	178,051.59
13-1		520.38	265,987.23	121,638.99	498.90	221,838.65	151,990.03
13-2		488.73	249,808.46	113,562.80	562.98	250,332.58	171,216.99
14-1	103 ↓	739.28	377,872.84	161,265.01	704.27	313,160.04	214,030.77
14-2		811.66	414,869.57	175,953.27	692.99	308,143.32	209,090.21

TABLE 21. COMPARISON OF TRAVERSE AND RAKE VOLUME FLOW MEASUREMENTS

Test	Location And Load (mw)	TRAVERSE (MANOMETER)			RAKE (MANOMETER)			RAKE (BAROCEL)		
		Velocity (fpm)	Volume Flow (acfm)	Volume Flow (scfm)	Velocity (fpm)	Volume Flow (acfm)	Volume Flow (scfm)	Velocity (fpm)	Volume Flow (acfm)	Volume Flow (scfm)
2-1	Stack 103	855.65	380,474.04	255,603.98	836.63	372,015.56	249,929.79			
3-2	Stack 103	889.32	395,444.76	266,347.31	683.86 679.70	304,084.11 302,234.27	204,813.42 206,066.99			
3-1	Economizer 103	1263.94	646,049.68	277,452.36						
5-2	Stack Economizer 103	848.70	377,379.00	257,470.95				754.44 1085.29	335,471.07 554,735.43	228,854.80 241,377.95
15	Stack 103				759.11	337,545.90	227,662.02			

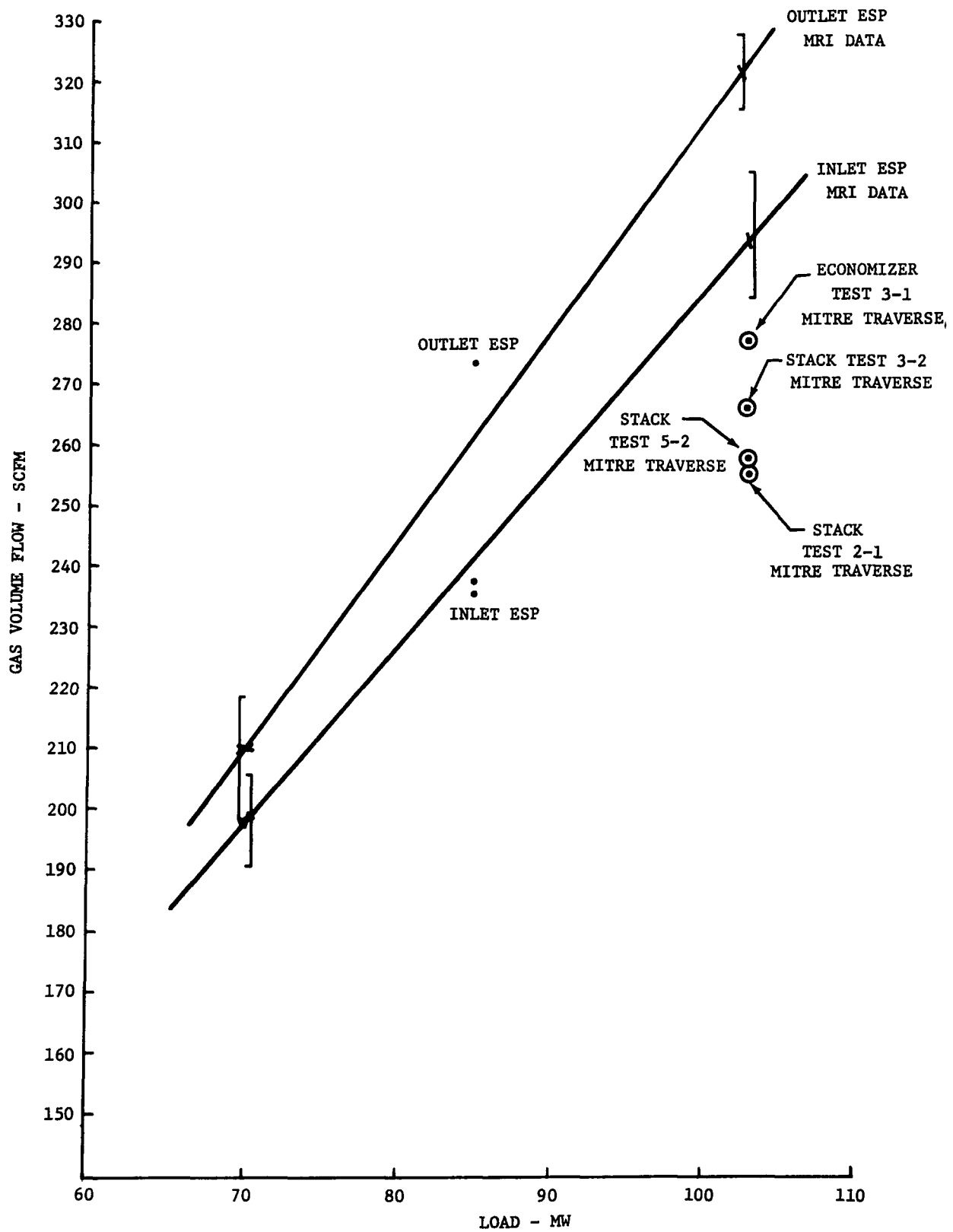


FIGURE 36
GAS VOLUME FLOW VERSUS LOAD FOR TRAVERSES

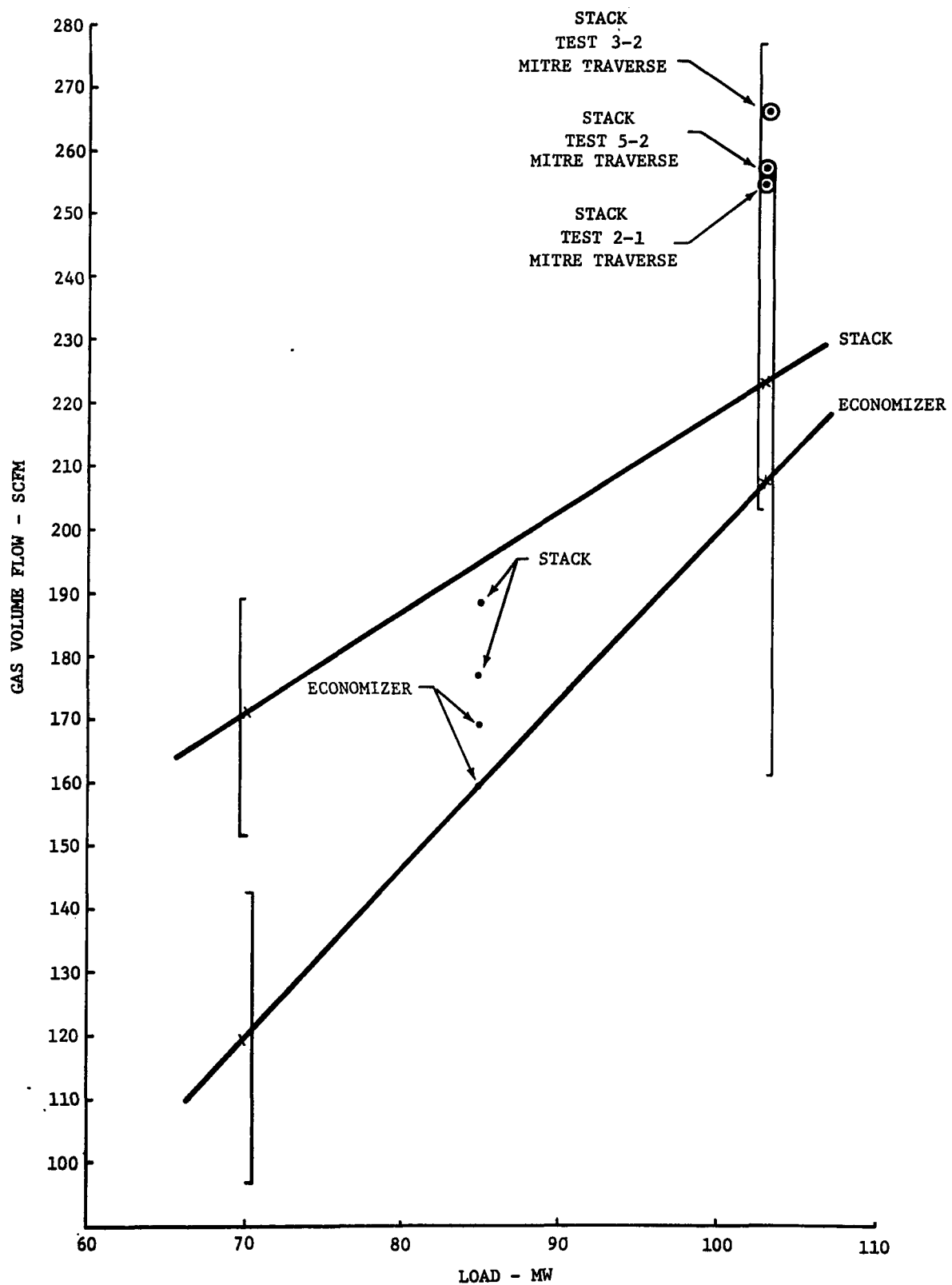


FIGURE 37
GAS VOLUME FLOW VERSUS LOAD FOR RAKES

APPENDIX III

ESP INLET AND OUTLET DUCTS

Cross-sections of the two inlet ducts to the electrostatic precipitator and the single outlet duct are shown in Figures 38, 39, and 40. The access ports and the sampling points are also indicated.

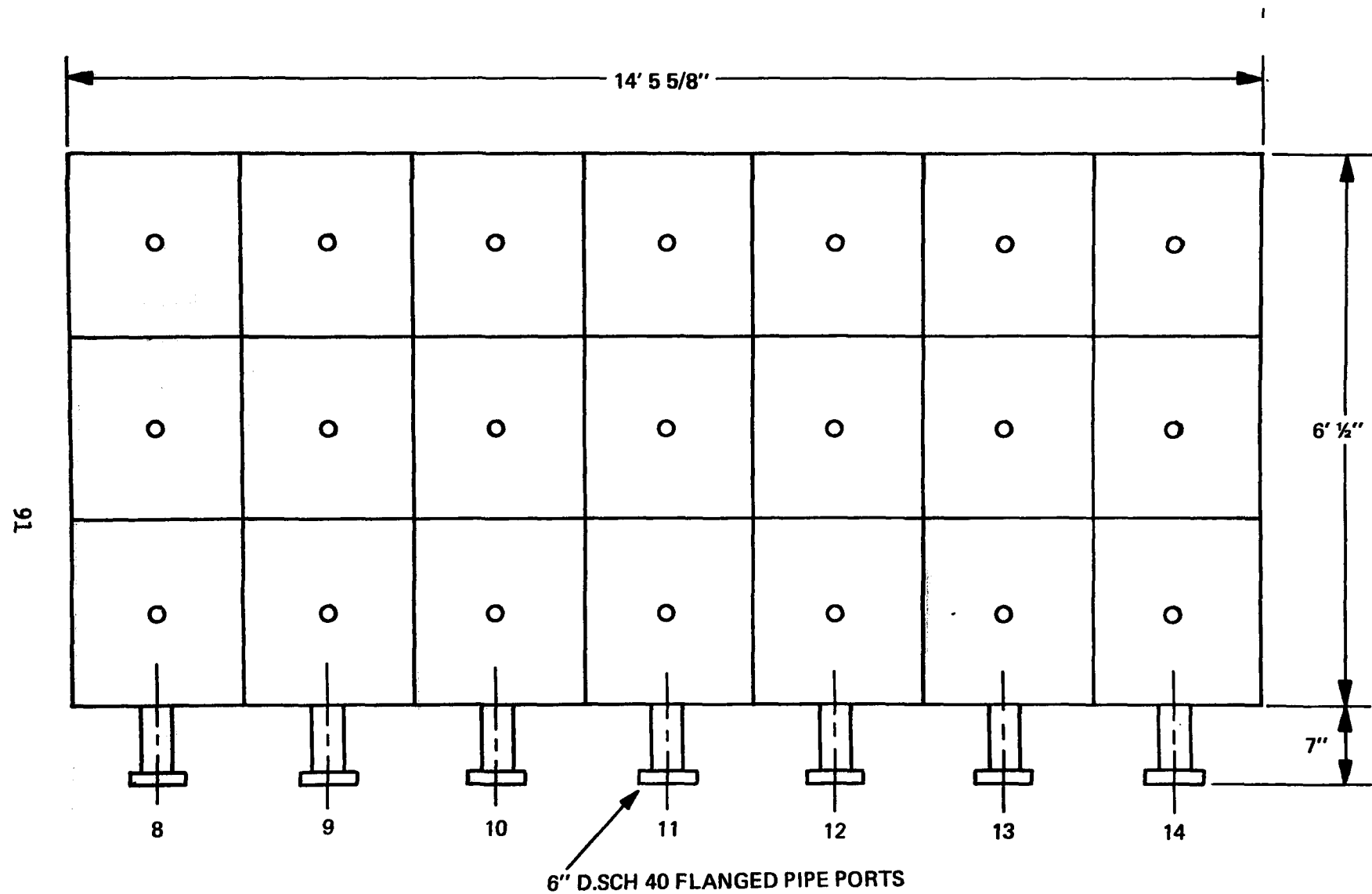


FIGURE 38
POINT 1—INPUT ELECTROSTATIC PRECIPITATOR
(LEFT SIDE FACING POWER PLANT)

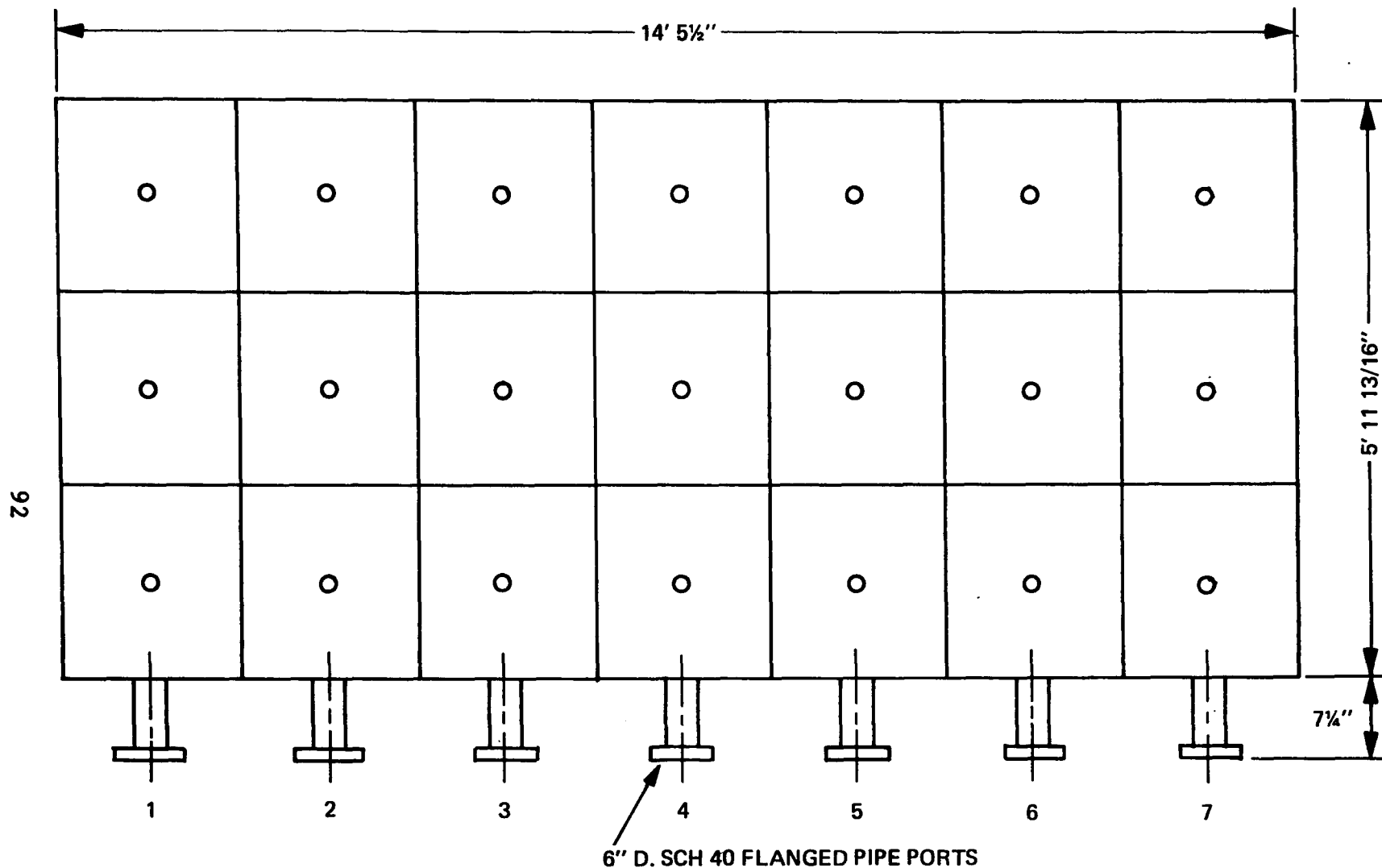


FIGURE 39
POINT 1—INPUT ELECTROSTATIC PRECIPITATOR
(RIGHT SIDE FACING POWER PLANT)

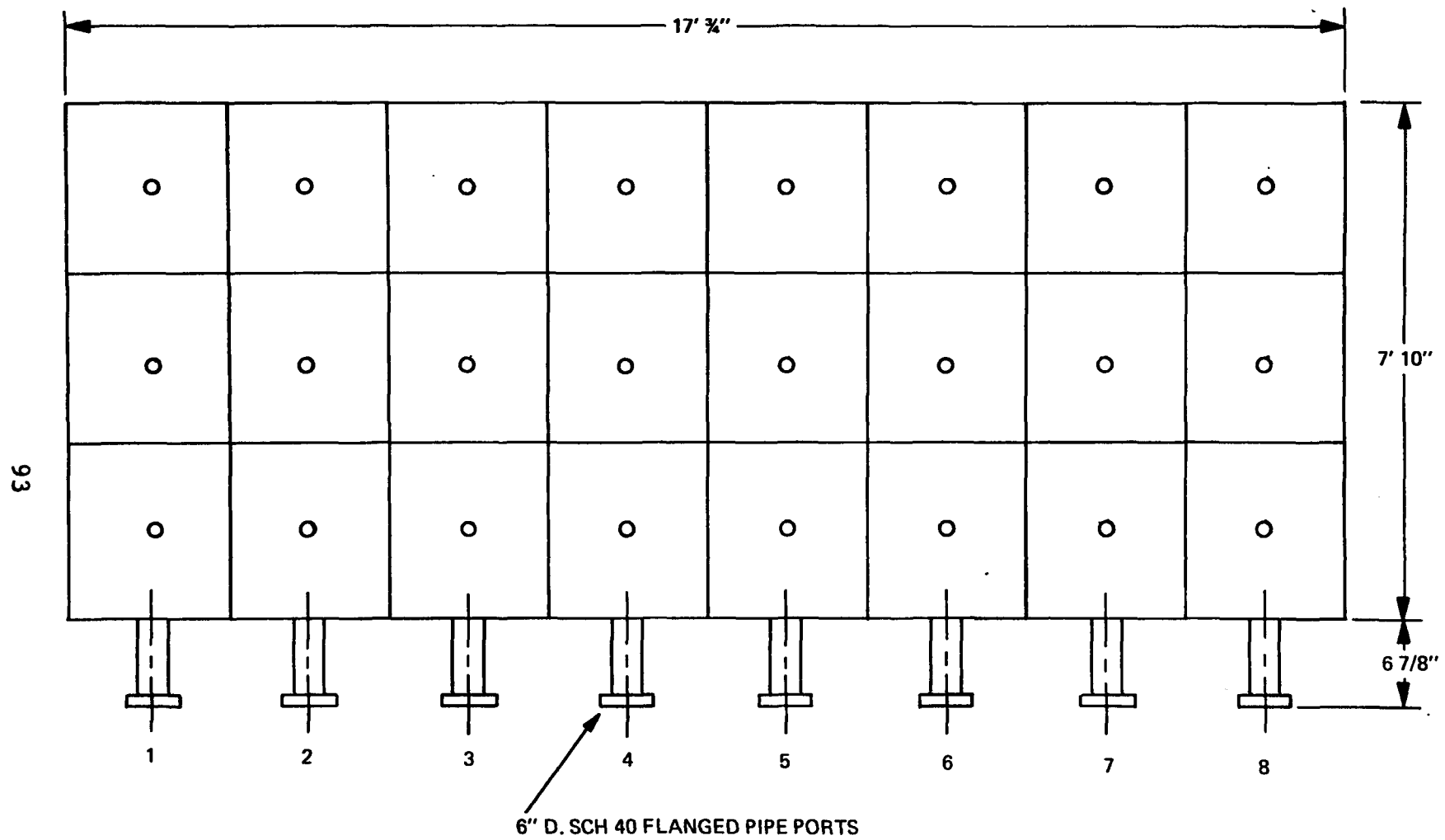


FIGURE 40
POINT 3-OUTPUT ELECTROSTATIC PRECIPITATOR

APPENDIX IV

CONVERSION FACTORS

TABLE 22. CONVERSION FACTORS

ENGLISH	METRIC
1.0 ft.	0.305 m.
1.0 lb.	0.454 kg.
1.0 grain	6.5×10^{-5} kg
1.0 Btu	1055 joules
1.0 °F	$\frac{^{\circ}\text{F} - 32}{1.8} = ^{\circ}\text{C}$

TECHNICAL REPORT DATA <i>(Please read Instructions on the reverse before completing)</i>			
1. REPORT NO. EPA-600/2-75-037		2. 	
4. TITLE AND SUBTITLE Test Evaluation of Cat-Ox High Efficiency Electrostatic Precipitator		3. RECIPIENT'S ACCESSION NO. 	
		5. REPORT DATE August 1975	
		6. PERFORMING ORGANIZATION CODE 	
7. AUTHOR(S) E. M. Jamgochian, N. T. Miller, and R. Reale		8. PERFORMING ORGANIZATION REPORT NO. M75-51	
9. PERFORMING ORGANIZATION NAME AND ADDRESS The Mitre Corporation Westgate Research Park McLean, Virginia 22101		10. PROGRAM ELEMENT NO. 1AB013; ROAP 21ACZ-003	
		11. CONTRACT/GRANT NO. 68-02-0650	
12. SPONSORING AGENCY NAME AND ADDRESS EPA, Office of Research and Development Industrial Environmental Research Laboratory Research Triangle Park, NC 27711		13. TYPE OF REPORT AND PERIOD COVERED Task Final; 9-12/74	
		14. SPONSORING AGENCY CODE EPA-ORD	
15. SUPPLEMENTARY NOTES 			
16. ABSTRACT <p>The report gives results of a test program to measure the performance of the high efficiency Research-Cottrell electrostatic precipitator (ESP) located at the Wood River Power Station, East Alton, Illinois. The overall efficiency of the ESP was measured as a function of steam generator and ESP operating conditions. Of particular interest was the efficiency of the ESP as a function of particle size over the range from 0.01 to 5 μm. In addition, fly ash resistivity, gas concentrations, coal analyses, and fly ash analyses were determined. The measured results were compared with those generated by an idealized computer simulation model.</p>			
17. KEY WORDS AND DOCUMENT ANALYSIS			
a. DESCRIPTORS		b. IDENTIFIERS/OPEN ENDED TERMS	
Air Pollution Electrical *Electrostatic Resistivity Precipitators Gases *Efficiency Concentration Measurement (Composition) *Fly Ash Coal *Flue Dust Chemical Analysis		Air Pollution Control Stationary Sources 	
		c. COSATI Field/Group 13B 20C 07D 21B 21D	
18. DISTRIBUTION STATEMENT Unlimited		19. SECURITY CLASS (This Report) Unclassified	
		20. SECURITY CLASS (This page) Unclassified	
		21. NO. OF PAGES 107	
		22. PRICE 	